

Editor-in-Chief B.E.Paton

Editorial board:

Yu. S. Borisov	V. F. Grabin
A. Ya. Ishchenko	V. F. Khorunov
B. V. Khitrovskaya	I. V. Krivitsun
S. I. Kuchuk	Yatsenko
Yu. N. Lankin	V. K. Lebedev
V. N. Lipodaev	L. M. Lobanov
V. I. Makhnenko	A. A. Mazur
O. K. Nazarenko	I. K. Pokhodnya
I. A. Ryabtsev	K. A. Yushchenko
N. M. Voropai	A. T. Zelnichenko

International editorial council:

N. P. Alyoshin	(Russia)
U. Diltey	(Germany)
Guan Qiao	(China)
D. von Hofe	(Germany)
V. I. Lysak	(Russia)
N. I. Nikiforov	(Russia)
B. E. Paton	(Ukraine)
Ya. Pilarczyk	(Poland)
P. Seyffarth	(Germany)
G. A. Turichin	(Russia)
Zhang Yanmin	(China)
A. S. Zubchenko	(Russia)

Promotion group:

V. N. Lipodaev, V. I. Lokteva
A. T. Zelnichenko (exec. director)
Translators:
I. N. Kutianova, T. K. Vasilenko,
N. V. Yalanskaya
Editor
N. A. Dmitrieva
<i>Electron galley:</i>
I. S. Batasheva, T. Yu. Snegiryova

Address:

E.O. Paton Electric Welding Institute,
International Association «Welding»,
11, Bozhenko str., 03680, Kyiv, Ukraine
Tel.: (38044) 287 67 57
Fax: (38044) 528 04 86
E-mail: journal@paton.kiev.ua
http://www.nas.gov.ua/pwj

State Registration Certificate
KV 4790 of 09.01.2001

Subscriptions:

\$324, 12 issues per year,
postage and packaging included.
Back issues available.

All rights reserved.

This publication and each of the articles
contained herein are protected by copyright.
Permission to reproduce material contained in
this journal must be obtained in writing from
the Publisher.

Copies of individual articles may be obtained
from the Publisher.

CONTENTS

SCIENTIFIC AND TECHNICAL

*Ishchenko A. Ya., Falchenko Yu. V., Ustinov A. I., Movchan B. A.,
Kharchenko G. K., Muravejnik A. N., Melnichenko T. V. and Rudenko
A. E.* Diffusion welding of finely-dispersed AMg5/27 % Al₂O₃
composite with application of nanolayered Ni/Al foil 2

Lobanov L. M., Pashchin N. A., Loginov V. P. and Smilenko V. N.
Effect of electrodynamic treatment on stressed state of welded
joints on steel St3 6

Skuba T. G. Spatial model of welded butt joint based on the data
of triangulation optical sensor 9

Royanov V. A. and Korostashevsky P. V. Selection of parameters of
the roller field of the line of sheet panel assembly and welding 14

INDUSTRIAL

*Paton B. E., Yushchenko K. A., Lychko I. I., Kovalyov V. D., Veliky
S. I., Pritula S. I., Chepurnoj A. D., Nikitchenko S. P. and Shalashny
A. N.* Equipment, procedures and technology for electrosag
welding of position circumferential butt joints 19

Kirian V. I., Knysh V. V. and Kuzmenko A. Z. Extension of the life of
metal span structures of railway bridges with fatigue damage 23

Ilyushenko V. M., Voropaj N. M. and Polyakov V. A. Technological
features of the processes of automated arc welding in repair of
large-sized tanks 26

Demchenko E. L. and Vasiliev D. V. Effect of structural-phase state
of high-strength weld metal on properties of welded joints in
hardening steels 30

*Salnikov A. S., Otkrovov V. V., Shelenkov G. M., Tsymbal E. A. and
Laktionov M. A.* Application of corrosion-resistant surfacing in
technological equipment operating in contact with sea water 35

BRIEF INFORMATION

Chajka N. K. Block of bias and cathode power of electron beam
gun using inverter-type converters 40

Theses for scientific degree 43

News 45

NEWS

International conference «Ti-2007 in CIS» 47

Railway transport. Welding 2007 (Workshop in Kakhovka) 48

M. L. Zhadkevich is 70 50

Developed at PWI 8, 13, 22, 42, 44



DIFFUSION WELDING OF FINELY-DISPERSED AMg5/27 % Al₂O₃ COMPOSITE WITH APPLICATION OF NANOLAYERED Ni/Al FOIL

A.Ya. ISHCHEENKO, Yu.V. FALCHENKO, A.I. USTINOV, B.A. MOVCHAN, G.K. KHARCHENKO, A.N. MURAVEJNIK,
T.V. MELNICHENKO and A.E. RUDENKO
E.O. Paton Electric Welding Institute, NASU, Kiev, Ukraine

It is shown that the presence of an interlayer between the surfaces being joined leads to formation of a strong (about 70 % of strength of the base metal) welded joint with no change in uniformity of distribution of the reinforcing particles (Al₂O₃). An activating effect of the interlayer on the process of diffusion welding is provided by the reaction of synthesis to form the NiAl₃ intermetallic phase within the joint zone, the phase being fragmented and dissolved in the composite matrix phase under the conditions of heating under pressure.

Keywords: diffusion welding, composite, electron beam deposition, nanolayered foil, solid-phase synthesis

Application of composite materials (CM) in development of complex mechanical systems (aircraft engines, hull components, missile stabilizers, connecting rods, and other car engine components) in a number of cases is limited by unsatisfactory weldability [1]. Use of the traditional methods of material joining by fusion usually leads to weld metal saturation by gases and (or) to disturbance of the uniformity of distribution of the CM strengthening component (for instance, in laser or electron beam welding). In addition, during the welding cycle time CM components usually enter into chemical interaction with each other and the material loses its strength properties.

Fusion welding of dispersion-strengthened aluminium-based CM is hindered also by the high viscosity of the metal in the weld pool, effects of agglomeration of the reinforcing particles (at application of Al₂O₃ as reinforcing particles), dissociation of the reinforcing particles at application of SiC particles. Conglomerates of strengthening particles or aluminium carbides forming in the weld in this case lead to lowering of strength and corrosion resistance of welded joints [2-4].

Use of the process of vacuum diffusion welding (VDW) for producing permanent joints of aluminium composites allows avoiding some of the above difficulties and producing sound joints of CM with the metal matrix [5].

Analysis of the phenomena running at VDW shows that the values of the welding process parameters (temperature, pressure, time of welded joint formation, etc.) strongly depend on the conditions providing activation of the surfaces being welded, i.e. breaking up of the oxide film, plastic deformation of the surface layers of the edges, etc. It is known that at VDW of high-strength materials the conditions for surface activation are greatly facilitated at introducing inter-

layers from ductile alloys between the surfaces being welded, namely from aluminium, copper, nickel, silver or gold, as well as in the form of galvanic or thin-film coatings. Powder-like materials are also used as interlayers in VDW, their effectiveness being associated with a highly developed free surface of the powders, and, consequently, their high diffusion activity [6].

Additional activation of the welded surface was achieved when using interlayers, consisting of two foils based on different elements, in which contact melting processes developed at temperature rise, which were accompanied by appearance of a liquid interlayer, promoting activation of the surfaces being welded at lower temperatures and pressure [7].

Thus, analysis of the studies devoted to development of the methods of producing permanent CM joints shows that using interlayers capable of plastic deformation and acceleration of diffusion process running (for instance, due to a high density of the interfaces), provides activation of the surfaces being welded and formation of the welded joint. From this viewpoint, laminated materials based on highly reactive elements can be used for this purpose.

It is known that at heating solid-phase reactions with intermetallics formation run in such laminated materials, which are accompanied by heat evolution. It may be assumed that under the conditions of external pressure application these processes will promote development of plastic deformation in the material subsurface layers and removal of oxide film from the surface.

The rate of running of solid-phase reactions in laminated materials depends on the layer thickness. With their reduction, the rate of running of the synthesis reaction increases [8], so that use of nanolayered materials is preferable for the most effective action of the interlayers on the surface being welded.

In view of the above, the possibilities for formation of welded joints using a nanolayered interlayer consisting of nickel and aluminium layers were studied in this work in the case of AMg5/27 % Al₂O₃ CM.



Procedure of sample preparation for investigations. Nanolayered foil based on Ni/Al system was produced by the method of layer-by-layer electron beam deposition of elements on a horizontally rotating substrate fastened on a vertical shaft of UE204 unit, by the procedure described in a number of works (for instance, [9]). Schematic of the process of foil formation is shown in Figure 1. In order to perform layer-by-layer deposition of elements the vacuum chamber was separated by a vertically mounted continuous screen into two equal parts, in each of which copper water-cooled crucibles were installed. A nickel ingot was placed into one of the crucibles, and aluminium ingot into another one. The substrate was fastened to a vertical shaft, the axis of which is located above the separating screen. Heating electron beam guns were used to heat the substrates up to the specified temperature, which was controlled during deposition by a thermocouple, the junction of which was fastened so that it was as close as possible to the surface, on which the condensate was deposited. Before the start of the condensate deposition, a thin layer of CaF_2 (1–2 μm) was deposited on the substrate surface, which promoted separation of the foil from the substrate furtheron. Then the evaporation guns were used to create on the ingot surface a molten pool, from which evaporation was performed, the intensity of which was adjusted by electron beam current. Substrate rotation and presence of the separating screen allowed successively depositing layers from pure elements. The proportion of the thickness of individual element layers was determined by the proportion of the intensities of ingot evaporation, and their total thickness was varied by changing the rate of substrate rotation. The total thickness of foil at the specified intensity of element evaporation was determined by the duration of the deposition process.

CM welding was performed in P-115 unit by the VDW process in forming matrices with forced formation of the contact zone.

CM samples of $15 \times 15 \times 4$ mm size were ground, degreased and scraped immediately before welding to remove the work-hardened layer formed during rolling. The prepared samples were fastened in forming matrices, which were mounted in a massive case between the upper and lower dies to ensure the coaxiality of welding pressure application and equalizing of the temperature field around the samples.

Heating was performed by plate heaters from molybdenum. For convenience of unit maintenance and access to the item, the heater consists of two halves, fastened on water-cooled copper brackets on vacuum chamber doors. In the working position with the closed chamber doors the heater forms a ring.

Welding temperature was measured by MPSHchPI-54 potentiometer. A chromel-alumel thermocouple was used as the sensor, which was fastened in the case in a special clamp.

Welding pressure was applied from a manual press through a wedge located below the vacuum chamber

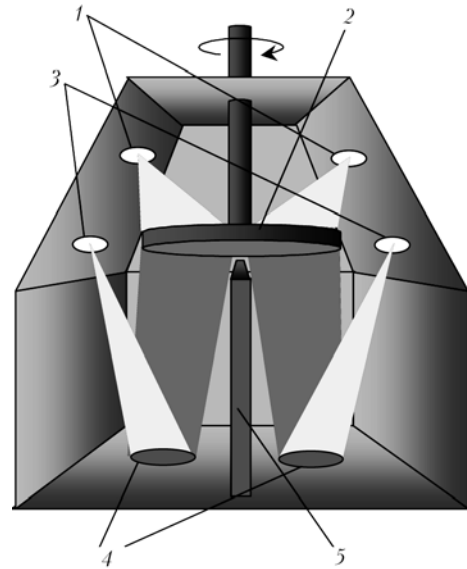


Figure 1. Schematic of the process of electron beam deposition of condensates with a laminated structure: 1 — heating electron beam guns; 2 — substrate; 3 — evaporation electron beam guns; 4 — crucibles with evaporation ingots; 5 — separating impermeable screen

and lower die contacting the billets to be welded. The applied pressure was controlled by ICh type indicator mounted in the dynamometer between the press and the wedge. Vacuum in the chamber was evaluated by the readings of ionization-thermocouple vacuumeter of VIT-3 grade.

After completion of the welding process and case cooling to the temperature of 100 °C the samples were taken out of the chamber. Sample cutting up for metallographic examination of the structure and mechanical testing was performed in electric erosion machine tool.

In order to prepare the metallographic sections of CM with reinforcing particles, the hardness of which is much higher than that of the matrix materials, elastic diamond discs with the grit between 125/100 and $3/2 \mu\text{m}$ were used with subsequent polishing with diamond paste. Composite structure was revealed by electrolytic etching in acetic-chloric electrolyte of the following composition: 1000 cm^3 of glacial acetic acid CH_3COOH and 70 cm^3 of chloric acid HClO_4 , as well as chemical etching in 10 % solution of H_3PO_4 . In order to reveal Ni/Al layers in nanolayered foil methods of selective chemical etching in Vasiliev reagent were used.

Microstructural studies were performed in MIM-8, «Neophote» microscopes, and CamScan4 scanning microscope fitted with energy-dispersive microanalyzer «Energy 200» for determination of the composition of the studied area of the microsection. Sample hardness was measured in «Rockwell» instrument at 600 N load, microhardness — in PMT-3 instrument at 0.2 N load.

Samples of the initial AMg5/27 % Al_2O_3 CM, as well as the welded joints, were subjected to tensile testing using standard MI-12 samples (type 1 to GOST 6996–66).

Results and their discussion. Figure 2 gives the microstructures of multilayered Ni/Al condensate of 77Ni–23Al, wt.%, composition consisting of nickel

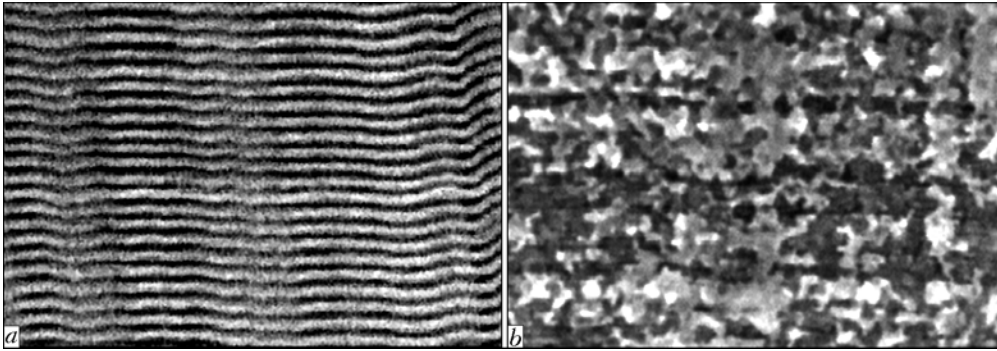


Figure 2. Microstructures of the cross-section of multilayered foil (light-coloured layers — nickel, dark-coloured — aluminium) in the initial condition (*a* — $\times 20000$) and after running of high-temperature synthesis reaction in it without pressure application (*b* — $\times 10000$)

and aluminium layers of 0.05 and 0.07 μm thickness, respectively. It is seen that the boundaries between the layers are quite sharp, i.e. electron beam technology enables production of laminated condensates with separated elements capable of reaction diffusion.

In addition, the contact between the layers creates the conditions for running of the synthesis reaction in such materials, which propagates at a high rate. Figure 2, *b* shows the microstructure of the foil after running of the solid-phase reaction in it, which propagated by the schematic of self-propagating high-temperature synthesis. As a result of running of this reaction the foil forms a consolidated compact structure with less than 1 μm grain size.

AMg5/27% Al_2O_3 CM was produced by casting method — mixing the dispersed strengthening particles of Al_2O_3 with the matrix material melt with subsequent compacting [10]. In the initial condition (Figure 3, *a*) CM is α -solid solution of aluminium with

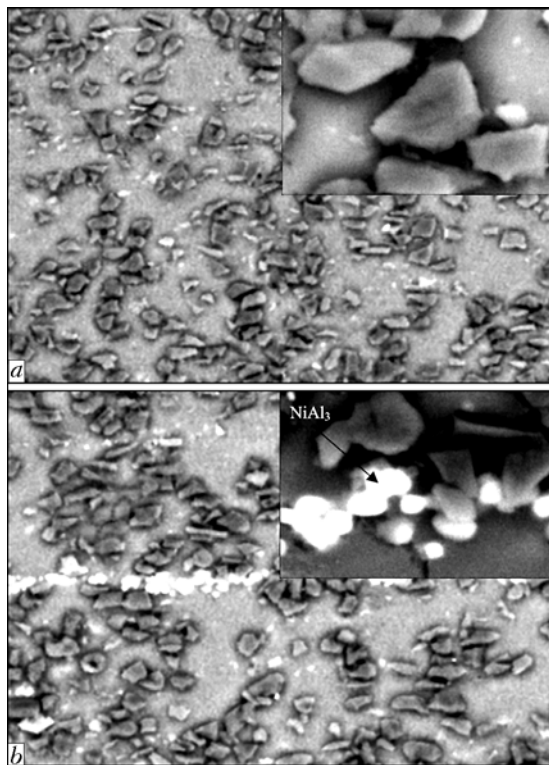


Figure 3. CM microstructures in the initial condition (*a*) and in the welded joint zone (*b*); $\times 300$, in the right upper squares — $\times 1500$

uniformly distributed dispersed intermetallic inclusions inherent to the matrix aluminium alloy and reinforcing particles of aluminium oxide. Al_2O_3 particles of an angular shape, dark-grey colour, 3–15 μm size with 3–20 μm interparticle distance are quite uniformly distributed in the matrix volume. The CM main defects are pores and discontinuities in the region of particle accumulation, which has an adverse effect on material properties. Compared to fusion welding, in solid-phase welding such defects of the base metal have a weaker influence on the joint quality.

Figure 3, *b* gives the microstructure of the zone of CM welded joint produced by VDW process using multilayer Ni/Al foil. Heating temperature in welding was 520 $^\circ\text{C}$ with subsequent soaking for 5 min. Unlike the initial material structure (Figure 3, *a*) a chain of precipitates formed in the joint zone. Local probe analysis of their composition showed that they are close in their composition to that of NiAl_3 intermetallics (39.5Ni–60.5Al, wt.%). In addition, in VDW process the nature of distribution and morphology of the reinforcing Al_2O_3 particles in the regions adjacent to the weld is not disturbed, and no agglomeration of the reinforcing particles is observed.

It should be noted that compared to the initial composition of the foil, synthesis of intermetallics enriched in aluminium, results from the high diffusion mobility of nickel in aluminium. Therefore, solid-phase reactions in the nanolayered interlayer, initiated by heating up to the welding temperature, activate reaction diffusion not only in the film proper, but also in the surface layers of the blanks being joined.

To clarify the possible influence of Al_2O_3 particles, strengthening the CM, on dispersion of the intermetallic interlayer resulting from the synthesis reaction at nonuniform plastic deformation in the joint zone and their local mechanical impact on the interlayer, experiments were conducted on VDW of an aluminium alloy close in its composition to matrix CM — AMg6 alloy.

In the initial condition AMg6 alloy is α -solid solution of aluminium, which contains dispersed particles of β -phase (Al_3Mg_2), and can also include AlMg_2Mn , $\text{Al}_6(\text{FeMn})$, Mg_2Si , $\alpha(\text{FeSiMn})$, Al_3Fe usually of less than 1 μm size (Figure 4, *a*).

Figure 4 gives the microstructure of the joint zone of samples from AMg6 alloy produced using multi-

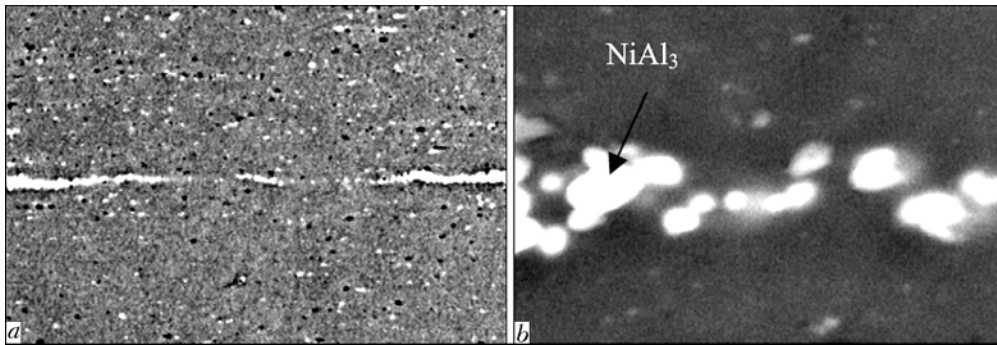


Figure 4. Microstructure of the joint zone of AMg6 alloy: a — $\times 300$; b — $\times 3000$

layered Ni/Al foil of the above composition. During VDW the reaction of solid-phase synthesis runs in the multilayered foil, which is accompanied by foil fragmentation into individual inclusions of 2–5 μm size, uniformly distributed along the weld. Comparison of microstructures of welded joints of CM and AMg6 alloy shows that the degree of fragmentation of intermetallic inclusions is close in both the cases.

Thus, during welding of AMg6 alloy, similar to CM, the interlayer is fragmented into individual dispersed particles, which is due to the features of running of the solid-phase reaction under the conditions of intensive plastic deformation of the material, which develops under the impact of pressure and is localized mainly in the joint zone, and is unrelated to the presence of strengthening Al_2O_3 particles in CM.

Mechanical testing of CM welded joints produced using nanolayered Ni/Al interlayer showed that their strength is 249 MPa, which is equal to 76 % of the base metal strength (Figure 5). The obtained results are indicative of the fact that interlayers with such a structure not only activate the processes providing diffusion welding of CM, but also do not lead to any essential lowering of the strength properties of CM welded joint.

Analysis of the obtained results shows that variation of the structure and properties of the interlayer, thermal cycle of diffusion welding and pressure application allows optimizing the VDW parameters to achieve the required level of mechanical characteristics of CM welded joints.

CONCLUSIONS

1. CM, based on aluminium alloy AMg5 strengthened by dispersed Al_2O_3 particles in the amount of 27 %, is used as an example to demonstrate that nanolayered interlayers in the form of foil, having a high diffusion activity, provide permanent joints at VDW without disturbance of the continuity and uniform distribution of the strengthening phase in the joint zone.

2. Activation of the joining process proceeds due to running of a solid-phase reaction of synthesis of NiAl_3 intermetallic phase in the nanolayered interlayer volume, which is fragmented and dissolved in the base material matrix phase under the conditions of heating under pressure.

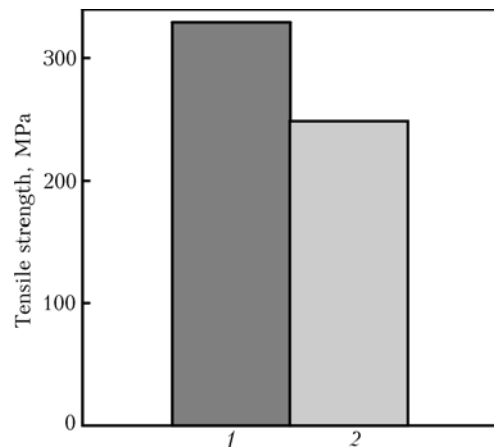


Figure 5. Strength of samples of initial material (1) and welded joint with a nanolayered interlayer of Ni/Al (2) at rupture testing

The work was performed with the financial support under the national program «Nanosystems, Nanomaterials and Nanotechnologies» (Project #11/06-N).

1. Krivov, G.A., Ryabov, V.R., Ishchenko, A.Ya. et al. (1998) *Welding in aircraft construction*. Kiev: MIIVTs.
2. Chernyshova, T.A., Kobeleva, L.I., Shebo, P. et al. (1993) *Interaction of metallic melts with reinforcing fillers*. Moscow: Nauka.
3. Ryabov, V.R., Muravejnik, A.N., Budnik, V.P. et al. (2001) Investigation of weldability of dispersion-strengthened Al + SiC composite material. *The Paton Welding J.*, **11**, 13–16.
4. Ryabov, V.R., Muravejnik, A.N., Bondarev, Andr.A. et al. (1999) Examination of structure of welded joints of dispersion-strengthened aluminium alloy. *Tekhnologiya Lyog. Splavov*, **1/2**, 139–144.
5. Calvo, F.A., Criado, A.J., Gomes de Salara, J.M. (1987) Soldadura por difusion de peliculas de oro electrodepositadas sobre aluminio. *Rev. Soldadura*, **17(2)**, 71–77.
6. Lyushinsky, A.V., Mazanko, V.F., Belyakova, M.N. et al. (1999) Mass transfer in pressure welding with application of ultradispersed nickel powder. *Svarochn. Proizvodstvo*, **6**, 10–14.
7. Lashko, S.V., Sukhacheva, G.N. (1968) Contact-reactive brazing of aluminium and its alloys. In: *Brazing in machine-building*. Riga: LatINTI.
8. Mann, A.B., Gavens, A.J., Reiss, M.E. et al. (1997) Modeling and characterizing the propagation velocity of exothermic reactions in multilayer foils. *J. Appl. Phys.*, **82(3)**, 1178–1188.
9. Bunshah, R.F., Nimmagadda, R., Doerr, H.J. et al. (1980) Structure and property relationships in microlaminar Ni–Cu and Fe–Cu condensates. *Thin Solid Films*, **72(2)**, 261–275.
10. Bondarev, B.I., Polkin, I.S., Romanova, V.S. et al. (1991) State-of-the-art and prospects of development of composite materials on the base of aluminium alloys reinforced by ceramic particles. In: *Transact. of the E.O. Paton Electric Welding Institute*. Kiev: PWI, 52–57.



EFFECT OF ELECTRODYNAMIC TREATMENT ON STRESSED STATE OF WELDED JOINTS ON STEEL St3

L.M. LOBANOV, N.A. PASHCHIN, V.P. LOGINOV and V.N. SMILENKO

E.O. Paton Electric Welding Institute, NASU, Kiev, Ukraine

The effect of electrodynamic treatment (EDT) with electric current pulses on the stressed state of low-carbon steel St3 and its butt welded joints was investigated. The experimental procedure was developed to study the mechanism of a discrete drop of the loading force on flat specimens under a single electrodynamic impact. EDT of butt welded joints on steel St3 was found to provide a more than 50 % decrease in the level of residual welding stresses.

Keywords: welded structures, low-carbon steel, electrodynamic treatment, current pulse, base metal, welded joint, tensile force, flat specimen, evaluation of stresses, residual stresses

The progress of modern engineering is determined by the application of welded structures with high preset technological and service characteristics. In this case, the problems of reduction in costs and consumption of metal for the fabrication of weldments are very important. Low-carbon steels are widely applied to manufacture welded members of critical structures, this requiring development of new approaches to improvement of mechanical properties of their welded joints.

Residual welding stresses (RS) are one of the causes of decrease in performance of metal structures. They have a negative effect on strength of the structures under cyclic loads, their corrosion resistance, etc. This leads to the need to investigate the efficient methods for controlling the stressed state of welded joints.

The impact by current pulses on metal subjected to tension to a level of ductility is known to lead to relaxation of its stressed state [1]. Tensile stresses close to the yield point of a material are effective in a welded joint. Treatment of the welded joint with the current pulses may initiate decrease in the level of RS in the weld metal and near-weld zone (NWZ).

Electrodynamic treatment (EDT) is one of the methods for affecting metals and alloys. It is based on initiation of electrodynamic forces in a material, which are induced during the transient processes accompanying propagation of the current pulses through the material [2]. Summing up of the electrodynamic forces and RS in the welded joints on a structure treated may cause formation of local regions of macroplastic strains in it, which leads to decrease in a general level of the stressed state of the material.

The purpose of this study was to investigate the effect of EDT on the stressed state of low-carbon steel St3 and its welded joints.

Flat specimens of the blade type were subjected to EDT to evaluate its effect on relaxation of mechanical stresses in a material [3]. The laboratory unit built on the base of a capacitor-type machine, the principle

of operation of which is described in [1], was used to generate single pulses of the electric current. Discharges of the capacitor bank were supplied to a specimen through contact of a copper electrode with the metal surface within the EDT zone.

Materials were tested using the tensile testing machine TsDM-10 with a maximal tensile force of 10 t at a strain rate of 6 mm/min. Variations in the tensile force were recorded during the entire cycle of loading of the specimens up to reaching the required stressed state in the material.

Peaks of the electrodynamic effect observed in the form of decrease in deformation resistance of the material under the effect of the current pulses were examined in the present study. The electrodynamic effect showed up as characteristic drops of the deformation force in tension diagrams.

During the experiments, a specimen held in grips of the testing machine was subjected to preliminary tension to a preset value of preliminary stress σ_{pr} , and then a discharge was applied. Drop of the deformation force, $\Delta\sigma_n$, was fixed by a recorder, which was part of the tensile testing machine TsDM-10. Tension was applied in a discrete manner with an interruption for EDT using n quantity of single pulses of the electric current, as well as fixation of the drop of the deformation force, $\Delta\sigma_n = \sigma_n - \sigma_{n+1}$, where σ_n and σ_{n+1} are stresses in a specimen material before and after a single pulse, respectively.

Characteristics of the drop of the deformation force were studied in a wide range of preliminary loading. The main consideration in this case was given to investigation of the electrodynamic effect at preliminary stresses, which were close to RS in welded joints on steel St3. Parameters of the treatment were as follows: electrode current $I_e = 3200$ A, voltage $U_e = 480$ V, current pulse duration $t_p = 0.0012-0.80036$ s, and capacitance of the capacitor bank $C = 4400$ μ F.

Discrete characteristics of the drop of the tensile force were investigated on the base metal and butt welded joints, the geometry features and treatment scheme of which are given in [3]. Samples of the welded joints were made in one pass by manual welding with 4 mm diameter covered electrodes of the ANO-4I grade under the following conditions: arc cur-



Variations in the stressed state parameters of specimens of steel St3 base metal and welding joints after EDT

Type of specimen	n	σ_{pr} , MPa	σ_n , MPa	$\Delta\sigma_n$, MPa	$\Delta\sigma_{\%} = \frac{\Delta\sigma_n}{\sigma_{pr}} \cdot 100 \%$	$\Sigma\Delta\sigma_{\%}$, MPa	Type of loading
Base metal	--	186.0	--	--	--	--	Elastic
	1		144.3	41.7	22.40	~40	
	2		130.4	13.9	7.47		
	3		116.6	13.8	7.42		
	4		111.0	5.6	3.00		
	--	230.0	--	--	--	--	Elasto-plastic
	1		180.37	49.63	21.57	~38	
	2		155.40	24.97	10.85		
	3		141.52	13.88	6.03		
	1	310.0	--	--	--	--	Plastic
			255.0	55.0	17.74	~18	
	Welded joint	--	205.0	--	--	--	--
1			185.90	19.10	9.31	~36	
2			155.40	30.50	14.80		
3			141.52	13.88	6.77		
4			130.42	11.10	5.41		
1		230.0	--	--	--	--	Elasto-plastic
2			183.15	46.85	20.36	~39	
3			160.95	22.20	9.65		
			144.30	16.65	9.09		
--		310.8	--	--	--	--	Plastic
1			255.3	55.5	17.85	~18	

rent $I_a = 150$ A, arc voltage $U_a = 70$ V, and welding speed $v_w = 5$ m/h.

The data on preliminary stress σ_{pr} and its discrete drop in the base metal and welded joints on steel St3 in EDT are given in the Table. It can be concluded from the Table that EDT of the samples of steel St3 with sequential current pulses causes a drop of the tension force in a material over all loading ranges. Maximal values of the drop of the tension force, $\Delta\sigma_{\%}$, are achieved in this case at the first current discharge ($n = 1$) in the EDT cycle. With subsequent effects by the current pulses, decrease in the efficiency of the treatment of a material occurs in such a way that at $n \geq 5$ the values of $\Delta\sigma_{\%}$ in the EDT cycle are not in excess of 1–2 %.

The total relative drop of the tension force in an elastic range, $\Sigma\Delta\sigma_{\%}$, in samples of the St3 base metal is about 40 %, and that in the welded joints is up to 36 %. This is attributable to the fact that an insignificant hardening of the overheated NWZ region subjected to EDT takes place in welding of low-carbon steels [4], which decreases the efficiency of this treatment. Under preliminary loads, which are much in excess of the elasticity limit of steel St3 ($\sigma_{pr} = 310$ MPa), the base metal and welded joint experience strain hardening, which also leads to decrease in the efficiency of EDT in the plastic loading region, where $\Sigma\Delta\sigma_{\%} \leq 18$ %.

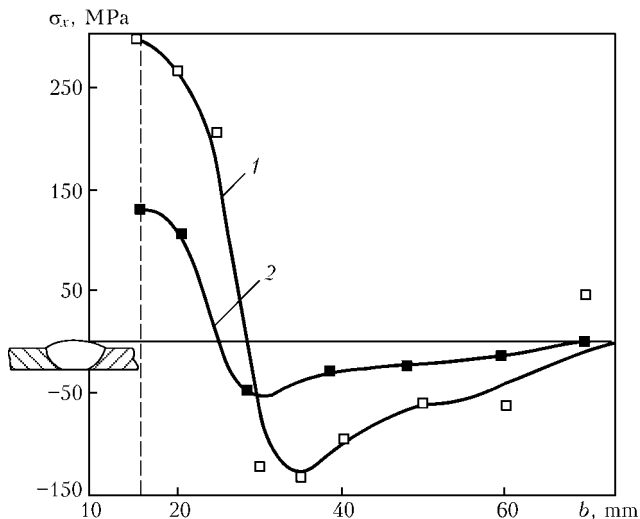
Stress of a flat specimen at $\sigma_{pr} = 230$ MPa corresponds approximately to the level of residual tensile stresses in NWZ of a welded joint on steel St3. Therefore, the electrodynamic effect on a specimen loaded to 230 MPa may cause a total drop of the tensile force,

$\Sigma\Delta\sigma_{\%}$, in it, that is similar to decrease in the level of RS in real welded joints of metal structures. As follows from the Table, EDT can lower the level of tensile stresses of the «active» zone of welded joints on steel St3 to 40 % of the initial one.

To prove the effect of the electrodynamic treatment on variations in the stressed state of thin welded metal structures, the treatment was performed on plates $500 \times 500 \times 3$ mm in size, having a longitudinal butt weld at their centre.

The level of RS was determined by the non-destructive ultrasonic inspection (USI) method, which is based on the dependence of propagation of ultrasonic waves upon the stresses in metal [5]. This method allows analysing the plane stressed state, the test object remaining intact.

The USI method made it possible to conduct multiple measurements of the current values of RS after each pulse in the EDT cycle. This method was used to evaluate the efficiency of EDT depending upon the quantity of the current pulses. Residual stresses were measured in the central cross section area of the plates. Longitudinal component σ_x of the plane stressed state of the plate material was determined before and after EDT. Each plate with the longitudinal weld was treated under conditions used earlier for EDT of flat specimens. A plate at the EDT moment was in a free state, i.e. without the application of static loads on it. This allowed evaluation of the pulsed effect by discharges of the electric current on relaxation of RS, which were formed as a result of the thermal welding cycle. EDT was performed by spot effects on the weld metal in a direction from its centre to ends with a step



Distribution of longitudinal residual stresses σ_x in welded joints on steel St3 without (1) and after (2) EDT: b — half-width of welded joint

of 90–100 mm. Totally, four discharges were performed, which corresponded to the conditions of treatment of blade-type flat specimens. The choice of the EDT direction was based on the fact that, according to the Table data, the first and second discharges in

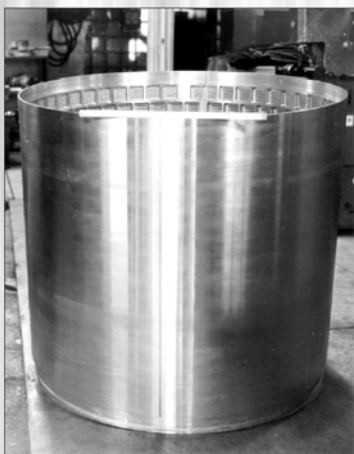
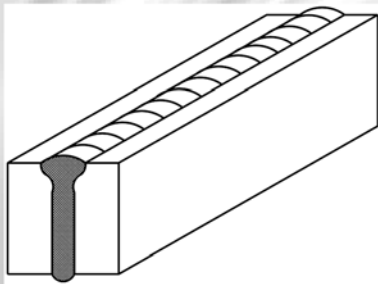
a series are most effective. So, it is expedient to apply them to the central part of the plate, where the RS level is maximal.

Distribution of longitudinal residual welding stresses σ_x on treated and non-treated plates is shown in the Figure. It can be concluded on the basis of the RS diagram that EDT of butt welded joints leads to a more than 50 % decrease in longitudinal component σ_x of the plane stressed state.

The above data prove the efficiency of application of EDT to control the stressed state of steel St3 and its butt welded joints.

1. Lobanov, L.M., Pashchin, N.A., Skulsky, V.Yu. et al. (2006) Influence of electrodynamic treatment on the stress-strain state of heat-resistant steels. *The Paton Welding J.*, 5, 8–11.
2. Aleksandrov, G.N., Borisov, V.V., Ivanov, V.L. et al. (1985) *Theory of electric apparatuses*. Moscow: Vysshaya Shkola.
3. Lobanov, L.M., Pashchin, N.A., Loginov, V.P. et al. (2007) Change of the stress-strain state of welded joints of aluminium alloy AMg6 after electrodynamic treatment. *The Paton Welding J.*, 6, 7–14.
4. Grabin, V.F. (1982) *Metals science of fusion welding*. Kiev: Naukova Dumka.
5. Guz, A.N., Makhort, F.G., Gushcha, O.N. et al. (1974) *Principles of non-destructive ultrasonic inspection method for determination of stresses in solids*. Kiev: Naukova Dumka.

TECHNOLOGY FOR EBW OF HIGH-STRENGTH ALUMINIUM ALLOYS WITH PROGRAMMED HEAT INPUT



Technology was developed for welding new structural materials, meeting high requirements for quality and strength of welded joints used in flying vehicles, cryogenic units or other heavy-loaded structures.

Welding with programmed heat input within the beam scan pattern holds a special place among various techniques of electron beam welding, such as welding with a scanning beam, tandem or double refraction welding. It offers researchers and technologists the fundamentally new possibilities in terms of active control of size and shape of the penetration zone, prevention of formation of root defects or structural heterogeneity, improvement of resistance to formation of hot cracks and porosity in the weld metal, and ensuring of stable strength values both within the welded joint and across the weld section in welding of thick billets.

Proposals for co-operation. Our specialists can conduct investigations on weldability of new structural materials using new equipment, develop the technology for welding of units and structures on which increased requirements for strength, density or wear resistance are imposed, and render technical assistance in arrangement of manufacture of parts in compliance with customer's specifications.

Contacts: Prof. Ishchenko A.Ya.
Tel.: (38044) 287 4406



SPATIAL MODEL OF WELDED BUTT JOINT BASED ON THE DATA OF TRIANGULATION OPTICAL SENSOR

T.G. SKUBA

E.O. Paton Electric Welding Institute, NASU, Kiev, Ukraine

The paper deals with the problem of construction of a spatial model of butt joint by the data obtained from triangulation optical sensor. Obtained work results can be used in systems of adaptive control of the process of arc welding of sheet structures 30–50 mm thick in different positions.

Keywords: welded structures, butt joints, geometrical size, triangulation optical sensor, spatial model, analytical description, approximation, point array

In preparation for welding of large-sized items it is impossible to produce butt joints, the geometrical dimensions of which correspond to those indicated in the drawings. Therefore, control of the welding torch manipulation system by a «rigid» program, which is compiled on the basis of drawings of edge preparation and parameters characterizing the gap and misalignment of edges formed at abutment of the parts of the item to be welded, does not provide a deposited metal layer of the actual geometry even at a rigorous following of the required welding modes. To guarantee an accurate correspondence of the geometry of the deposited metal layer to the actual groove geometry, and not the one specified by the drawings, which is what directly influences the weld quality, it is necessary to apply additive control of the welding torch manipulation system [1, 2], the algorithm of which allows for the position of the items being welded and geometrical parameters of the butt groove.

This study deals with the problem of construction of a spatial model of the actual butt for the case of welding thick-walled sheet structures, which is called the transverse «hill» technique. It essentially consists in a successive filling of the butt by parallel metal layers, deposited at a fixed angle to the butt axis. The above welding technique allows conducting single-pass welding of butt and fillet position and roll butt joints of thick-walled structures in the position from the downhand to the vertical one, also in the vertical plane.

To ensure sound deposition of the layers, it is necessary to move the welding torch along a complex path, which should correspond to the actual spatial parameters of the butt and provide a uniform thickness of the deposited metal layer. To implement this process, it is necessary to periodically measure the geometrical parameters of the butt being welded at a fixed distance ahead of the welding torch; construct a spatial model of the butt by the measured data; calculate the path of welding torch displacement corresponding to the actual butt geometry and providing a constant thickness and quality of metal layer depo-

sition allowing for transportation lag; perform adaptive control of the welding torch in real time and in keeping with the geometry of each deposited layer.

Accuracy of measurement of the geometrical parameters of the welded butt joint and welding torch positioning as a tool fastened on the last link of the manipulation system, should be not less than 0.25 of the minimum diameter of the electrode used for welding. With this welding process, the accuracy of measurement and positioning should be not less than 0.2 mm.

This work gives the results of solving the problem of construction of a spatial model of the butt by the data obtained from a triangulation optical sensor (TOS) with the light section of the butt joint.

TOS application. TOS is designed for forming an analog video signal, which is an image of a section of the butt of items being welded, and its transmission to the welding process control system. It consists of the lighting device forming the light plane and video-camera, mounted in one case.

TOS principle of operation [3] consists in the following. The lighting device generates the light plane, which is projected to the butt of items as a light band (Figure 1). Its contour follows the shape of the butt with formation of salient points. Salient points (1–4) of the light band at sensor displacement along the groove in time are shown in Figure 2.

TV camera receives the image of the light band projected onto the items being welded. Because of the non-uniformity of treatment of the surface of items being welded, the light band, being reflected from the groove faces, forms flares, which are the source of noise. In most of the cases, the applied software (SW) of TOS filters the noise and determines the spatial coordinates of the light band salient points with the required accuracy. In some cases, TOS applied SW calculates the point coordinates with a certain error, and in the case, if the sought points cannot be found, the program generates an error signal. In this connection, it is impossible to guarantee generation of data with the required accuracy after a specified time interval. In addition, it is impossible to determine the coordinates of the start of the metal layer, which should be deposited, and of its end directly by TOS readings. This is attributable to the fact that the in-

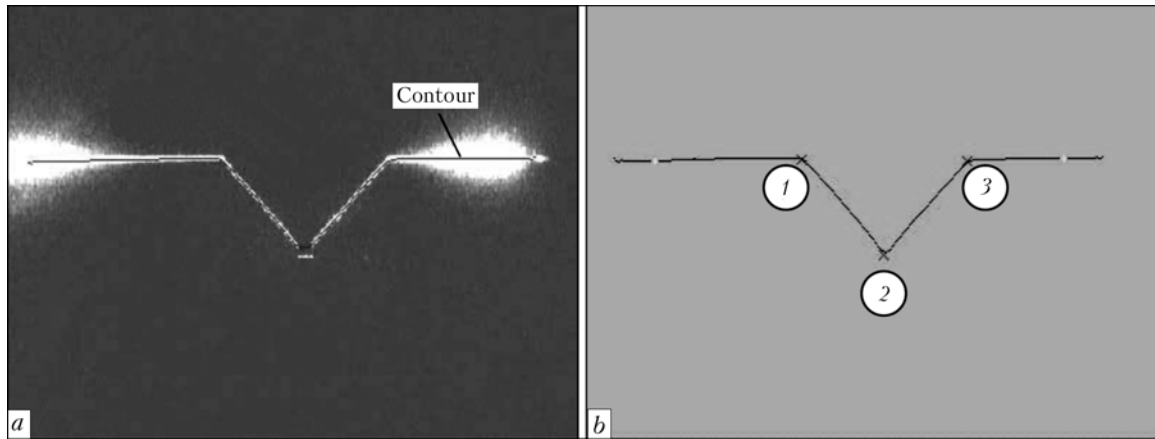


Figure 1. Projection of the light plane on the butt (a) and light band contour (b): 1-3 — points located on the left edge, in its root and on the right edge, respectively

quiry for obtaining information from TOS is issued not continuously, but after some time intervals, and, in addition, there is a limit of TOS operation. Until this limit has been overcome, the sensor SW cannot perform a correct numerical calculation of the light line salient point co-ordinates, not can the weld root toe be measured directly using the sensor. This is attributable to the fact that the side surfaces of the groove in the butt joint root are turned at an angle of 90° , so that the reflected beams of the laser band generator do not penetrate into the camera and, therefore, cannot be measured.

The formed data array of co-ordinates of the light band salient points is transmitted as a structure through the file, represented in the computer memory, to the applied SW of plotting the spatial model of the butt joint (SMBJ).

Substantiation of selection of the method of statistical processing of measurement results. The task of applied SW for SMBJ construction realizing the

selected method of statistical processing of measurement results, consists in the butt presentation in the analytical form. The faces of the latter are described by equations of planes, which are derived as a result of approximation of a set of data obtained from applied SW of the TV sensor (TVS). The above method allows with the specified accuracy reproducing the surface of the butt groove. Applied SW of SMBJ obtains the data on its position relative to the zero point selected in advance, and groove geometry of the parts being welded from TOS mounted on the welding tractor. Each light section, which represents the spatial co-ordinates of the salient points of laser emitter band contour, is entered into a list, which furtheron is the base for analytical description of the butt and calculation of the path of manipulation system link displacement on its basis. In this case the values of parameters, which cannot be directly measured with TOS (for instance, weld root toe), but are known beforehand from design documentation, are also taken into account.

To find the line of the «hill» start and lines limiting each deposited layer from the left, right, top and bottom, systems of equations are solved, which consist of equations of plane. These equations are derived by plane approximation of an array of points (see Figure 2), which are located on the edges of the left and right faces of the groove, «hill» faces, upper and lower faces of items being welded. Number of points on each face is taken to be equal to the number of correct lines of the light band, obtained from the sensor during scanning of the «hill» plane. To plot the equation of plane describing the right edge of the groove, an array of points designated as 1, 1', ..., 1''' and 2, 2', ..., 2''' in Figure 2, is made. The plane describing the left edge of the groove, is constructed by the array of points designated as 3, 3', ..., 3''' and 4, 4', ..., 4''' in Figure 2. Equation of planes describing the «hill» plane, is calculated by points 3, 3', ..., 3''' and 2, 2', ..., 2''' . As the butt has a variable shape along the entire length of the items being welded, equations of plane are recalculated in keeping with the current position of the metal layer being deposited. For this purpose, the points, which described the po-

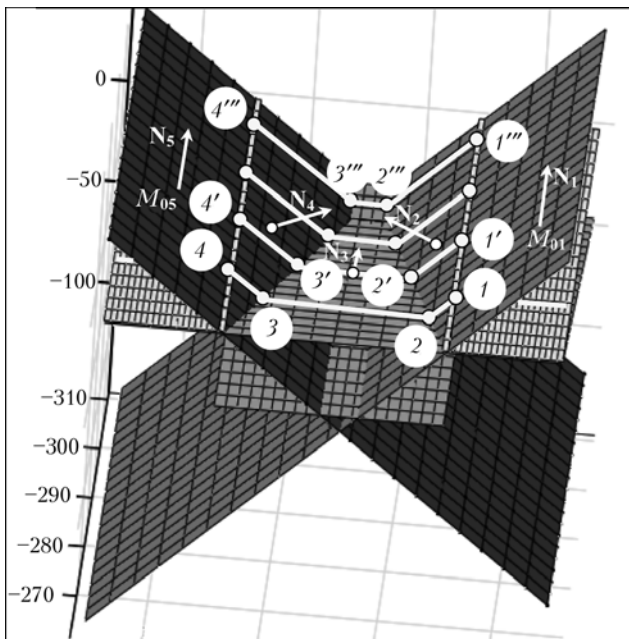


Figure 2. Groove geometry obtained as a result of approximation by planes: M_{01} – M_{05} — points on the respective plane; N_1 – N_5 — normal to the plane drawn from the respective point

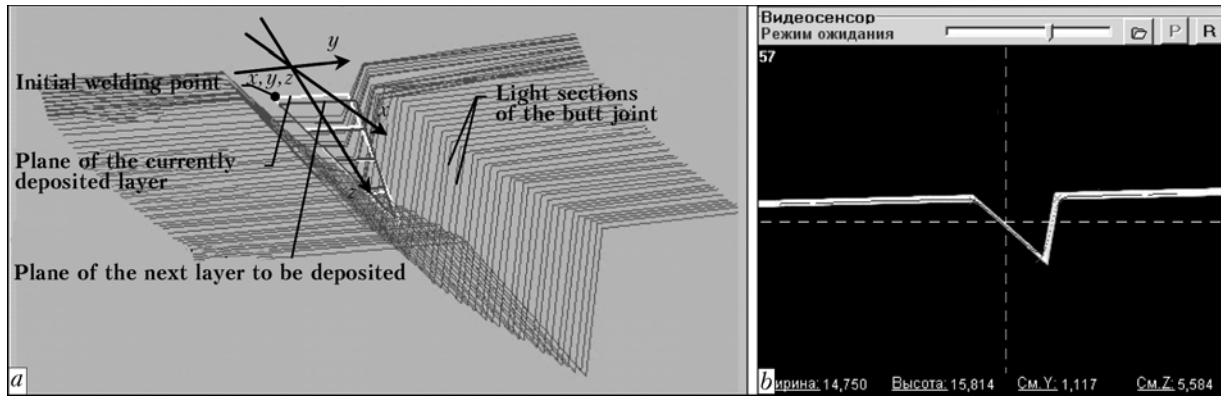


Figure 3. Spatial model of the butt joint (a) and TOS video signal (b)

sition of the first light section are removed from the point array, by which equations of plane are calculated for this layer, and points describing the position of the next light section, not included into the previous data array, are added to the end of the array. Formation of a new array of light sections is performed only in the case, if value of x co-ordinate of the initial point on the next layer to be deposited (Figure 3) is higher than x co-ordinates of the last light section, included into the current data array. Otherwise, equations, describing the butt side faces, remain unchanged, and position of the plane, which represents the «hill» plane, is corrected so that it was shifted relative to the previous one by the deposited layer thickness. Its slope remains unchanged along the entire butt length.

Subprogram of plane approximation of a set of n points in space calculates the normal to plane $N\{A, B, C\}$ (unit vector) and point $M_0(x_0, y_0, z_0)$, through which the plane passes. Point co-ordinates are calculated as the mean arithmetic value of initial point coordinates. Jacobi method is used to find the normal vector, i.e. finding eigen values and eigenvectors for symmetrical matrices [3]. Components of the sought normal vector are those of the initial matrix eigenvectors. The matrix is made up as follows:

$$A = \begin{vmatrix} xx & xy & xz \\ xy & yy & yz \\ xz & yz & zz \end{vmatrix}, \quad (1)$$

where

$$\begin{aligned} xx &= \sum_{i=0}^n x_i x_i; & xy &= \sum_{i=0}^n x_i y_i; & xz &= \sum_{i=0}^n x_i z_i; \\ yy &= \sum_{i=0}^n y_i y_i; & yz &= \sum_{i=0}^n y_i z_i; & zz &= \sum_{i=0}^n z_i z_i, \end{aligned} \quad (2)$$

x_i, y_i, z_i are the co-ordinates of point $u_i(x_i, y_i, z_i)$; $u_i = v_i - M_0$; v_i are the initial points in space; $M_0(x_0, y_0, z_0)$ is the point, the co-ordinates of which are the arithmetic mean of the respective co-ordinates $v_i(x_i, y_i, z_i)$ of the initial points.

As A matrix is a symmetrical real one and its dimension is equal to 3, it has three eigen values λ_i , each of which is matched to eigenvector V_i . Compo-

nents of the normal vector are calculated as follows: if $\lambda_0 < \lambda_1$ and $\lambda_0 < \lambda_2$, then normal vector $N\{x_{v_1}, x_{v_2}, x_{v_3}\}$; if $\lambda_0 < \lambda_1$ and $\lambda_0 > \lambda_2$, then $N\{z_{v_1}, z_{v_2}, z_{v_3}\}$. Otherwise, if $\lambda_0 > \lambda_1$ and $\lambda_1 < \lambda_2$, then $N\{y_{v_1}, y_{v_2}, y_{v_3}\}$; if $\lambda_0 > \lambda_1$ and $\lambda_1 < \lambda_2$, then $N\{z_{v_1}, z_{v_2}, z_{v_3}\}$.

Having calculated the normal vector and point through which the respective plane runs (plane describing the left and right faces of the groove, «hill», etc.), it is possible to present each of the planes by equation of the following kind:

$$A(x - x_0) + B(y - y_0) + C(z - z_0) = 0. \quad (3)$$

By solving a system of equations describing the horizontal plane of the metal surface and plane at an angle of 45° , we will determine the coordinates of the start of the first deposited metal layer. Solution of this system of equations, describing the horizontal plane on the level of the groove root and the same plane at an angle of 45° , yields coordinates of the end of the layer, which should be deposited.

Time interval, after which the data coming to TOS are read, is found by setting the respective values of system timer properties, and is equal to 150 ms. Data reading and storage are performed in real time at the stage of looking for the initial welding point, as well as displacement of welding torch to each next layer to be deposited. The spatial model of the butt groove is shown in Figure 3.

Synthesis of SMBJ construction algorithm.

SMBJ SW fulfills three main functions: reading of the data structure from the file represented in the memory, analytical description of the butt faces as equations of plane; plotting of a spatial graphic image of the butt of items to be welded.

The butt model is plotted on the basis of data received from TOS, with their subsequent approximation by planes. The size of the list, into which the data from applied SW of TOS are entered, is determined with a transportation lag --- distance from the welding torch nozzle edge to TVS. Values of co-ordinates of light band salient points are entered by TVS into a list, starting from finding the co-ordinates of the start of the butt and up to placing the torch into the initial welding point. During welding the list is updated at transition to the next deposited layers.

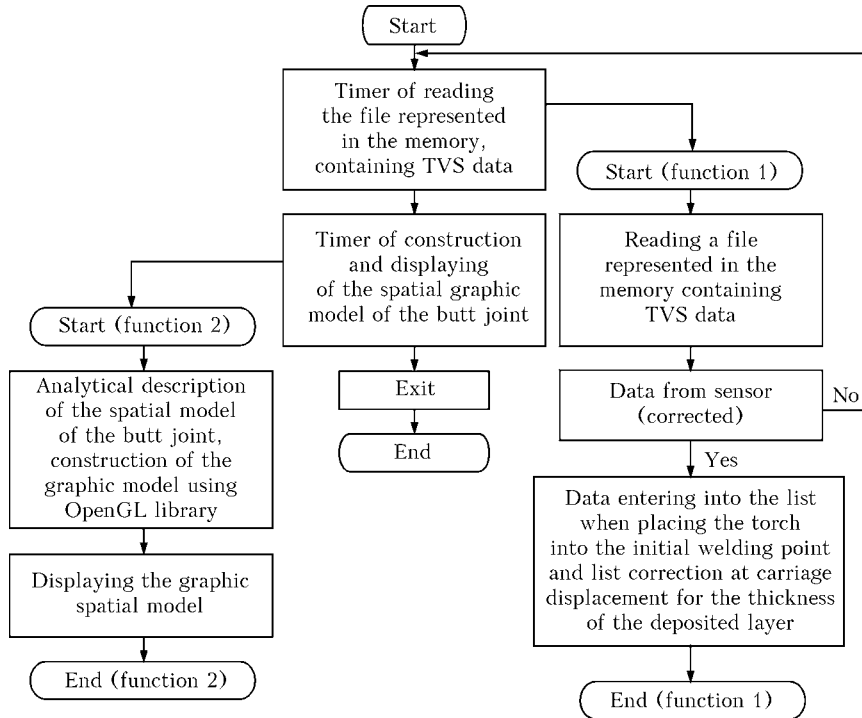


Figure 4. Block-diagram of the algorithm of construction of the spatial model of the butt joint

First the co-ordinates of salient points of the first light section are removed from the list, and the respective coordinates of light section registered by TVS during welding carriage movement to the next layer to be deposited, are added to its end. Such an approach allows storing a small but sufficient for calculation scope of data in the computer working memory, which enables continuous welding of an item of any length.

The decision on recalculation of planes at welding carriage displacement to the next layer to be deposited is taken, proceeding from the condition that x co-ordinate of the initial welding point in the next metal layer (see Figure 3), which is calculated on the basis of the welding process modes, exceeds x co-ordinate of point 1 (see Figure 1) of the light section contour. In order to take the decision, the first light section in the queue for entering into the list is taken, which is the basis to perform the current calculation of the equations of plane.

The spatial model was displayed using OpenGL graphic library, which provides the body of mathematics for manipulating 3D objects in space.

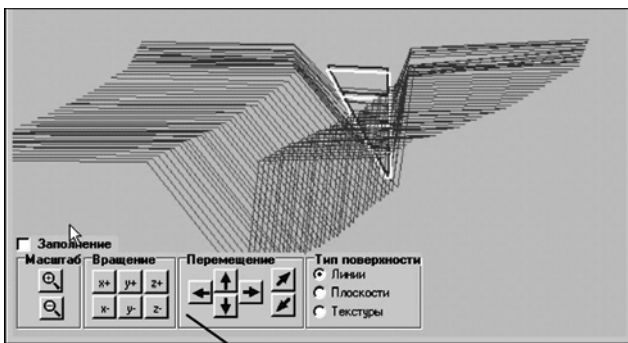


Image adjustment panel

Figure 5. Appearance of butt joint model at different settings

The algorithm of plotting the spatial model of the butt is shown in Figure 4. The block-diagram incorporates two system timers, assigning the time interval for data reading from the file represented in the memory, as well as calculation and drawing the 3D image of the butt of the items to be welded. Two timers are used in connection with the fact, that the defined tasks are fulfilled after different time intervals. Image drawing should be performed more often than reading of new data from the sensor. This is attributable to the need of a fast updating of the image at its rotation and displacement in the mapping window.

Results of simulation and experimental studies of operation of SMBJ program module. Results of the performed work were used to construct the spatial model of the butt of the items being welded, which was used to obtain initial data for calculation of the path of welding torch displacement required to perform welding by the transverse «hill» technique. The panel of image adjustment shown in Figure 5 allows changing the appearance, scale and position of the image in the mapping window, until the image has taken the form preferred by the operator.

Student's criterion was used to verify the adequacy of the obtained results of construction of the spatial model of the butt [4, 5]. For this purpose, the differences in selective average values of coordinates of points obtained from TVS ($\bar{x}_1, \bar{y}_1, \bar{z}_1$) and falling on the calculated plane ($\bar{x}_2, \bar{y}_2, \bar{z}_2$) were calculated:

$$|t_x| = \frac{|D_x|}{S} = \frac{|\bar{x}_1 + \bar{x}_2|}{S}, \quad |t_y| = \frac{|D_y|}{S} = \frac{|\bar{y}_1 - \bar{y}_2|}{S},$$

$$|t_z| = \frac{|D_z|}{S} = \frac{|\bar{z}_1 - \bar{z}_2|}{S}, \quad (4)$$



where $S = \sqrt{S_1^2 + S_2^2} = \sqrt{\left(\frac{1}{g} + \frac{1}{h}\right) s^2}$; $S_1^2 = \frac{1}{g} s^2$;
 $S_2^2 = \frac{1}{h} s^2$; D is the difference of coordinates; averaged
 weighted value is equal to

$$s^2 = \frac{\sum_{i=0}^g (x_{1_i} - M_{x_1})^2 + \sum_{i=0}^g (x_{2_i} - M_{x_2})^2}{g + h - 2},$$

g is the number of points, used to calculate the equation of approximating plane ($g = 20$); h is the calculated number of points falling on plane ($h = 7$);

$$M_{x_1} = \frac{1}{g} \sum_i x_{1_i}, \quad M_{x_2} = \frac{1}{h} \sum_i x_{2_i};$$

$$D_x = -8.699 + 8.8125 = 0.113;$$

$$s^2 x = (93.516 + 177.881) / (20 + 7 - 2) = 10.856;$$

$$S^2 x = (1/20 + 1/7) \cdot 10.856 = 2.094;$$

$$t_x = 0.113 / \sqrt{2.094} = 0.078;$$

$$t_y = 0.260 / \sqrt{0.082} = 0.906;$$

$$t_z = 0.361 / \sqrt{2.153} = 0.177.$$

If absolute values of $|t_x|$, $|t_y|$ or $|t_z|$ ratio exceed t_β values taken from the Table given in study [5], the hypothesis about the true average value being equal to $\hat{x}_1 = \hat{x}_2$, $\hat{y}_1 = \hat{y}_2 d$ or $\hat{z}_1 = \hat{z}_2$, respectively, should be rejected. With the probability of 0.95 it may be assumed that $\hat{x}_1 = \hat{x}_2$, $\hat{y}_1 = \hat{y}_2$ and $\hat{z}_1 = \hat{z}_2$, if $t_x < 2.086$, $t_y < 2.086$ and $t_z < 2.086$ at $g = 20$.

Values of Student's criterion $t < 2.086$ (t_x , t_y , t_z) lead to the assumption that the set of points is correctly approximated by the plane.

Thus, the 3D model of the butt constructed in this work is described in the form of equations of plane and provides the initial data for calculation of any paths of welding torch displacement, the accuracy of reproduction of which is one of the important factors, influencing the welded joint quality. To enable visual assessment by the operator of the correctness of the constructed graphic spatial model of the butt, the functions of image rotation around all the axes of the Cartesian system of co-ordinates, its displacement along the axes and change of the image scale, are envisaged. When the graphic presentation of the spatial model of the butt was plotted, one of the standard OpenGL libraries was used for graphic programming. This is a graphic standard, which provides broad possibilities and optimum response. The system is designed so that it may be incorporated into any (not just graphic) operating system.

Experimental studies showed that the butt model is constructed correctly and the error of the butt description in the analytical form does not exceed the admissible value equal to 0.25 of the minimum electrode diameter (0.8 mm) used with the above welding process, i.e. not more than 0.2 mm.

1. Pol, R. (1976) *Modeling, planning of paths and control of robot-manipulator movement*. Moscow: Nauka.
2. Korenev, G.V. (1979) *Task-oriented mechanics of controlled manipulators*. Moscow: Nauka.
3. Boillot, J.-P., Noruk, J. (2002) The benefits of laser vision in robotic arc welding. *Welding Technique*, **8**, 33-34.
4. Wilkinson, J.H. (1970) *Algebraic problem of eigen values*. Moscow: Nauka.
5. Varden, B.L. van der (1960) *Mathematical statistics*. Ed. by N.V. Smirnov. Moscow: Inostr. Literatura.

TECHNOLOGY OF MANUFACTURING LIGHT-WEIGHT WELDED CYLINDERS

The technology was developed at the E.O. Paton Electric Welding Institute and is aimed at solving two priority problems, namely lowering the specific weight and increasing the operating reliability. The novelty consists in the laminated structure of the cylinder wall and a rational combination of metals with different physico-mechanical properties.

The new approach to the technology of cylinder manufacturing allows using metals with a high specific strength, and, therefore, reducing the item weight by 30 to 50 %; increasing the operating reliability by minimizing the structure imperfections associated with the welds located on the cylindrical part and the nozzle; making the technology simple and accessible for implementation under the factory conditions.

There are no foreign analogs.

Pilot production batches have been made of cylinders of small and medium volume for the working pressure of 14.7 MPa (150 kg/cm²) with the strength margin of 2.6 according to the DNAOP 0.00-1.07-94 Rules. Technical documentation for cylinders manufacture has been developed.

Application. Storage and transportation of pressurized gases.

Contacts: Prof. Garf E.F.
 E-mail: yupeter@ukr.net



SELECTION OF PARAMETERS OF THE ROLLER FIELD OF THE LINE OF SHEET PANEL ASSEMBLY AND WELDING

V.A. ROYANOV¹ and P.V. KOROSTASHEVSKY²

¹Priazovzovskiy State Technical University, Mariupol, Ukraine

²OJSC «GSKTI», Mariupol, Ukraine

Dependence of deflection of sheet panel ends at transportation over the roller field on the extension of a free hanging end, distance between the neighbouring rows of rollers, material properties and sheet thickness was established. Schemes were developed for selection of roller spacing and distance between the neighbouring rows of rollers of the roller field for transportation of panels from sheets of different thickness and different materials.

Keywords: welding, roller field, assembly and welding line, sheet panel

Assembly and welding of sheet panels of shells of different tanks, including the barrels of railway tank cars and tank containers is performed in combined-production lines of panel assembly and welding, one of the important elements of which is the roller field. The smoothness of panel displacement, power of the transporting device drives and efficiency of the line as a whole depend on the main parameters of the roller field (roller diameter, bearing type, roller spacing, distance between the adjacent roller rows). On the other hand, dimensions and number of rollers influence the equipment weight and cost. At determination of the main parameters of roller fields of panel lines, the choice is usually made in favour of the rolling bearings in view of the their universally recognized advantages. Criteria for selection of the other parameters of the roller field are practically absent. Their development is an important scientific and practical task.

In publications devoted to this problem [1–6], special attention is given to selection of the roller conveyor roller spacing for transportation of long cargo and hot rolled sheets. Transportation of sheet panels of shells in large-sized tanks, the width of which is 2–3 times higher than the maximum width of the rolled sheets, similar to the design of the respective roller fields, has their features, which are practically not reflected in the technical literature. One of them is the considerable deflection (overhanging) of the edges of the sheet panel transported in the cold condition, under the action of its own weight, particularly of the front edge coming first in the direction of motion, which prevents normal sliding of the panel onto the rollers at its displacement and transportation. Edge deflection depends on the panel sheet material, and roller field parameters.

This study gives the results of investigation of the dependence of deflection of sheet panel edges on different parameters of the roller field and sheets being

welded, and criteria and procedures of selection of the main parameters of the roller fields of the lines of assembly and welding of sheet panels have been developed, ensuring normal operation, optimum metal content and cost of the equipment.

In order to reduce the metal content and cost of equipment for the roller fields, idle disc rollers with the spherical rolling surface mounted in staggered rows are used for the roller fields. Idle rollers of the roller conveyor are mounted in the places of the panel pressing to the jig to increase the contact surface and prevent dents in the sheets. Roller diameter is between 100 and 360 mm (the greater it is, the lower the resistance to panel displacement), and ball or roller rolling bearings are used. Panel displacement in different sections of the assembly lines is performed using special push (pull) devices and individual blocks of live rollers in their different combinations.

At displacement of a sheet panel over the roller field with roller spacing S , the front edge of the panel of width b , develops deflection f_c as it comes off the rollers, bending downwards relative to the overall plane of transportation under the action of its own weight (Figure 1, a). Side edges of the panels are deflected by f'_c , and part of the panel located between the roller rows --- by f_n (Figure 2, a); deflections f'_c and f_n are absent in the points of roller conveyor rollers mounting.

Let us determine for the case of the front edge, the deflection of panel edges hanging over during transportation. For this purpose let us represent the overhanging front edge of the panel as a beam with one end fixed, which is under uniformly distributed load --- its own weight. The calculated schematic of such a beam is given in Figure 1, b, panel extension l being the function of time t and displacement rate v : $l = vt$. At panel displacement from roller to roller with change of time t from zero to t_{\max} the extension changes from zero up to l_{\max} , while sagging of the front edge --- from zero to $f_{c\max}$. Considering that the rate of panel displacement is uniform and relatively small (less than 0.2 m/s), the formula of front edge



deflection at any moment of time, proceeding from differential equation of bent axis [7], becomes

$$f_c = \frac{q(vt)^4}{8EI_x} = \frac{ql^4}{8EI_x}, \quad (1)$$

where q is the uniformly distributed load (in this case the weight of overhanging edge of the panel, conditionally reduced to beam axis and uniformly distributed along extension length l); E is the modulus of normal elasticity; I_x is the moment of inertia of the section relative to bending axis.

Panel weight at any moment of time, allowing for the small value of the speed of displacement, is equal to

$$G_n = \gamma hb(vt) = \gamma hbl, \quad (2)$$

where γ is the specific weight of panel sheet material; h is the thickness of overhanging edge; b is the sheet length (panel width).

Then the uniformly distributed load is defined as

$$q = \frac{G_n}{l} = \gamma hb. \quad (3)$$

The moment of inertia of the section relative to the bending axis is equal to

$$I_x = \frac{bh^3}{12}. \quad (4)$$

Substituting the derived values into (1), we obtain

$$f_c = \frac{ql^4}{8EI_x} = \frac{\gamma hbl^4}{8E \frac{bh^3}{12}} = \frac{3\gamma}{2Eh^2} l^4. \quad (5)$$

From (5) it follows that deflection f_c of the panel front edge overhanging under the action of its own weight, is directly proportional to the fourth degree of the extension, depends on the specific weight and material of the sheets and is inversely proportional to the square of thickness of overhanging edge of the panel sheet. Designating value $3\gamma/2Eh^2$ constant for sheets of a specific material and specific thickness, as $K_{th,m}$ — coefficient of material and thickness, we obtain the formula of front edge deflection in the following form:

$$f_c = K_{th,m} l^4. \quad (6)$$

Panels of shell of barrels of railway tank cars and tank containers are made from structural low-alloyed steels 09G2S, corrosion-resistant steels 12Kh18N10T and AD0 aluminium 4–26 mm thick. $K_{th,m}$ values for sheets of 4–26 mm thickness from the above materials are given in Table 1. To calculate deflection f_c we will use the range of panel extension lengths from zero up to 2000 mm with the interval of 100 mm.

Analysis of data in Table 1 showed that from the three studied materials AD0 aluminium is the most rigid, i.e. having minimum deflection at the same thickness of the sheet and extension, and steel

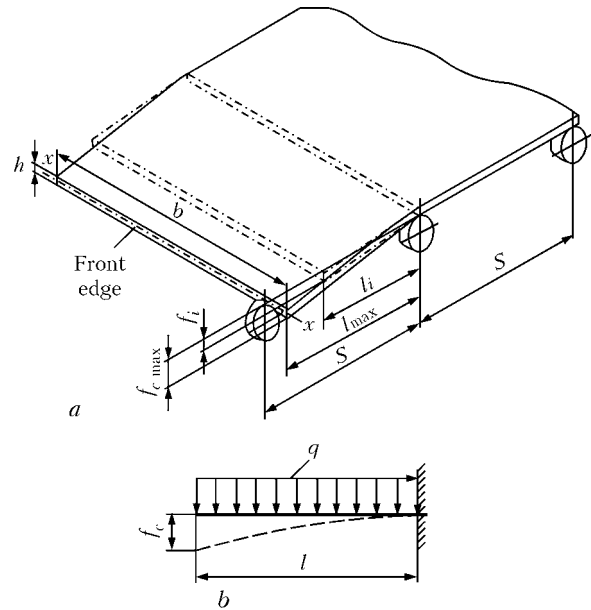


Figure 1. Schematic of the position of front edge of a sheet panel overhanging in cantilever (a), and design schematic of determination of edge deflection (b)

12Kh18N10T is the least rigid. Dependence of deflection on panel extension for sheets from steel 12Kh18N10T of different thickness is given in Figure 3.

Deflection of side edges f'_c varies by the same dependencies, as deflection of the front edge f_c . To determine the deflection (sagging) of part of the panel between two adjacent rollers (roller rows) f_n (Figure 2, a) let us consider it as a beam lying on two supports, which is under a uniform continuous load — its own weight. Figure 2, b gives the design schematic of the beam. Proceeding from the differential equation of a bent axis [7] maximum deflection of the beam is located in the span middle and is equal to

$$f = \frac{5q_n L^4}{384EI_y}, \quad (7)$$

where I_y is the moment of inertia of the section. Making the same transformations as for (1), we obtain

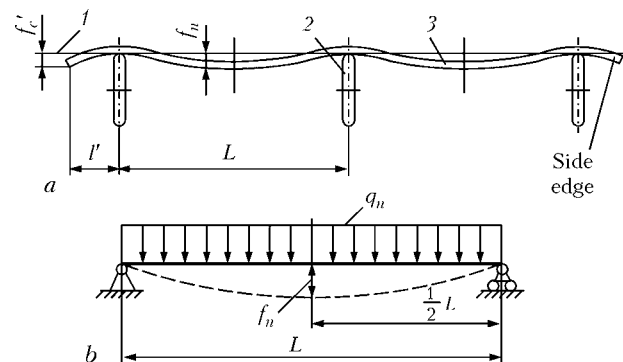


Figure 2. Deflections of a sheet panel at displacement over the roller field: a — schematic of deflections; b — calculated schematic of deflection between two adjacent roller rows; 1 — common transportation plane; 2 — roller; 3 — sheet panel; L — distance between two adjacent rows of rollers; l' — extension of the panel side edge; f'_c — deflection of overhanging side edge; f_n — deflection of panel part between the rollers; q_n — uniformly distributed load at panel sagging



of the roller journal r_n ; OC being the radius of the roller rolling surface R_r . Let us calculate the deflection:

$$f_c = R_r - R_r \sin \psi = R_r (1 - \sin \psi) = 2R_r \sin^2 (45^\circ - \psi/2);$$

$$\psi = 90^\circ - \beta = 90^\circ - (90^\circ - \alpha - \theta) = \alpha + \theta; \quad (10)$$

$$f_c = D_r \sin^2 \left(45^\circ - \frac{\alpha + \theta}{2} \right),$$

here angle $\alpha = \arcsin (r_n / R_r)$ and is constant for each roller.

We will take the formula of the section rotation angle from the differential equation of bent axis of a beam with one end fixed, which is under the uniform load (its own weight) [7]:

$$\theta = \frac{qI^3}{6EI_x} \quad (11)$$

Transforming this equation similar to (1), we obtain

$$\theta = K_\theta I^3, \quad (12)$$

where K_θ is the coefficient of the section rotation angle, equal to $2\gamma / EH^2$.

Values of coefficient K_θ for sheets from steels 09G2S, 12Kh18N10T and AD0 aluminium 4–26 mm thick are given in Table 2. Analysis of the tabulated data showed that at the same thickness sheets from 12Kh18N10T steel have the maximum angle of rotation, those from AD0 aluminium have the minimum angle. This confirms the conclusion about the relative rigidity of sheets from these materials made on the basis of the data in Table 1.

Substituting the value of angle θ into formula (10) and replacing the value of deflection f_c by its value derived from formula (6), we have

$$K_{th.m} I^3 = D_r \sin^2 \left(45^\circ - \frac{\alpha + K_\theta I^3}{2} \right) \quad (13)$$

Conditionally replacing I by x , designating $D_r / K_{th.m}$ as K and transforming this equation, we have

$$x^2 - \sqrt{K} \sin \left(45^\circ - \frac{\alpha + K_\theta x^3}{2} \right) = 0. \quad (14)$$

Having graphically solved this equation, we obtain two functions: $y_1 = x^2$ and $y_2 = \sqrt{K} \sin \times \left(45^\circ - \frac{\alpha + K_\theta x^3}{2} \right)$. Point of intersection of the derived curves gives us the value of panel extension, at which the front edge has deflection f_c at contact with the roller, i.e. has the maximum admissible overhanging for a smooth sliding onto the roller. The line of force in the point of panel contact with the roller runs in the plane normal to the edge face along a tangent to journal diameter (see Figure 4). Let us designate this deflection as critical f_{cr} , and the length of panel extension, at which it occurs, as

Table 2. Values of coefficient $K_\theta \cdot 10^{-17}$ (deg/m³) for sheets from different materials of different thickness

Sheet thickness $h \cdot 10^{-3}$, m	09G2S steel ($E = 200$ GPa, $\gamma = 7.85 \cdot 10^3$ kg/m ³)	12Kh18N10T steel ($E = 198$ GPa, $\gamma = 7.90 \cdot 10^3$ kg/m ³)	AD0 aluminium ($E = 81$ GPa, $\gamma = 2.70 \cdot 10^3$ kg/m ³)
4	281108	285756	238733
5	179909	182884	152789
6	124937	127003	106103
7	91790	93308	77954
8	70277	71439	59683
9	55527	56446	47157
10	44977	45721	38197
11	37171	37786	31568
12	31234	31751	26526
14	22948	23327	19488
16	17569	17860	14921
18	13882	14111	11789
20	11244	11430	9549
22	9293	9446	7892
24	7809	7938	6631
25	7196	7315	6112
26	6653	6763	5650

L_{cr} . The first function (parabola) will be the same for all the rollers and sheets of the applied materials of different thickness, and the second will have its own curve for each of these parameters. We will plot the curves (Figure 5) for 8 mm thick sheet from the least rigid material — steel 12Kh18N10T — for rollers having an optimum (25 to 60 mm) diameter of the journal and discs with 100–360 mm diameter around the rolling circle. Knowing values of critical extensions L_{cr} and using dependencies of panel edge deflection on its extension, we obtain the values of critical deflection (overhanging) of the panel front edge (Figure 6). As the situation shown in Figure 4 is the same both at sliding onto the roller of a panel front edge overhanging in cantilever, and at its deflection between two rows of rollers at roller arrangement in staggered rows,

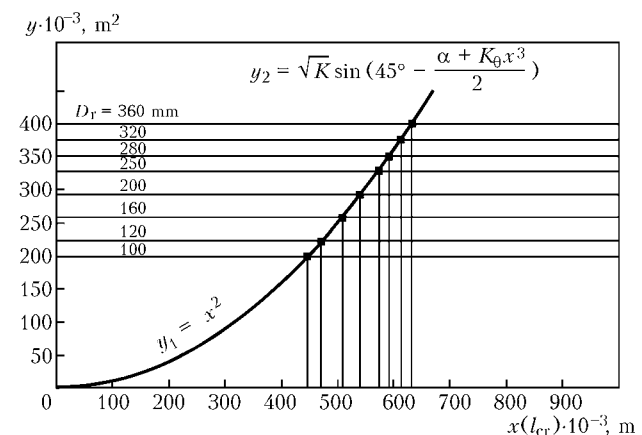


Figure 5. Schematic of determination of critical extensions L_{cr} for 12Kh18N10T steel sheet 8 mm thick and rollers of different diameter

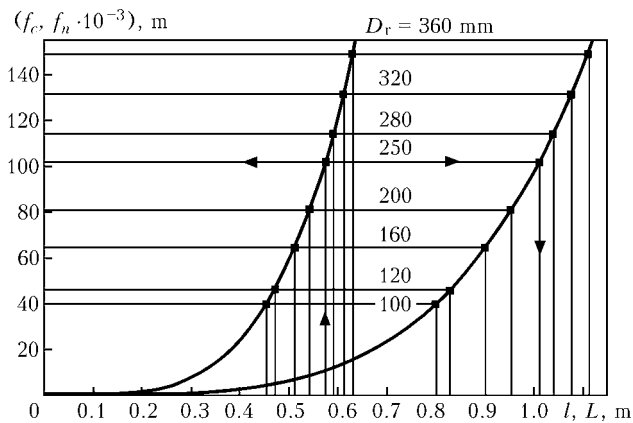


Figure 6. Schematic of determination of critical deflections f_{cr} and distance L_{cr} between adjacent rows of rollers of different diameters for 12Kh18N10T sheet steel 8 mm thick

using the values of critical deflection we will determine from f_n curves also the critical (maximum) distances L_{cr} between two adjacent rows of rollers (Figure 6).

Knowing the values of critical extensions, we will find the maximum roller spacing S_{max} of the roller field, equal to critical extension plus section OD from CDO triangle (see Figure 4, b):

$$S_{max} = L_{cr} + R_r \cos \left(\arcsin \frac{R_r - f_c}{R_r} \right) \quad (15)$$

where $f_c = f_{cr}$.

Upgrading of the roller field of the line of sheet panel assembly and welding in OJSC «Azovmash» taking into account the presented studies, allowed improvement of the quality of welds on panels, with reduction of the number of rejects.

Further studies are being conducted to establish the forces of additional resistance to displacement of sheet panels over the roller field, arising at sliding of the overhanging edge onto the roller, to determine the power of the transportation devices.

CONCLUSIONS

1. Main criterion for determination of the parameters of the roller field for transportation of sheet panels is

providing a guaranteed sliding onto the rollers of edges overhanging under the action of their own weight (sagging) at panel displacement, first of all of the front edge.

2. Deflection of a panel edge overhanging in cantilever or sagging between the rollers under the action of its own weight, is directly proportional to the fourth degree of extension (distance between two adjacent roller rows), depends on the material (specific weight and normal elasticity modulus) and is inversely proportional to the square of sheet thickness.

3. Selection of roller field parameters requires derivation of a dependence of panel edge deflection on the extension and distance between adjacent roller rows, as well as plotting graphs for determination of maximum deflections and extensions for sheets of all the used materials of different thickness.

4. Specific selection of parameters of the roller field should be performed after determination of the material and thickness of sheets of the produced panels and assigning the roller diameters (allowing for journal diameter) by the tables of values of maximum admissible spacing and distances between the adjacent roller rows, which should be developed for all the applied materials of different thickness.

5. Selection of roller spacing and distance between the adjacent rows should be performed taking into account the roller diameter, their arrangement in the roller field, quantity, weight, cost, as well as other data.

1. Ivanovsky, K.E., Rakovshchik, A.N., Tsoglin, A.N. (1973) *Roll and disc conveyors and systems*. Moscow: Mashinostroenie.
2. Plavinsky, V.I. (1969) *Machines of continuous transport*. Moscow: Mashinostroenie.
3. Zenkov, R.L., Ivashkov, I.I., Kolobov, L.N. (1987) *Machines of continuous transport*. Moscow: Mashinostroenie.
4. Spivakovsky, A.O., Diachkov, V.A. (1983) *Handlers*. Moscow: Mashinostroenie.
5. Kruzhkov, V.A. (1989) *Metallurgical lifting-and-shifting machines*. Moscow: Metallurgiya.
6. *GOST 5332-75: Rollers and spacing of mill roller beds*. Moscow: Standart.
7. Belyaev, N.M. (1976) *Strength of materials*. Moscow: Nauka.



EQUIPMENT, PROCEDURES AND TECHNOLOGY FOR ELECTROSLAG WELDING OF POSITION CIRCUMFERENTIAL BUTT JOINTS

B.E. PATON¹, K.A. YUSHCHENKO¹, I.I. LYCHKO¹, V.D. KOVALYOV¹, S.I. VELIKY¹, S.I. PRITULA¹,
A.D. CHEPURNOJ², S.P. NIKITCHENKO² and A.N. SHALASHNY²

¹E.O. Paton Electric Welding Institute, NASU, Kiev, Ukraine

²Open Joint Stock Company «Azovmash», Mariupol, Ukraine

The paper considers features of equipment and technology for electroslag welding of position circumferential butt joints on supporting rings of oxygen-blown vessels using the Ash 115 M machine at the Company «Azovmash». Described are advantages of the new machine that provides a high technical level of the technology and cost effectiveness of fabrication of large-size welded metal structures.

Keywords: electroslag welding, position circumferential welds, welding machine, information recording system, welding parameters, visualisation

Application of electroslag welding in machine-building provided a substantial increase in the efficiency of fabrication of large-size welded metal structures. Quality and performance of welded joints in electroslag welding (ESW) depend upon a number of technological factors (choice of welding consumables, heating temperature and type of heat treatment, welding parameters, methods for elimination of defects, and methods for fixation of billets to be welded), as well as upon the welding procedure (feeding of electrode consumables to the welding zone, methods for formation of the external surface of the weld, ensuring of the continuous and stable electroslag process, keeping to the preset welding parameters, modes of connection of power sources, and manipulation with a workpiece). It is obvious that these factors are closely related to each other and should be simultaneously considered and allowed for.

The efficiency of application of ESW is determined in many respects by the availability, technological capabilities and technical level of welding equipment, as well as by the rational handling of issues associated with procedure and technology of making a weld.

Design features of the ESW machines depend upon the peculiarities of the ESW method (wire electrode, consumable nozzle or large-section electrode), size and configuration of a billet to be welded. This determines whether the welding machine should be stationary or portable, moving along a workpiece or along a special column.

Many years' experience and current trends in building of welding equipment for ESW allowed development of an ingenious design of the modular type, based on modern mass-produced drives.

The new stationary welding machine Ash 115 M was developed and manufactured by the Pilot Plant for Welding Equipment of the Science and Technology

Complex «E.O. Paton Electric Welding Institute» particularly for ESW of position circumferential butt joints on supporting rings of oxygen-blown vessels produced by the OJSC «Azovmash». The machine differs fundamentally from its precursor (machine A-1555M) both in design and in its functional and technical capabilities.

The machine consists of the following main mechanical units: displacement mechanism, modular unit for feeding of wire electrodes, electrode oscillation mechanism, mechanism for variation of electrode inclination angle and crosshead hanger. Electrical equipment of the control systems is housed in a cabinet located near the machine. Buttons to control the process are mounted on a rotary plug-in panel fixed directly on the machine. The latter is equipped with two DC power sources of the VDU-1250 type and an information recording system.

Design and functional capabilities of the machine are adapted as much as possible to actual requirements the welding production of «Azovmash» should meet.

As to its design, the Ash 115 M machine has the following distinctive advantages:

- modular design allows an easy and prompt mounting of the machine on a guide rail, as well as its subsequent dismantling in any location of the joint;

- mode «setting» provided for in the control system allows setting of the process parameters (electrode wire feed speed v_e , oscillation amplitude A , time t of stopping of electrodes at the crosshead, etc.) before the beginning of the welding process;

- separate feeding of welding wires and powering from independent welding current sources provide the possibility of regulating the thermal power of the process depending upon the position of electrodes relative to the slag pool surface, which is particularly important for ESW of curvilinear welds;

- possibility of prompt adjustment of main process parameters from the control panel;

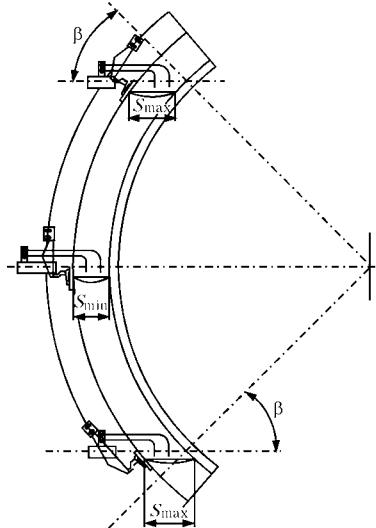


Figure 1. Scheme of ESW of an element of supporting ring for oxygen-blown vessel using the ASh 115 M machine

- mechanised correction of the nozzle inclination angle depending upon the spatial position of the slag pool;
- high reliability of operation of the machine control panel (with continuous monitoring of calculated parameters of the welding process);
- high reliability of operation of the drives: mechanisms for displacement of the machine along the rail, for feeding of electrode wires, and for transverse oscillations, which are based on using reduction gear-motors with frequency regulation of the rotation speed;
- presence of the information recording system equipped with personal computer, having a special software for visualisation of the process and recording of the process parameters.

The ASh 115 M machine is intended for ESW of vertical, inclined and curvilinear joints with curvature radius $R > 4.0$ m and angle of inclination to the vertical line adjustable within $\pm 25^\circ$.

Specifications of the ASh 115 M machine

Thickness of weld edges, mm	40–200
Quantity of electrodes, pcs	2
Diameter of electrode wire, mm	3.0, 4.0
Welding current per electrode at duty cycle = 100 %, A	up to 800
Electrode feed speed, m/h	80–450
Electrode feeding scheme	independent
Vertical displacement speed, m/h	0.6–12.0
Turning of electrodes in ESW of inclined joints, deg	± 25

Correction of position of electrodes:	
along the groove	± 60
across the groove	± 20
Driving force of traverse gear, kg	≥ 800
Oscillation amplitude, mm	100
Guide rail	flexible strip with involute gear rack

The special procedure and technology for ESW of position circumferential butt joints on billets of supporting rings for oxygen-blown vessels were developed for the machine.

The choice and setting of process parameters for ESW of the straight-line joints are based on the requirement that the welding machine or its main units should be moved during welding along a joint, and not change their position with respect to the slag pool surface. Therefore, the process parameters remain unchanged during the welding process.

In the case of welding of position butt joints, the spatial position of the entire machine continuously changes with respect to the welding zone, and thickness of the weld edges also changes depending upon the length of the weld (Figure 1). This causes changes (decrease or increase) in value of the so-called «dry» extension of electrodes, L_d , as well as the angle of inclination of the electrodes to the slag pool surface, β (Figure 2). Increase or decrease in L_d relative to the accepted values may lead to an inadmissible violation of the electroslag process. Variations in angle β have a substantial impact on the weld formation, and may cause the lack of fusion between the edges. Moreover, increase or decrease in thickness of the weld edges, S , causes variations in electrode oscillation amplitude A , which makes it necessary to adjust the gaps between the electrodes and crosshead, Δ_2 , and permanent cover plate, Δ_3 . To ensure normal conditions for the welding process, it is necessary to constantly maintain the value of L_d at the required level. Besides, these manipulations should be carried out during welding, simultaneously with constant control of the entire process.

The choice of welding parameters is based, first of all, on the size of a joint (thickness of the weld edges, curvature radius and weld length), as well as on the welding speed.

The range of thicknesses to be welded for the ASh 115 M machine is 40–200 mm. Practice of the welding production shows that one electrode can weld metal up to 50 mm thick. At a larger thickness it is necessary to apply electrode oscillations, or increase the quantity

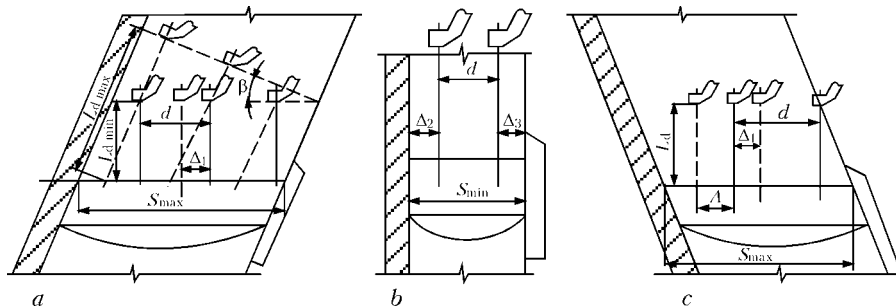


Figure 2. Schematic of location of electrodes within the ESW zone in the initial region (a), horizontal diameter (b) and final region (c) of the joint



of electrodes. It is recommended to weld metal up to 100 mm thick using two electrodes without oscillations, and metal up to 200 mm thick --- with oscillations.

The welding speed depends, primarily, upon the properties of a structural material welded (chemistry, and carbon content in the first turn), thickness of the weld edges and their fixation conditions. For carbon and low-alloy steels, satisfactory values of the welding speed for thicknesses under consideration (40–200 mm) are 2.0–0.5 m/h, the welding speed being rapidly decreased with increase in thickness. Under conditions of the rigid fixation of workpieces (permanent cover plate), widening of the existing ranges may lead to formation of solidification cracks in the weld metal.

In welding with oscillations, distance between the electrodes, d , should be selected proceeding from ratio $d = (S + \Delta_1 - \Delta_2 - \Delta_3) / n$ (mm). The required electrode wire feed speed is calculated on the basis of electrode quantity n and welding speed v_w selected for a specific thickness of the joint: $v_e = v_w F_h / \Sigma F_e$ (m/h), where F_h is the gap cross section, and F_e is the total cross section of electrodes.

For welding of joints in billets of half-rings with wall thickness $S = 100$ mm, it is necessary to apply oscillation of electrodes, as thickness of the metal welded changes from $S_{max} = 130$ mm (at the beginning and end of the joint) to $S_{min} = 100$ mm (at the centre). This requires that extra manipulations should be performed during the welding process, such as changing the oscillation amplitude (amplitude A) and distance between the electrodes, d .

Sound welds were produced by ESW of samples (wall thickness of a shell --- 60 mm, weld length --- 1500 mm) at a welding speed of $v_w = 1.8$ –2.4 m/h under laboratory conditions of the E.O. Paton Electric Welding Institute. Optimal values of L_d at the initial and final stages of welding were determined, and values of Δ_2 and Δ_3 were optimised in tests of the new machine under factory conditions (on full-scale samples). The required values of the process parameters were selected by manipulating with the mechanisms for transverse oscillations and rotating of the feed modules with respect to the slag pool surface.

The satisfactory weld formation is achieved by a combined regulation of L_d and β (Figures 1 and 2), periodic adjustment of the Δ_2 and Δ_3 values, as well as regulation of v_e and U_w at each electrode depending upon the position of the welding zone.

For ESW of circumferential welds with a shell wall thickness of $S = 60$ mm, it is possible to use one electrode with oscillations. However, in this case v_e will range from 250 to 450 m/h, which may cause certain technical difficulties associated with stability of the welding process. Therefore, it is recommended to weld this thickness using two electrodes without oscillations at $v_e = 110$ –250 m/h.

Joints with a shell wall thickness $S = 60$ –80 mm should be welded using two electrode wires without

oscillations at a welding speed of $v_w = 0.8$ –1.5 m/h, and those with a shell wall thickness above 80 mm should be welded using two electrodes with oscillations at a welding speed ranging from 0.6 to 1.2 m/h.

Procedure for performing ESW of position circumferential butt joints with electrode oscillations is more difficult than welding with stationary electrodes. In the process of position butt welding, because of continuous changes in thickness of the weld edges (see Figure 1), a welding operator should periodically change the A and d values according to a changing value of S . Parameter A is changed using the transverse oscillations control buttons, which are located on the panel, and d --- using the electrode separation buttons. The values of «dry» electrode extension L_d are also variable. Moreover, they can be increased (decreased) approximately two times (Table). The values of L_d are regulated by the machine tilting mechanism.

Electrode wire feed speed v_e in the initial and final regions of a joint is regulated in such a way that welding speed v_w matches thickness of the weld edges in a corresponding region allowing for the L_d value. As thickness of the weld edges approaches the S value, the values of v_e for both electrodes are made almost equal to each other.

When welding a joint with thickness $S = 100$ mm, oscillation amplitude A will vary from 37 to 20 mm, the value of dry electrode extension L_d will also change in this case. For an external joint the L_{d2} / L_{d1} ratio at the beginning of the weld is equal to 0.8, that at the weld centre is 1.0, and at the end of the weld it is 1.25. In welding of an internal joint, the L_{d2} / L_{d1} ratio is equal to 1.25, 1.0 and 0.8 mm, respectively, depending upon the weld position. At a constant electrode wire feed speed a 20–25 % increase (or decrease) in the dry electrode extension may lead to some decrease (increase) in the welding current at electrodes. Therefore, it is necessary to allow for the current values of I_d during the welding process and maintain

Variations in dry extension of electrodes, L_d , depending on welding zone position

Metal thickness, mm	Welding zone position	L_{d1} max, mm	L_{d1} min, mm	L_{d2} max, mm	L_{d2} min, mm
150	Weld beginning	90	75	70	50
	Weld centre	70	70	70	70
	Weld end	70	55	90	75
100	Weld beginning	80	70	65	55
	Weld centre	70	70	70	70
	Weld end	65	55	80	70
80	Weld beginning	80	70	65	50
	Weld centre	70	70	70	70
	Weld end	60	50	80	70

Note. L_{d1} and L_{d2} --- dry extension at the leading and tailing electrode, respectively.

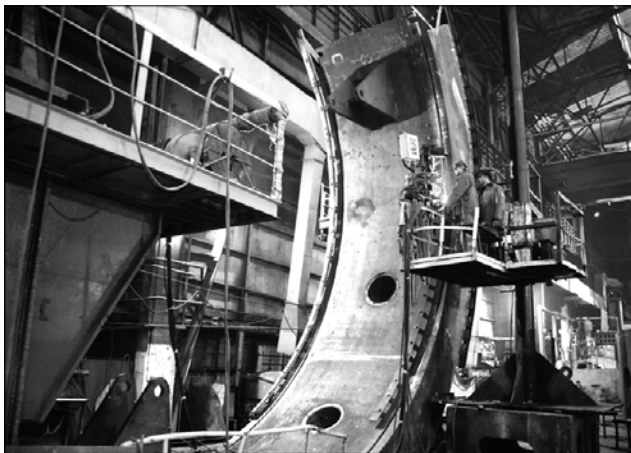


Figure 3. Working moment of ESW of standard workpiece under workshop conditions

them at a preset level by regulating the electrode feed speed according to the welding zone position.

Maintaining the required values of Δ_2 and Δ_3 in all regions of the weld is a critical operation in ESW with electrode oscillations. This requirement is particularly difficult to meet (because of a poor vision) for an internal electrode. That is why, prior to welding it is necessary to determine Δ_2 and Δ_3 along the length of the joint (with an interval of 300–500 mm) and enter these values into a Table. Utilisation of the Table data makes the control of the welding process much easier.

To practically apply the new machine, representatives of the E.O. Paton Electric Welding Institute trained the Chief Welder's Department specialists and welders of the workshop in the procedure and technology of ESW using the new machine. A special

rig, i.e. model with the full-scale external and internal joints, was equipped for training.

ESW of curvilinear joints on standard billets of supporting rings for oxygen-blown vessels (Figure 3) was performed by the «Azovmash» specialists with technical supervision provided by representatives of the E.O. Paton Electric Welding Institute. Eight welds (four internal welds with edge thickness of 100 mm, and four external welds with edge thickness of 80 mm) with a total length of about 48 m were made using the ASh 115 M machine without the application of the nozzle oscillation mechanism, and one weld with edge thickness of 160 mm and total length of 3 m was made by oscillating the nozzles along the gap. All the actuating mechanisms and control systems of the machine were working without any failures and deviations from the standard. The main process parameters were close to the calculated ones, and were fixed with the information recording system in the form of protocols. Subsequent 100 % ultrasonic inspection of all the welds confirmed the absence of defects in metal of the resulting welded joints.

The ASh 115 M machine for ESW using wire electrodes is the first in series of a new generation of the welding equipment developed by the E.O. Paton Electric Welding Institute of the NAS of Ukraine, which should provide application of ESW in welding production at a higher technical level.

Verification of technological recommendations for ESW of position circumferential butt joints on elements of oxygen-blown vessels using the ASh 115 M machine at the OJSC «Azovmash» proved a high technical level and cost effectiveness of application of the new equipment.

TECHNOLOGY OF MANUFACTURE OF WELDED LARGE-SIZED STIFFENED PANELS AND SHELLS OF LIGHT ALLOYS

The new technology is based on application of both electron beam and also argon-arc consumable-electrode welding, performed at a high speed, in combination with a preliminary deforming of parts being joined. The stiffeners are welded to a thin-sheet element by a double-sided fillet weld with small legs and complete penetration across the stiffener thickness.

As a result, the high accuracy of manufacture of large-sized structures, low level of residual welding stresses and strains, narrow zone of weakening of the parent metal in the near-weld zone, high quality of welded joints are provided.



Panels of 2700 × 760 mm size of aluminium alloy 6063 (3 (2) mm sheet thickness, 2 mm stiffener) manufactured by the new technology using EBW

As compared with widely used milling of thick sheets and hot pressing of panels, the cost of manufacture of panel structures, using the offered technology, is lower, the metal utilization factor is increased greatly in this case and the design opportunities of manufacture of highly-efficient structures are widened.

Application. Ship building (deck substructures, hulls of light ships and partitions), aircraft industry (fuselage, floor), rocketry (fuel tanks), railway industry (car bodies), and also the building of light metal structures.

Contacts: Prof. Lobanov L.M.
E-mail: office@paton.kiev.ua

EXTENSION OF THE LIFE OF METAL SPAN STRUCTURES OF RAILWAY BRIDGES WITH FATIGUE DAMAGE*

V.I. KIRIAN, V.V. KNYSH and A.Z. KUZMENKO
E.O. Paton Electric Welding Institute, NASU, Kiev, Ukraine

Considered are the features of early accumulation of fatigue damage, initiation and development of fatigue cracks in welded components of metal span structures of railway bridges. A high effectiveness of application of high-frequency mechanical peening (HFMP) for extension of residual life of welded joints after accumulation of considerable damage in them, including development of cracks up to 1 mm deep, was established. Methods of retardation have been studied for propagating cracks, and the most efficient of them have been determined, namely inducing compressive residual stresses in the fatigue crack propagation path by applying local heating of the metal; placing a high-strength bolt in the drilled-out hole near the crack tip; repair of the metal zone damaged by the fatigue crack using welding with HFMP.

Keywords: metal span structures, railway bridges, fatigue cracks, welded joint, high-frequency mechanical peening, extension of fatigue life

Rated operating life of metal span structures of railway bridges is equal to 80–100 years. Fatigue strength analysis of their main (load-carrying) elements is performed proceeding from limited endurance based on $2 \cdot 10^6$ cycles of alternating load. In this case it is taken into account that one load cycle of the span structure corresponds to passage of one echelon.

On the other hand, as indicated by the experience of operation, fatigue cracks initiate much earlier than after 1–7 years and in those elements and welded joints, in which they were not anticipated and which were not analyzed for fatigue [1]. They arise the most often in welded span structures, in which vertical stiffeners, gusset plates and transverse beams are welded to the web of the beam (Figure 1).

The main causes for early accumulation of fatigue damage, initiation and propagation of fatigue cracks are due to the design shortcomings of typical span structures. They include selection of the design of welded components similar to the riveted ones without allowing for the specific features of welding technology characterized by a higher rigidity of the joints and formation of residual stresses; use of upper girths of a considerable width (420–620 mm), through which the load from train passage is transferred to the structure; irrational arrangement of the longitudinal and transverse ties to the main beam webs; connection of vertical stiffeners with the tensioned girths through split keys.

All this led to a considerable eccentricity of load transfer from the rails to the main beams, development of additional local stresses in the span structure ele-

ments and their vibration. Vibration frequency and levels of additional stresses are determined by the train speed and Q -factor (qualitative characteristic of the resonance properties of the vibratory system) of the component. High-frequency component of stresses due to element vibration is superposed on the secondary low-frequency stresses. Bi-frequency, and in the general case, poly-frequency load essentially lowers the cyclic fatigue life. Therefore, in order to ensure the design operating life of span structures of railway bridges improvement of their design is necessary, i.e. prevention of appearance of inadmissible additional local stresses and vibrations.

This work is devoted to consideration of the methods of life extension of operating span structures of railway bridges with fatigue damage of different degrees and propagating fatigue cracks.

Over the last years a lot of attention has been given to high-frequency mechanical peening (HFMP) of welded joints as one of the most promising methods of improvement of their fatigue strength. This method

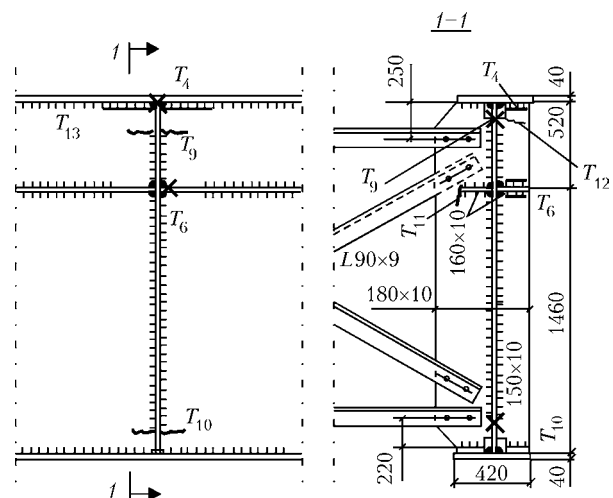


Figure 1. Sites of fatigue crack initiation in the elements of typical span structures of railway bridges designed in 1960–1970s (Projects 541 and 821). Designation of crack types by letter T with a subscript is in compliance with recommendations of [2]

* The paper was prepared by the results of fulfillment of the purpose-oriented integrated program of NASU «Problems of residual life and safe operation of structures, constructions and machines» (2004–2006).



Figure 2. Equipment of 0.3 kW power for HFMP of welded joints of metal structures: 1 — manual tool with a piezoceramic radiator; 2 — ultrasonic generator; 3 — computer

is quite well-studied, the main regularities of improvement of cyclic fatigue life and endurance limit of welded joints by HFMP strengthening immediately after their manufacturing have been established, and its advantages have been demonstrated compared to other known techniques of plastic deformation of the metal surface [3]. The main advantages of HFMP technology allowing its broad application for extension of the residual life of metal structures in service, are high efficiency and cost-effectiveness, compactness and mobility of equipment, treatment in any position in space (Figure 2). It is important that in order to improve the fatigue resistance of welded joints it is sufficient to treat a narrow zone of transition from the weld metal to the base material 4–7 mm wide. The main factors of increasing the cyclic fatigue life and endurance limit of welded joints at HFMP are as follows: inducing compressive residual stresses in the transition zone; lowering the coefficient of concentration of working stresses α_σ ; strain ageing of the surface layer of metal.

Given below are the results of investigation of the effectiveness of HFMP application to improve the cyclic fatigue life of welded joints of metal structures,

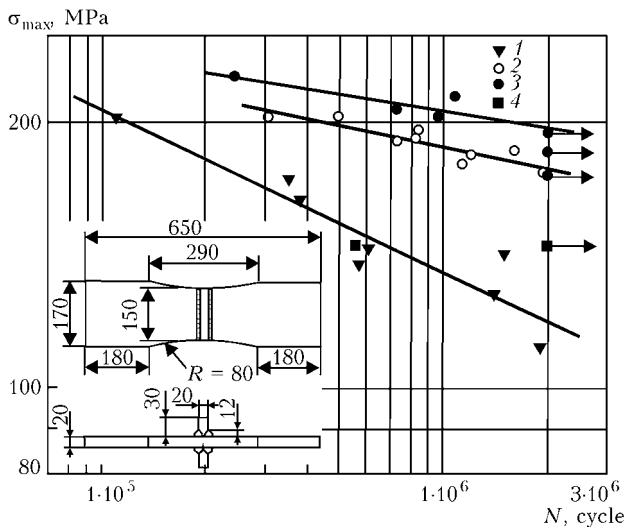


Figure 3. S–N curves of tee welded joints (St3sp steel): 1 — initial as-welded condition; 2 — HFMP directly after welding; 3 — HFMP after operation up to 50 % of fatigue life; 4 — HFMP after operation up to 95 %

which are in operation and which already have a significant level of accumulated fatigue damage in the stress raiser zones, and in individual cases fatigue cracks up to 1 mm deep [4].

Fatigue testing was conducted at from-zero cycle of alternating loading ($R_\sigma = 0$) on samples of steel St3sp (killed) with transverse stiffeners welded with complete penetration by manual electric-arc welding. The first series of samples was in the initial as-welded condition, the second was treated by HFMP immediately after welding, the third was treated by HFMP after cyclic loading and accumulation of fatigue damage in the welded joints on the level of approximately 50 % of those which correspond to crack initiation.

The obtained fatigue curves (Figure 3) demonstrate an increase of fatigue life of samples of the third series (filled circles) tested in the stress range $\sigma_{max} = 175\text{--}225$ MPa in comparison with samples of the first (filled triangles) and second (light circles) series by an order of magnitude and more than 2 times, respectively. In this case the endurance limits based on $2 \cdot 10^6$ cycles also increased compared to the initial condition by 66 and 50 %. Increase of the stress level $\sigma_{max} = 175\text{--}225$ MPa at treatment for 50 % fatigue life and testing of third series samples is related to the fact that even after accumulation of about 95 % of fatigue damage and HFMP the fatigue life turned out to be higher than the norm value — $2 \cdot 10^6$ cycles (filled squares in Figure 3). Such a high (close to the yield point) stress level promoted an essential plastic deformation of the metal near the raiser and formation of residual compressive stresses (as at overload). As a result of this additional effect fatigue resistance of welded joints increased after operation and HFMP (filled circles in Figure 3) compared to those treated

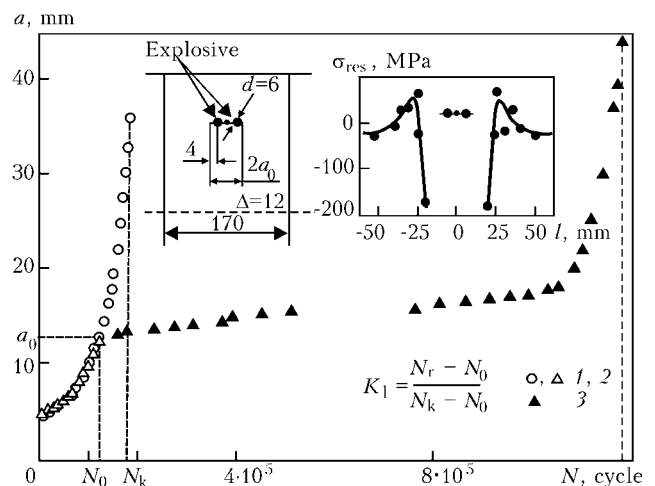


Figure 4. Dependence of the fatigue crack half-length ($a = a_0 + \Delta a$) on the number of cycles of alternating load in the steel 10KhSND sample at retardation of fatigue crack by inducing residual compressive stresses in its propagation path by local explosion treatment: a_0 — crack half-length by the start of retardation; N_0 — number of cycles up to the start of crack retardation; N_k — number of cycles up to sample fracture in initial condition; N_r — number of cycles up to sample fracture under the condition of crack retardation; 1, 2 — initial condition; 3 — application of local explosion treatment



Results of experimental studies of the effectiveness of the fatigue crack retardation processes in flat samples of steel Vst3sp ($2a_0 = 76$ mm, $R_\sigma = 0$, $\sigma_{\max} = 150$ MPa)

Sample No.	Crack retardation method	Fatigue life N , cycle	Coefficient of fatigue life extension K_1
1	Initial condition	35000	
2	Drilling out a hole of 23 mm dia. near the crack tip	52200	1.45
2'	Same with subsequent work hardening of hole surface by HFMP	84500	2.41
3	Placing a high-strength bolt of 22 mm dia. into the hole with 20 tf tension	730,550	20.87
4	Local explosion treatment	277,700	7.93
5	Local heating	668,300	19.09
6	Crack repair by welding	1,450,000	41.43
6'	Same and HFMP	$> 2 \cdot 10^6$	

by HFMP directly after welding (light circles in Figure 3).

An essential increase of fatigue life after HFMP is also observed in welded joints of metal structures, which have fatigue cracks up to 1 mm deep. Fatigue life of the tee joint of 10KhSND steel in as-welded condition has reached approximately 300,000 cycles of stress alternation ($\sigma_{\max} = 220$ MPa, $R_\sigma = 0$). Due to HFMP of the zone of transition from the metal of the fillet weld to the base metal, in which the fatigue crack initiated (up to 1 mm deep), sample fatigue life exceeded $2 \cdot 10^6$ cycles.

Load-carrying elements of span structures of railway bridges with fatigue cracks, which are developing and have considerable dimensions, were studied at different methods of their retardation. For comparison purposes, known techniques currently used in practice, were considered simultaneously with the new ones, in particular, hole drilling in the fatigue crack tip with or without placing a high-strength bolt into it to induce compressive stresses.

Large-scale flat samples for investigation of steels 10KhSND and Vst3sp 12 and 14 mm thick, respectively, had an initial central through-thickness fatigue crack of $2a_0$ length. After application of the methods of fatigue crack retardation shown in the Table, the cyclic loading of the samples was conducted in a soft mode (maintained by constant force) at from-zero cycle asymmetry ($R_\sigma = 0$) and maximum stress $\sigma_{\max} = 150$ MPa. The plotted dependencies of crack growth on the number of cycles up to complete fracture of the samples were used to determine the coefficient of fatigue life extension K_1 (Figure 4, Table).

From the considered methods inducing compressive fatigue residual stresses in the path of fatigue crack propagation is of interest. This is achieved by short-term local heating of the metal up to the temperature of about 350°C at a short distance from the crack tip ($K_1 = 19$). For specific cases the technological parameters of heating are determined by solving the thermoelasticity problem provided maximum com-

pressive stresses are induced in the path of fatigue crack propagation. Quite effective ($K_1 \approx 21$) is placing a high-strength bolt with 20 tf tension into the hole near the fatigue crack tip. At $K_1 > 41$ a crack can be repaired by welding, and fatigue life of repair welds after HFMP is higher than the standard one of $2 \cdot 10^6$ cycles.

Produced results of experimental investigation allow recommending the HFMP technology developed at the E.O. Paton Electric Welding Institute for wide application for extension of the life of welded metal structures, the operating life of which has reached the specified value (up to 1 mm fatigue cracks have developed) or is close to it. Restored fatigue life after HFMP can rise up to the specified life of $2 \cdot 10^6$ cycles depending on the level of acting alternating stresses in operation.

The most effective methods of retardation of fatigue cracks, which are propagating, is inducing residual compressive stresses in the path of their propagation using local metal heating, drilling out holes near the crack tip and placing high-strength bolts with 20 tf tension and crack repairing by welding and HFMP of the transition zone from the weld metal to the base material.

Proceeding from the conducted investigations for «UkrSaliznytsa» «Recommendations on reinforcement, repair and extension of the life of solid-wall welded span structures» have been complied.

1. Mirolyubov, Yu.P., Panin, E.M., Frolov, V.V. et al. (1983) Fatigue cracks in solid web spans. In: *Problems of design and service of artificial constructions*. Leningrad: V.N. Obraztsov IIZhDT.
2. (1990) *Recommendations on inspection and strengthening of welded span structures in service*. Moscow: MPS, GUP NII-mostov LIIZhTA.
3. Lobanov, L.M., Kirian, V.I., Knysh, V.V. et al. (2006) Improvement of fatigue resistance of welded joints in metal structures by high-frequency mechanical peening (Review). *The Paton Welding J.*, **9**, 2–8.
4. Lobanov, L.M., Kirian, V.I., Knysh, V.V. (2006) Increase of life of welded metal structures by high-frequency mechanical peening. *Fizyko-Khimichna Mekhanika Materialiv*, **1**, 56–61.



TECHNOLOGICAL FEATURES OF THE PROCESSES OF AUTOMATED ARC WELDING IN REPAIR OF LARGE-SIZED TANKS*

V.M. ILYUSHENKO, N.M. VOROPAJ and V.A. POLYAKOV
E.O. Paton Electric Welding Institute, NASU, Kiev, Ukraine

Comparative analysis has been performed of the processes of automated gas-shielded, self-shielded flux-cored wire arc and submerged-arc welding for repair of metal structures of large-sized tanks. Considered are the technological features of performance of various types of welds, as well as principles of development of specialized site welding machines. Experience of and prospects for application of new developments are described.

Keywords: automated arc welding, low-alloyed steels, butt welds, overlap joints, tee joints, shielding gas, self-shielded flux-cored wire, site welding machine, tanks

Modern welded structures of large-sized tanks are critical constructions with high technical requirements to their leak-tightness, safety and operating lives. Analysis of performance of these structures shows that in site joints with horizontal and vertical welds the most common defects are crack-like damage, corrosion wear and loss of geometrical shape. Individual sections of the tanks are exposed to deformations due to skewing and non-uniform settlement, which requires their restoration or complete replacement of sections [1].

Up to now coated-electrode manual arc welding and mechanized gas-shielded welding were mostly used for current repair and overhauling of the tanks. These processes are characterized by low efficiency and quality of welded joints. Evaporation of petroleum products in defective locations leads to considerable material expenses. In view of an abrupt increase of the cost of new tank construction great attention should be given to restoration of performance of the existing fleet. Most often it is necessary to repair or replace the damaged sections of the bottom and adjacent parts of the vertical wall.

For the bottom, instead of the traditional feeding of individual sheets inside the tank, it is proposed to feed a continuous strip, which has already been butt welded from separate sheets [2]. Sections of the required length are made from this strip. Thus, all the girth joints are made as butt joints, and overlap joints are located on one line. In this case, conditions are in place for automation of welding technology.

This paper deals with the technological features of highly efficient means of automated arc welding of

butt and fillet welds in different positions in repair of large-sized tanks.

Types of welds and joints of tank structures. Various tanks are used in local and foreign practical operations for oil and petroleum product storage. These primarily are vertical cylindrical tanks of up to 50,000 m² capacity. Low-alloyed steels of different grades are used for tank wall and bottom sections, depending on the volume and type of the products, service features and climatic conditions. For oil tanks of up to 20,000 m³ capacity, steel 09G2S is used as the base metal in the four lower girths of the wall [1], and in those of 30,000 and 50,000 m³ capacity --- steel of 16G2AF grade. The range of thicknesses of low-carbon low-alloyed steels is equal to 10–40 mm.

Based on comprehensive consideration of the design and analysis of operation of typical tanks, four kinds of welds and joints can be noted, namely horizontal butt welds on the vertical plane of the wall; vertical butt welds on the vertical plane of the wall; fillet welds in the downhand position of the overlap joint on the bottom; fillet welds, which connect the horizontal bottom with the vertical wall (downhand position, tee joint).

Depending on the thickness of base metal sheets one-sided or two-sided edge preparation is used in welding horizontal and vertical butt welds on the tank walls. Tee joint of fillet welds of the bottom with the vertical wall on up to 16 mm thick metal is welded without edge preparation, and that of thicker metal --- with two-sided edge preparation.

Selection of the processes of automated arc welding. Technological capabilities of the processes of automated CO₂ arc welding with solid electrode wire Sv-08G2S and process of self-shielded flux-cored wire PP-AN19N [3] were evaluated for making of horizontal and vertical butt welds on the vertical plane. Automated self-shielded flux-cored wire welding provides the highest efficiency at satisfactory weld formation. With this welding process it is necessary to additionally feed carbon dioxide gas into the weld pool zone in site to prevent weld metal porosity. Self-shielded flux-cored wire PP-AN19N provides a high arcing sta-

* The paper was prepared by the results of fulfillment of the purpose-oriented integrated program of NASU «Problems of residual life and safe operation of structures, constructions and machines» (2004–2006).



Mechanical properties of joints of low-alloyed steel 09G2S 10–40 mm thick

Metal thickness, mm	Weld type	Number of passes	KCU, J/cm ² (not less than) at T, °C							
			Weld center				HAZ			
			+20	-20	-40	-60	+20	-20	-40	-60
10	Horizontal butt (one-sided)	2	160	130	120	60	130	100	90	50
15	Same	4	150	120	110	50	120	105	80	45
25	Horizontal butt weld (two-sided)	6 + 6	140	110	105	55	140	105	75	40
40	Same	9 + 9	130	105	90	40	120	95	80	35
40	Vertical butt	2	130	100	80	35	120	90	70	35

bility, medium-drop transfer of electrode metal and easy separation of the slag crust.

Tentative mode of automated self-shielded wire arc welding is as follows: $d_{\text{wire}} = 3.0$ mm; $I_w = 320$ – 380 A; $U_a = 24$ – 28 V; $v_w = 16$ (horizontal welds) and 3 m/h (vertical); $Q_{\text{CO}_2} = 16$ – 20 l/min. Number of passes of horizontal welds depending on metal thickness was equal to 2 (for $\delta = 10$ mm) and 4 ($\delta = 15$ mm) in one-sided welding. For thick metal two-sided welding is rational, in which the number of passes corresponds to 6–7 at $\delta = 25$ mm and 9–10 at $\delta = 40$ mm. Such modes promote a uniform formation of multilayered weld without defects of the type of pores, cracks or oxide inclusions.

Mechanical properties of welded joints of low-alloyed steel 09G2S 10–40 mm thick at temperatures of $+20$ – -60 °C were studied (Table). Welded joints with horizontal and vertical welds made with self-shielded flux-cored wire of PP-AN19N type in optimum modes meet the existing technical requirements for building metal structures for similar purposes. Mechanical properties of welded joints with horizontal welds are, as a rule, better than those of welded joints with vertical welds made in one pass. Increase of base metal thickness from 10 up to 40 mm somewhat lowers the mechanical properties of the joints at room and minus temperatures.

The need for automation of downhand welding of fillet welds in welded joints is urgent, considering that complete replacement of the bottom panel is often required. As shown by investigations, it is rational to perform these technological operations by automated submerged-arc welding with AN-60SM flux and Sv-08GA electrode wire of 3.0 mm diameter [4].

In order to select effective methods of making fillet welds which join the tank horizontal bottom with the vertical wall, the technological capabilities of three processes of automated arc welding were studied, namely submerged-arc, self-shielded flux-cored wire and gas-shielded solid wire. Considering that self-shielded flux-cored wire is 4–5 times more expensive than the solid wire, automated submerged-arc welding and welding in shielding gas mixtures were selected for further testing.

Experiments on submerged-arc welding of low-alloyed 09G2S steel 10–30 mm thick were made using

AN-66 flux and Sv-08G2S electrode wire of 2.5 mm diameter. Welding modes are as follows: $I_w = 380$ – 420 A; $U_a = 28$ – 30 V; $v_w = 30$ – 38 m/h; electrode wire extension ---- 25 mm; welding position ---- downhand.

Technique of welding tee joints on the metal of the above thickness envisaging edge opening (at up to 16 mm metal thickness) and two-sided non-symmetrical edge opening with the angle of $(45 \pm 5)^\circ$ (at more than 16 mm metal thickness) has been optimized. The optimum angle of electrode wire inclination to the horizontal plane was selected depending on base metal thickness and groove shape. To ensure the necessary weld leg in the range of 6–12 mm welding was performed in 1–4 passes from each side of the tee joint. Compared to coated-electrode manual arc welding, the developed technology of automated submerged-arc welding allowed increasing the process efficiency 3–4 times.

Mechanical properties of welded joints on low-alloyed 09G2S steel were studied. The obtained results of mechanical testing meet the requirements of SnIP 3.03.01-87 «Load-carrying structures and frame fillings». Results of mechanical testing of impact toughness of welded joints of 09G2S steel 20 mm thick at different temperatures are as follows: at the temperature of -20 °C — 90–110 J/cm²; -40 °C — 75–90; -60 °C — 65–100. Considering the possible difficulties of submerged-arc welding application in site associated mainly with flux feeding and removal, technology of making such welds with solid wire of 2.0–2.5 mm diameter in a mixture of Ar + 20 % CO₂ gases is currently being optimized.

Some techniques of controlling the characteristics of the processes of automated arc welding of horizontal and vertical welds have also been studied, namely by increasing electrode extension, modulation of current and electrode wire feed rate. Self-shielded flux-cored wire PP-AN19N and electrode wire Sv-08G2S in combination with carbon dioxide gas were used as welding consumables. To perform automatic arc welding with an increased electrode extension the current-supplying nozzle and electrode wire feed mechanism were upgraded in site welding AD-333M machine. As a result it ensured adjustment of electrode extension in the range of 40–120 mm with up to 500 m/h rate of electrode wire feed.

It is established that as a result of increase of electrode extension to 80–100 mm the deposition factor



increases by 20–30 %, and the HAZ decreases by the same value. No significant change of weld metal composition, lowering of the reliability of protection of the weld pool or mechanical properties of welds was observed. It should be noted that simultaneously with the noted positive factors the working range of current, in which the necessary stability of the welding processes is preserved, is somewhat reduced at increase of electrode extension.

When studying the influence of current modulation on the process of arc welding the following technique was used: at a constant rate of electrode wire feed the welding current was switched off momentarily [5]. Optimum values of the duration of pulses and pauses were tentatively equal to 1.2 and 0.5 s, respectively. At a shorter duration of the pulses the process only slightly differed from the stationary mode. In all the cases pores and nonmetallic oxide inclusions were observed in the weld metal. For this reason use of an increased electrode extension and current modulation is not rational in site.

The essence of the process of arc welding with a controllable transfer of electrode metal consists in imparting to the electrode a motion pulse directed towards the pool, under the impact of which the molten metal drop at the electrode tip acquires considerable kinetic energy [6, 7]. The latter at an instantaneous stopping of the electrode is capable of causing a forced separation of the drop or guarantee its contact with the weld pool metal. The force of inertia should exceed the equivalent force of electromagnetic origin and surface tension force. The main characteristic parameters of the process of welding with pulsed feed of electrode wire are step, repetition frequency and duration of the feed pulses and pauses. As a result of the conducted testing, optimum values of step (0.5–3.0 mm) and frequency of pulses (10–50 s⁻¹) were selected for making welds in different positions.

Development of site welding machines for repair of tank structures. Considering the specific require-

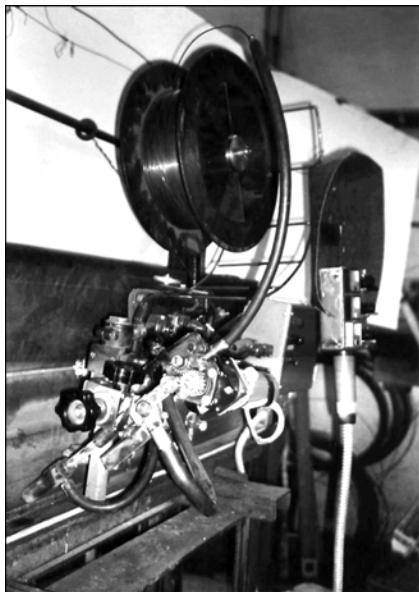


Figure 1. Test sample of a site machine for fillet welding

ments to site equipment — small weight and overall dimensions, capability of mounting directly on the welded item, optimum automation level, diverse components of light-weight machines used in special equipment for automated arc welding were tested in repair of metal structures. Such components include, primarily, travel carriage, electrode wire feed mechanism, process control schematic and arc power source. For horizontal butt welds the technique of automatic welding with partial forced weld formation was proposed. The essence of this technological procedure consists in that the welding arc runs in the zone limited by base metal (or forming device) from one side, and copper water-cooled shoe from the other side. The pool is open from two sides — from the top and the front, while the angle of inclination of the nozzle of electrode wire feed mechanism can vary in the range of $\pm 30^\circ$.

Specialized site rail machine of AD-330M type was developed for implementation of the above technique of automatic arc welding of horizontal butt welds. The travel mechanism of the machine is a compact three-wheel carriage, which allows making curvilinear welds with minimum radius of curvature (up to 1000 mm). The mechanism of electrode wire feed and electric circuit of the machine enable remote control of the mode parameters. The machine moves along the tank wall over a guide rail. The technological capabilities of the tested welding arc power sources (VDU-504, VDU-506, VDU-601 and VS-600M) are practically equivalent in welding with solid electrode wire and flux-cored wire.

For vertical butt welds made by automated self-shielded flux-cored wire arc welding with forced formation, both the currently available rail machines of A-1381 type and upgraded by us machine of AD-333M type can be used, depending on sheet thickness.

For automation of welding of fillet welds in overlap joints (bottom) and welds joining the bottom to the vertical wall, R&D work is performed on development of specialized tractor-type machines based on unified components, which were successfully used in machines of AD-330M and AD-333M type. A feature of these machines is their compactness, small dimensions and weight, as well as the possibility of moving over the surface of welded sheets, and reliably following the welded joint line. In particular, in the machine for welding overlap joints, special attention is given to ensuring a reliable maintenance of the electrode wire position relative to the joint line. In the machine for making fillet welds selection of the travel mechanism of magnetic roller type is due to the need to place the machine directly on the vertical wall, as the bottom edge, which extends outside is not more than 40–50 mm, and cannot be the base for machine displacement.

Figure 1 shows a test sample of the machine for fillet welding, which connects the bottom edge with the tank vertical wall.

Practical result. The technology developed by the E.O. Paton Electric Welding Institute of NASU to-

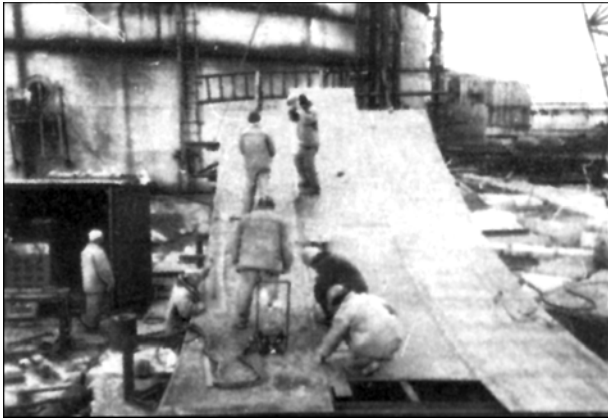


Figure 2. Automatic submerged-arc welding of mounting blocks in repair of a tank in CJSC LINOS (Lisichansk)

gether with «Ekorembud» Company (Rovno) was used to repair a cylindrical tank of 20,000 m³ capacity in Lisichansk of Lugansk district. The vertical wall had to be replaced along the entire tank height. This section was equal to almost 25 % around the case perimeter. Under the conditions of tank repair two processes of automated arc welding were used, namely submerged arc --- for joining individual sheets into mounting blocks, and self-shielded flux-cored wire arc welding --- for horizontal welds on a vertical plane in mounting the blocks on the vertical wall. In down-hand submerged-arc welding for metal thickness of 9–12 mm, electrode wire Sv-08GA of 5 mm diameter and AN-60SM flux were used. Welding was performed by ADF-1002 tractor with VDU-1201 power sources in the following mode: $I_w = 720\text{--}850\text{ A}$; $U_a = 30\text{--}38\text{ V}$; $v_w = 20\text{--}28\text{ m/h}$. Sound formation of the weld reverse side was achieved using a flux-copper pad. To replace the tank wall, it was necessary to weld six individual blocks in a special fixture (Figure 2).

Automatic arc welding of horizontal butt welds by self-shielded flux-cored wire with semi-forced formation of the deposited metal was conducted either by the site welding machine AD-330M with remote control, or VDU-506 power source. The reverse side of the horizontal welds was formed on a copper backing, which had a groove of the respective geometry. The mode of welding the main welds is as follows: $I_w = 360\text{--}380\text{ A}$; $U_a = 24\text{--}26\text{ V}$; $v_w = 12\text{--}20\text{ m/h}$. At metal thickness of 9 and 12 mm welding was performed in two and three passes, respectively (Figure 3).

Successful performance of repair work on a tank of 20,000 m³ capacity allowed application of the technology and equipment for automatic arc welding also in construction of new tanks, in particular, in Smiga of Rovno district and Nadvornaya of Ivano-Frankovsk district [8]. At the first stage mainly the block method of mounting was used. The tank wall was divided into three tiers of blocks by height and 5–10 blocks across the width of each tier. Sheet assembly into blocks and their automatic submerged-arc welding were performed in a rotary fixture with ADF-1002 machine. Technology of automatic multilayer arc welding in AD-330 machine with self-shielded flux-cored wire PP-AN19N with pool additional protection by CO₂



Figure 3. Automatic welding of a horizontal weld on a tank wall by AD-330M machine

and partial forced formation of the welds was used for making horizontal butt welds on the wall vertical surface. For vertical butt welds the technology of welding with self-shielded wire PP-AN19N with forced metal formation is recommended. Depending on sheet thickness and shape of edge preparation, welding is performed by rail machine of AD-333M type or railless machine of A-1150 type.

The advantages of the above technologies of automated arc welding are as follows:

- ability of direct viewing of the arcing zone;
- improvement of the conditions of weld pool protection, which is important in site;
- reduction of the number of passes in welding of thick metal;
- ensuring the correct geometry of weld formation;
- increase of welding efficiency 1.5–2 times compared to welding under the conditions of free weld formation.

Considering the need for construction of large-capacity of oil tanks (50–70–100 ths m²), the method of sheet-by-sheet mounting of such metal structures appears to be promising. The technologies of automated arc welding will certainly become widely accepted.

1. (1997) *Welded building structures. Types of structures*. Ed. by L.M. Lobanov. Vol. 2. Kiev: PWI.
2. Barvinko, Yu.P., Golinko, V.M., Barvinko, A.Yu. (1999) New technologies of restoration of the performance of vertical cylindrical tanks for oil and petroleum product storage. *Svarshchik*, 4, 6–8.
3. Pokhodnya, I.K., Suptel, A.M., Shlepakov, V.N. et al. (1980) *Flux-cored wires for arc welding*: Catalogue-reference book. Kiev: Naukova Dumka.
4. Polyakov, V.A., Tokarev, V.S., Goncharov, I.A. et al. (2003) Experience of application of AN-60SM flux in welding of tanks. In: *Proc. of Math. Sci.-Techn. Seminar on Advanced Welding Technologies in Industry* (Kiev, May 20–22, 2003), 105–106.
5. Voropaj, N.M., Ilyushenko, V.M., Lankin, Yu.N. (1999) Features of pulsed-arc welding with synergic control of mode parameters. *Avtomatich. Svarka*, 6, 26–32.
6. Voropaj, N.M. (1996) Parameters and technological capabilities of arc welding with pulsed feed of electrode and filler wire. *Ibid.*, 10, 3–9.
7. Voropaj, N.M., Ilyushenko, V.M. (2006) Tendencies of development of combined and hybrid methods of arc and plasma welding. In: *Proc. of Sci.-Techn. Seminar on Welding and Related Processes in Industry* (Kiev, April 12, 2006). Kiev: Ekotekhnologiya, 3–6.
8. Ilyushenko, V.M., Polyakov, V.A., Lashkevich, V.R. et al. (2003) Automated arc welding of butt joints in sheet-by-sheet method of tank mounting. In: *Proc. of Int. Conf. on Current Problems of Welding and Life of Structures* (Kiev, Nov. 24–27, 2003), 28–29.



EFFECT OF STRUCTURAL-PHASE STATE OF HIGH-STRENGTH WELD METAL ON PROPERTIES OF WELDED JOINTS IN HARDENING STEELS

E.L. DEMCHENKO and D.V. VASILIEV

E.O. Paton Electric Welding Institute, NASU, Kiev, Ukraine

It is established that the high-strength ($\sigma_t \geq 1000$ MPa) austenitic-martensitic weld metal has a positive effect on the kinetics of formation of structure and properties of HAZ of the welded joints in alloyed steels made without preheating and postweld heat treatment. Offered is the composition for the high-strength weld metal using flux-cored wire welding, which provides high cold crack and delayed fracture resistance of the welded joints.

Keywords: arc welding, hardening steels, welded joints, high-strength steels, HAZ metal, structure, welding consumables

Handling of the problem of producing quality welded joints in high-strength alloyed steels with properties equal to those of the base metal involves certain difficulties. High-strength steels ($\sigma_y \geq 800$ MPa) are characterised, as a rule, by an increased sensitivity to formation of brittle hardening structures in the HAZ metal of a welded joint under the effect of the thermal cycle of arc welding. Unfavourable structural transformations combined with behaviour of diffusible hydrogen lead to formation of cold cracks during the welding process. Increased sensitivity of the welded joints in hardening steels to delayed fracture often causes a substantial decrease in operational reliability of welded structures [1–4]. Modern engineering makes use of such technological operations in welding of hardening steels as preheating and postweld heat treatment to provide a favourable structure of the HAZ metal of a welded joint and reduce the level of residual stresses, as well as to impart the welded joint the required properties. However, there are cases, especially in welding of large-size structures, where the preheating and postweld heat treatment operations are absolutely impossible to perform [5]. Then in such cases the use is made of high-alloy austenitic welding consumables.

The authors of studies [6, 7] note a positive effect of the high-alloy austenitic weld metal on the process of formation of structure of the HAZ metal in high-strength steel welded joints. The latter is attributable to formation of a more favourable stressed state in a welded joint with the austenitic weld, as this state promotes displacement of the major mass of martensite transformation to a region of increased temperatures (> 250 °C), and improvement of properties of martensite formed in the HAZ metal as a result of its self-tempering.

It is reported [3] that temporary stresses in welded joints with different types of the weld metal differ in value and kinetics. Elasto-plastic strains formed in a joint before the beginning of martensite transformation in the HAZ metal have a substantial effect on

the kinetics of transformation of overcooled austenite within the said zone, and, as a result, on its final structure and properties. It was established that in joints with the austenitic weld the level of tensile stresses formed by the moment of cooling of the HAZ metal to a temperature of 500 °C is very high (120–140 MPa), which causes the austenite transformation to start in this zone at a higher temperature ($M_s = 460$ °C), compared with a joint with the ferritic-pearlitic weld ($M_s = 340$ °C). The stress level in this case is 60–80 MPa. Mostly upper bainite and temper martensite are formed in the HAZ metal of welded joints with the austenitic weld, which explains high resistance of the welded joints to cold cracking. However, substantial drawbacks of the austenitic weld metal are its low strength, compared with the base metal, and high cost. Therefore, this method can be applied only at the absence of requirements for ensuring full-strength welded joints. Achievement of the strength of the welded joints equal to that of the base metal by reinforcing the weld through depositing extra metal (weld reinforcement in this case amounts to 40 % of steel thickness) leads to a considerable increase in the amount of the deposited metal [5].

As an alternative to the technology for welding alloyed high-strength steels without preheating and postweld heat treatment, study [8] suggests a method providing for the use of the welds, the alloying system and properties of which are similar to chrome-nickel-molybdenum austenitic-martensitic steels (or steels of the transition grade). Decomposition of overcooled austenite ($\gamma \rightarrow \alpha_m$) in such steels occurs at lower temperatures compared with the temperature of the end of structural transformations in HAZ of the base metal ($T_m < 200$ °C). The effect of the austenitic-martensitic weld on formation of structure of the HAZ metal in a welded joint was assumed to be similar to the effect of the austenitic weld. In addition, such welds in the as-welded state, unlike the austenitic ones, should acquire a sufficient strength ($\sigma_t = 900$ –1200 MPa). As reported [9–11], mechanical properties of austenitic-martensitic steels depend to a considerable degree upon the proportion of their main structural components, e.g. martensite, retained austenite and δ -ferrite.

In this connection, the purpose of the study was to investigate the effect of the structural-phase state of the austenitic-martensitic weld metal on properties of the welded joints in high-strength alloyed steels in welding without preheating and postweld heat treatment. Experimental cast steel of the 03Kh12N8M2GST type, which is characterised by the required level of mechanical properties: $\sigma_{0.2} = 780\text{--}820$ MPa, $\sigma_t = 1000\text{--}1050$ MPa, $\delta \geq 16\%$, $\psi \geq 35\%$, and $KCU_{+20} = 100$ J/cm², was chosen for the investigation as a basic prototype of the weld metal. According to the metallography data, structure of the steel in the initial state is a mixture of lath (packet) high-alloy substitution martensite ($HV_{0.05}$ 3200 MPa) and retained austenite (Figure 1). Low-carbon (0.03 wt.% C) high-alloy substitution martensite in steel of the chosen composition has the form of rectangular packets of laminae (laths) located along the boundaries of the initial austenite grains. Thickness of laminae in a packet varies from 0.3 to 2.3 μm . According to microstructural examinations, crystalline grains are mostly of an irregular shape. A band, i.e. mid-rib, was detected in the largest of them, this band being composed of clusters of twins with a characteristic dislocation structure of the crystalline grains.

The methods of high-temperature vacuum metallography and dilatometry were used to investigate the kinetics of phase $\gamma \rightarrow \alpha_m$ transformation. Special specimens of the steel studied were heated in a vacuum chamber with a residual air pressure of 0.013–1.3 Pa at a rate of 100 °C/s to 1100 °C, and held there for 20 s to complete austenisation. After that the specimens were cooled at a rate of 4–5 °C/s. That reproduced conditions close to the thermal cycle of one-pass fusion arc welding.

Structural changes in the steel studied were examined during the cooling process. Microstructures resulting from vacuum etching in cooling of the specimens from 1100 °C to room temperature ($\gamma \rightarrow \alpha_m$ transformation) are shown in Figure 2.

Investigations of mechanical properties and results of metallography of the steel studied, which was chosen as a prototype, show that the high-alloy martensite should be the base of the structure of the austenitic-martensitic weld metal of a chrome-nickel-molybdenum composition. Low-carbon high-alloy martensite ($HV_{0.05}$ 2800–3200 MPa) provides a high strength ($\sigma_t = 1000\text{--}1200$ MPa) of the austenitic-martensitic weld metal, the level of which does not decrease too much provided that the total content of other structural components (retained austenite and δ -ferrite) is not in excess of 25 wt.%. If the weight content of martensite in the weld is higher than 90 %, ductile properties and toughness will substantially decrease, the strength values being $\sigma_t = 1200\text{--}1300$ MPa and $\sigma_{0.2} = 1000\text{--}1100$ MPa. The weld metal with such properties is hardly suitable for the use because of a low brittle fracture resistance. For this reason, the optimal content of martensite should range from 75 to 90 wt.%.



Figure 1. Microstructure of steel 03Kh12N8M2GST (prototype of weld metal) ($\times 500$)

The second phase as to the weight content in the structure studied is austenite (retained after completion of $\gamma \rightarrow \alpha_m$ transformation), as well as an insignificant amount of δ -ferrite. According to the literature data, retained austenite has a significant effect on mechanical properties of steels close in composition to the chosen weld metal, particularly on their ductile properties. It is reposted in studies [12–14] that this effect may show up in a diverse manner and depends upon the composition of austenite, its morphology, fine structure and stability, as well as upon the composition and properties of the martensitic matrix surrounding it. The authors of studies [12, 13] emphasise the positive effect of retained austenite on toughness of stainless steels of the transition grade, especially at low temperatures. As shown in [14], retained austenite increases ductility and decreases sensitivity to cracking of this type of cast stainless steels. In such cases the optimal amount of retained austenite is provided both as a result of variation (adjustment) of chemical composition of steel in a range limited by specifications, and as a result of special heat treatment [14, 15].

The effect of the structural-phase state on properties of the chrome-nickel-molybdenum austenitic-martensitic weld metal was evaluated on specimens of the weld metal with preset amounts of retained austenite, which was achieved by varying the ratio of weight contents of the main alloying elements (chromium, nickel, molybdenum and manganese) in the weld metal. Weight contents of other elements (carbon, nitrogen, silicon, sulphur and phosphorus) were kept almost unchanged. Variations of chemical composition of the weld metal were provided by varying the composition of the flux core of an experimental wire (alloying elements were added to it in the form of ferroalloy powders). An experimental flux-cored wire was used to make welded joints in alloyed steel of the 15Kh2N4MDA type.

Specimens were made from the weld metal to evaluate mechanical properties, and specimens treated by special etching to remove surface layers of metal with cold working structures due to machining were prepared to conduct metallographic examinations. The amount of retained austenite in the weld structure was determined by X-ray diffraction analysis using the procedure developed by PWI, which is based on

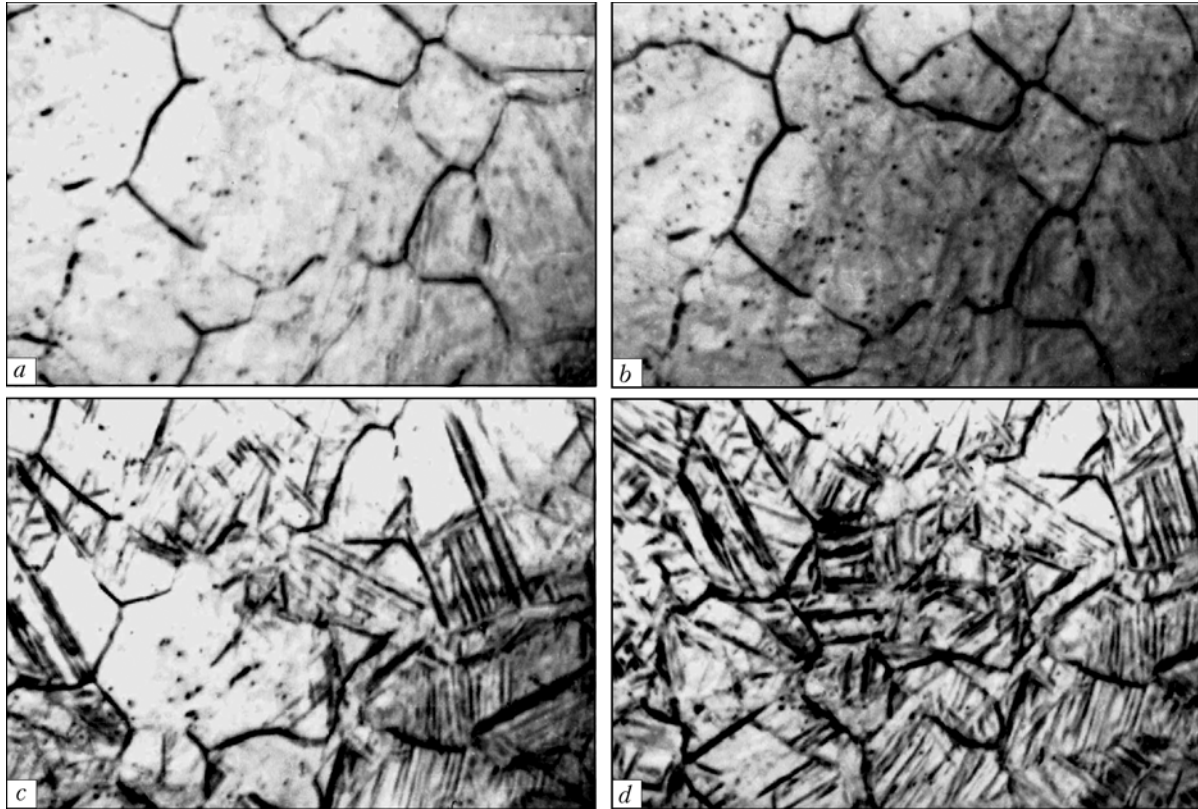


Figure 2. Microstructure of experimental steel after cooling from point A_{c3} to 800 °C (austenite) (a), 430 °C (austenite) (b), 180 °C (beginning of $\gamma \rightarrow \alpha_t$ transformation) (c) and 20 °C (martensite) (d) (high-temperature metallography, $\times 100$)

comparison of the intensities of selected diffraction lines of austenite and martensite.

Dependence of mechanical properties of the weld metal upon the content of retained austenite in it is shown in Figure 3. Analysis of the results shows that ductile properties (elongation, reduction in area and impact toughness) can be improved 1.5–2 times by varying the weight content of retained austenite in structure of the austenitic-martensitic weld metal from 0 to 10 wt.%, the tensile strength σ_t and yield stress $\sigma_{0.2}$ being kept at a sufficiently high level. Further increase in the weight content of retained austenite from 10 to 20 wt.% provides even higher values of

ductility and toughness without decrease in tensile strength ($\sigma_t = 1100$ MPa), the values of yield stress being substantially decreased ($\sigma_{0.2} = 600$ MPa). The effect of retained austenite formed during the $\gamma \rightarrow \alpha_m$ transformation on ductility of high-alloy maraging steels [14] is attributed not only to its initial ductility, but also to increase in ductility at the apex of a crack developing as a result of the $\gamma \rightarrow \alpha_m$ transformation in testing, which leads to a substantial growth of energy intensity of the process of crack propagation. The positive effect of retained austenite on ductility of the chosen type of the austenitic-martensitic weld metal can have a similar explanation.

The presence of 3–6 wt.% of δ -ferrite in structural composition of the weld metal provides its high resistance to hot cracking and some improvement of ductile properties. Increase in the weight content of δ -ferrite in structure up to 8% and more makes the austenitic-martensitic weld metal sensitive to brittle fracture (in ferrite interlayers), especially at low temperatures.

Therefore, the optimal proportion of structural components of the high-alloy austenitic-martensitic weld metal with a preset level of mechanical properties should be within the following range, wt.%: martensite — 75–85, retained austenite — 6–15, and δ -ferrite — 3–6.

As properties of welded joints in alloyed hardening steels, containing the high-strength ($\sigma_{0.2} = 800$ MPa) austenitic-martensitic weld metal, were insufficiently studied, particularly concerning their resistance to cold cracking, it seemed reasonable to investigate the effect of the above type of the weld metal on the

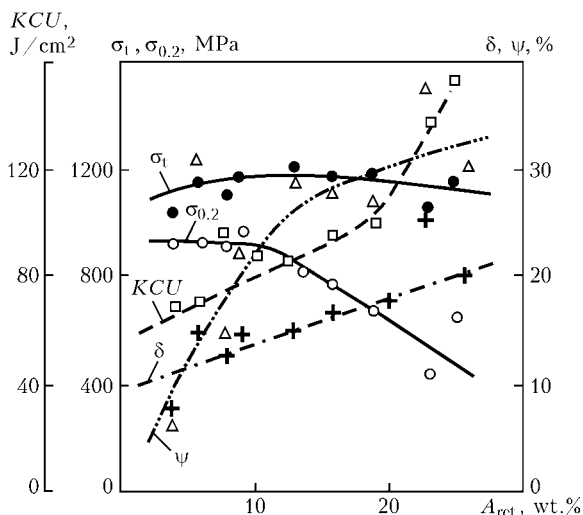


Figure 3. Dependence of mechanical properties of austenitic-martensitic weld metal on weight content of retained austenite



process of formation of structure of the HAZ metal, and compare it to the effect of the austenitic and ferritic-pearlitic welds.

Investigations were conducted using experimental flux-cored wires that provided the weld metal of a chrome-nickel-molybdenum composition of the 05Kh12N8M2GST type with an austenitic-martensitic structure, which meets requirements to chemical and phase composition, and in mechanical properties is at a level of the alloyed steels studied: $\sigma_{0.2} = 800$ MPa, $\sigma_t = 1000$ MPa, $\delta \geq 20$ %, $\psi \geq 35$ %, and $KCU_{+20} \geq 100$ J/cm².

Given below are the results of comparative evaluation of structure and properties of the HAZ metal of restrained welded joints made by CO₂ metal arc welding without preheating and postweld heat treatment on steel of the 30Kh2N2M type with the weld metal of the ferritic-pearlitic, austenitic and austenitic-martensitic grades. The use was made of wires of the Sv-10KhG2SMA and Sv-08Kh20N10G7T grades, as well as experimental flux-cored wire of the

05Kh12N8M2GST type (PP-ANVP-80), which provided deposited metal with the ferritic-pearlitic, austenitic and austenitic-martensitic structure, respectively. In all the three cases the welds were made in the flat position using 2.0 mm diameter wires. The welding procedure was of the penetration type with layer-by-layer cooling to a temperature of +20 °C, direct current of reverse polarity, and positive electrode. In this case the welding parameters were as follows: $I_w = 280$ – 300 A, $U_a = 30$ – 32 V, and $v_w = 12$ m/h. After air cooling to a temperature of 20 °C, templates for micro- and macrosections were cut from the experimental welded joints by the machining method. To avoid the probability of an additional heat effect, all the operations for making the sections were performed by using a forced cooling.

Examination of surfaces of the sections revealed cold cracks of the cleavage type in the HAZ metal of the welded joint with the ferritic-pearlitic weld (10KhG2SMA) (Figure 4, a). No cracks were detected in welded joints with the austenitic and austenitic-martensitic welds.

Microstructure of the HAZ metal of a welded joint with the ferritic-pearlitic weld is a bainitic-martensitic mixture of hardening martensite and lower bainite (HV0.05 4100–4300 MPa). It is characterised by coarser grains, compared with the mostly bainitic (HV0.05 3200–3400 MPa) structure of the HAZ metal of welded joints with the austenitic or austenitic-martensitic welds (Figure 4, b, c). Analysis of the results of measuring hardness and microhardness in the fusion zone shows that welded joints with the austenitic-martensitic and austenitic welds have substantial advantages over a joint with the ferritic-pearlitic weld.

Analysis of the dilatometry curves (Figure 5) characterising phase transformations in welded joints with the austenitic and austenitic-martensitic welds shows that formation of structure of the HAZ metal in cooling

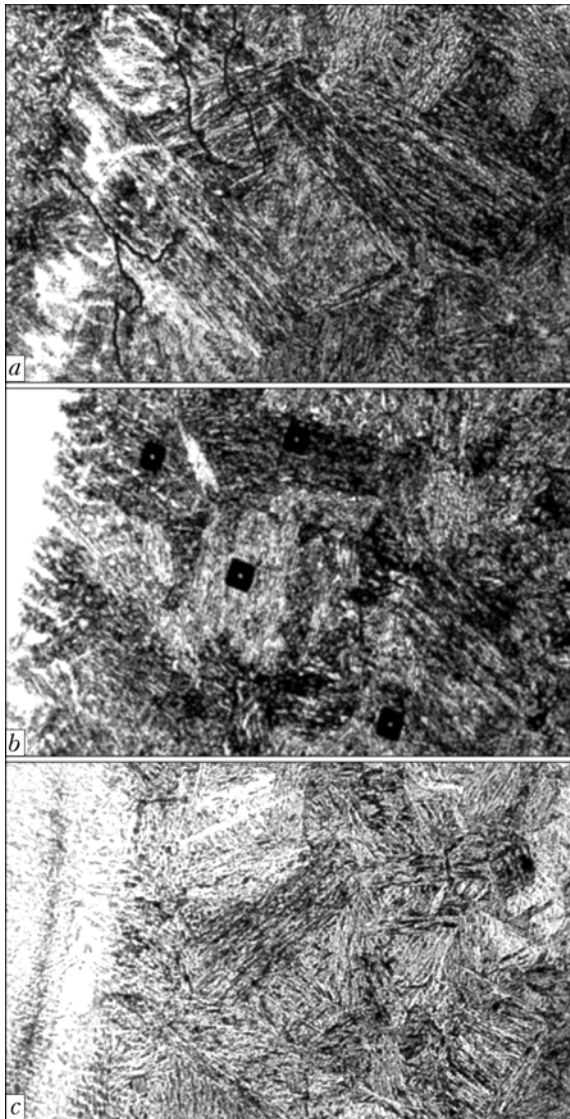


Figure 4. Microstructure of HAZ metal of welded joints in steel 30Kh2N2M with ferritic-pearlitic (a), austenitic (b) and experimental austenitic-martensitic welds (c) ($\times 500$)

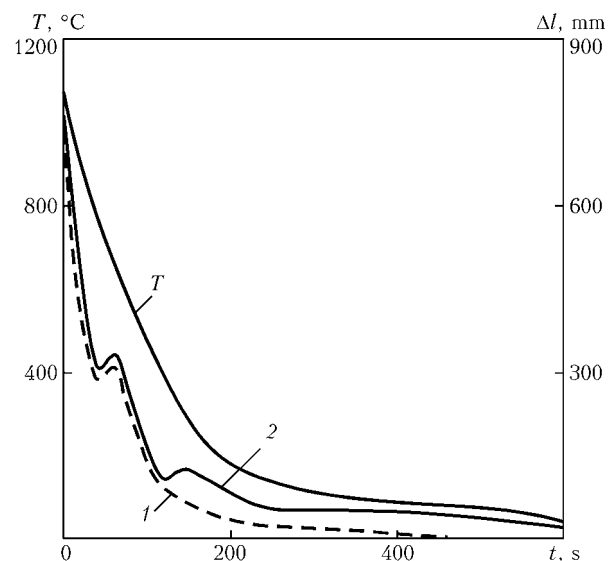


Figure 5. Dilatometric measurements of specimens of a welded joint with the austenitic (1) and austenitic-martensitic weld (2) in steel 15Kh2N4MDA in cooling from 1100 °C: T — temperature versus time

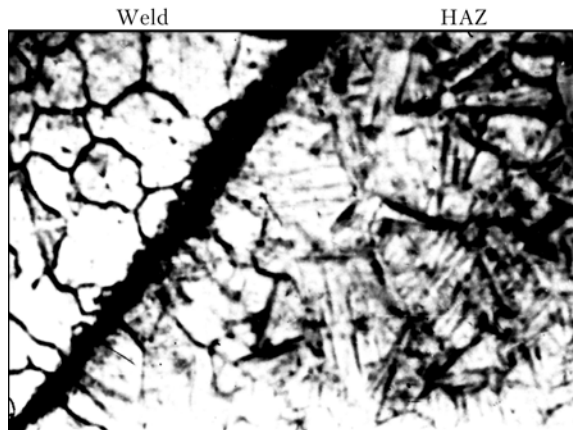


Figure 6. Microstructure of the HAZ metal of welded joint in steel 15Kh2N4MDA with weld of the 05Kh12N8M2GST type at the moment of completion of the HAZ metal structure formation (430 °C). Weld structure — austenite (high-temperature metallography, $\times 100$)

from a temperature of 1100 °C (A_{c3}) in both cases starts and finishes actually in the identical temperature range (450 → 400) °C. All subsequent transformations characteristic of the austenitic-martensitic weld occur now at the fully completed phase transformations in the HAZ metal (Figure 6). It should be noted that in cooling to temperatures of about 180 °C and below, the dilatometer fixes a sudden increase in linear sizes of the specimens, which is attributable to a volume character of the martensitic $\gamma \rightarrow \alpha_m$ transformation in welds of the type under investigation. The process of phase transformations in the weld metal has a positive effect on formation of the stress-strain state of a welded joint. Partial relaxation of residual stresses takes place. Metallography shows that the HAZ metal of welded joints both with the austenitic-martensitic and austenitic welds comprises tempering structures (mixture of martensite of a low degree of tetragonality and upper bainite, see Figure 4, c), which are ductile and insensitive to cracking and brittle fracture.

Therefore, it is established that the effect of the austenitic-martensitic weld metal on structural transformations in the HAZ metal of high-strength alloys steel of the 30Kh2N2M type is similar to the effect of the austenitic weld. In addition, the weld under investigation has high strength ($\sigma_t = 1150$ MPa), which is proved by a high level of hardness ($HV_{0.05} 270\text{--}330$, $HV_{0.05} 2700\text{--}3000$ MPa).

Results of investigations of the effect by the structural-phase state of the high-strength austenitic-martensitic weld on properties of the welded joints in alloyed steels were used as a basis for the development of a new generation of welding consumables: electrodes and flux-cored wires of the ANVP series, intended for welding of high-strength alloyed steels with a yield stress of 600 to 1000 MPa, involving no preheating and postweld heat treatment. The process of arc welding and surfacing using the experimental welding consumables is characterised by high welding-technological properties.

Low level of the concentration of hydrogen in the weld metal produced by using the new welding consumables (1.9–2.5 cm³/100 g of metal) is provided by taking special technological measures [16, 17] com-

bined with other favourable factors [18]. This ensures a satisfactory cold crack and delayed fracture resistance of the welded joints in alloyed steels.

Based on the results of pilot-industrial verifications, the new welding consumables were recommended for welding and surfacing of high-strength alloyed steels without preheating and postweld heat treatment for manufacture and repair of equipment applied in different sectors of domestic engineering (special, transport, power, oil refining, mining, etc.).

CONCLUSIONS

1. Kinetic of $\gamma \rightarrow \alpha_m$ transformation in low-carbon austenitic-martensitic weld metal has a positive effect on formation of structure of the HAZ metal of welded joints in hardening alloyed steels, promoting formation in it of mostly such ductile structures as upper bainite and temper martensite.

2. Sparsely alloyed austenitic-martensitic welds with a preset structural-phase state are not inferior in their mechanical properties to the base metal, which allows producing high-strength welded joints in alloyed steels by welding without preheating and postweld heat treatment.

3. Welded joints in alloyed steels with high-strength ($\sigma_t \geq 1000$ MPa) austenitic-martensitic welds are resistant to cold cracking and delayed fracture.

1. (1974) *Technology of fusion electric welding of metals and alloys*. Ed. by B.E. Paton. Moscow: Mashinostroenie.
2. Makarov, E.L. (1981) *Cold cracks in welding of alloyed steels*. Moscow: Mashinostroenie.
3. Makara, A.M., Mosendz, N.A. (1971) *Welding of high-strength steels*. Kiev: Tekhnika.
4. Gotalsky, Yu.N. (1992) *Welding of pearlitic steels with austenitic consumables*. Kiev: Naukova Dumka.
5. Grishchenko, L.V. (1961) New electrodes for welding of steel 15Kh2N4MDA. *Svaroch. Proizvodstvo*, **3**, 22–26.
6. Barishnikov, A.P. (1969) Influence of weld metal composition on cold crack formation in welding of medium-alloy steels. *Avtomatich. Svarka*, **7**, 1–4.
7. Birman, S.R. (1974) *Sparsely-alloyed maraging steels*. Moscow: Metallurgiya.
8. Gotalsky, Yu.N., Snisar, V.V., Demchenko, E.L. *Method of arc welding of hardening steels*. USSR author's cert. 880671. Int. Cl. B23K 28/00. Publ. 14.07.81.
9. Goldshtejn, M.I., Grachev, S.V., Veksler, Yu.G. (1985) *Special steels*. Moscow: Metallurgiya.
10. Goudremont, E. (1966) *Special steels*. Moscow: Metallurgiya.
11. Potak, Ya.M. (1972) *High-strength steels*. Moscow: Metallurgiya.
12. Kozlovskaya, V.I., Potak, Ya.M., Orzhekhovskiy, Yu.F. (1969) Increase of toughness of martensitic steels by heat treatment. *Metallovedenie i Term. Obrab. Metallov*, **5**, 61–66.
13. Tikhomirov, V.V., Shakhnazarov, Yu.V., Pankov, A.G. et al. (1971) Relationship between toughness of steel N18K9N5T at –196 °C and amount and stability of retained austenite in fracture. *Fizika Metallov i Metallovedenie*, **32**(3), 641–643.
14. Nikolskaya, V.L., Pevzner, L.M., Orekhov, N.G. (1975) Influence of retained austenite on properties of cast stainless steels. *Metallovedenie i Term. Obrab. Metallov*, **9**, 35–39.
15. Yushchenko, K.A., Pustovit, A.I. (1977) Influence of alloying elements on structure and cold resistance of high-strength maraging welds. In: *Steels and alloys for cryogenic engineering*. Kiev: Naukova Dumka.
16. Demchenko, E.L., Bovsunovskiy, A.N., Yankina, O.I. (1990) Effect of hydrogen on mechanical properties of austenitic-martensitic weld metal of the 03Kh12N8M2GST type. *Avtomatich. Svarka*, **7**, 30–33.
17. Demchenko, E.L., Snisar, V.V., Lipodaev, V.N. (1991) Ways of decreasing hydrogen content in weld metal of the 03Kh12N8M2GST type in arc welding. *Ibid.*, **10**, 23–27.
18. Sterenbogen, Yu.A., Vasiliev, D.V., Demchenko, E.L. et al. (2006) Role of peak stresses in formation of cold cracks in welded joints of hardenable steels. *The Paton Welding J.*, **4**, 9–16.



APPLICATION OF CORROSION-RESISTANT SURFACING IN TECHNOLOGICAL EQUIPMENT OPERATING IN CONTACT WITH SEA WATER

A.S. SALNIKOV, V.V. OTROKOV, G.M. SHELENKOV, E.A. TSYMBAL and M.A. LAKTIONOV

OJSC «M.V. Frunze Sumy NPO», Sumy, Ukraine

The results are given on comparative testing of anticorrosion deposits used for protection of power generation equipment operating in sea water. KhN65MV (EP-567) alloy has the highest pitting corrosion resistance in sea water. As to tribotechnical parameters, KhN65MV alloy in contact with FUT coal-plastic is inferior to FUT + bronze pair. KhN65MV alloy can be recommended for protection from pitting and contact corrosion of low-load components operating under the conditions of their wetting by sea water.

Keywords: arc surfacing, technological equipment, power generation systems, corrosion failure, corrosion-resistant surfacing, deposited metal, tribotechnical tests, deformation hardening, pitting corrosion

Sea water is used for cooling technological equipment in power generation systems, located in coastal sea territories. High-alloy chromium-nickel-molybdenum stainless steels that provide the necessary level of corrosion resistance in the given medium are used when manufacturing such equipment. However, protective measures preventing local corrosion failure — pitting and crevice corrosion, corrosion cracking, should be taken for keeping the metal in the passive state in the stagnant zones of the items, refrigerated friction components, components exposed to corrosion-mechanical wear. Such types of failure are possible in rotary pumps of VA 4500-50A, VA 5500-50A types from 12Kh17N13M3T steel grade taking into account their design and operating conditions.

Surfacing of critical zones of the items with materials providing the required level of corrosion resistance is one of the ways of solving the mentioned problem.

In world practice, the rational selection of corrosion-resistant steels for equipment operating under the conditions of possible local failure, is performed on the basis of an empirical dependence [1, 2]

$$PRE = \% Cr + 3.3 \% Mo + 16 \% N,$$

where PRE is the equivalent of resistance to pitting corrosion (PC).

Alloys with $PRE > 40$ are characterized by high resistance to PC in sea water. Such a property is found in steels (deposits) that contain 19–20 % Cr and not less than 6 % Mo [2–4].

The Table gives the calculated PRE values of welding consumables designed for anticorrosion surfacing to PNAE G-7-009–89, as well as those recommended by Federal State Unitary Enterprise Central Research Institute of Structural Materials «Prometej» and Azov Marine Institute of Odessa National Academy [5, 6].

PNAE G-7-009–89 recommends welding wire Sv-03Kh15N35G7M6B for this case. This is special-purpose wire so that it is practically impossible to purchase it in small volumes. More over there are no data in literary sources as to its industrial application for surfacing. Welding consumables given in the Table (except for KhN65MV alloy) have $PRE < 40$. Analysis of the given data allows making the conclusion that KhN65MV (EP-567) alloy is expected to have the highest resistance to PC.

The information on application of KhN65MV alloy for operation in sea water is rather limited. In study [7] the good prospects for application of KhN65MV alloy for corrosion protection of FUT + Kh65MV contact pair when operating in sea water are suggested proceeding from polarization diagram analysis. As to application of surfacing by KhN65MV alloy for protection from corrosion and corrosion-mechanical wear, these data are practically not available.

The problem of providing corrosion resistance in sea water in the zones subjected to corrosion-mechanical wear and contact pairs of slider bearings is studied even less. Continuous cladding of working surfaces by alloys with high corrosion resistance in sea water [8] (tin bronzes, copper-nickel alloys and other) is recommended by the Sea Register for protecting contact surface of steel shafts with a bearing from corrosion damage.

Application of protective casings leads to corrosion-fatigue strength decrease because of fretting-effect, considerable consumption of deficit materials and mass increase of the item [9]. Surfacing is the most promising method for protection of steel shafts from corrosion. However, the process of surfacing, even in the absence of defects in deposited layer, can decrease the endurance limit to 30 % [5]. The essence of fatigue failure consists in initiation of a fatigue crack, which simultaneously spreads in the deposited and base metal near the fusion boundary under the influence of alternating loads and residual stresses [5, 10]. One of essential factors influencing the fatigue crack initiation are the properties of the deposited metal and surfacing

Calculated values of PRE and results of PC testing of the deposits

No.	Material grade	Material compliance	PRE calculated (max/min)	Corrosion rate by GOST 9.912-89, g/(m ² ·h); susceptibility to PC
1	KhN65MV (EP-567)	GOST 5632-78	72.6 / 64.0	N/D
		Deposited metal	65.7	No losses of mass; PC is not found
2	PP-AN-163 (PP-Np-07Kh12M3N3G2)	TUU 05416923.020-97	21.9 / 16.6	N/D
		Deposited metal	19.3	max 10.5; up to 2 mm depth
3	OZL-17U (E-03Kh23N27M3D3G2B)	TU 14-4-715-75	39.2 / 29.6	N/D
		Deposited metal	34.34	max 06; 1 point per 1 cm ²
4	EA 400 / 10U (E-07Kh19N11M3G2F)	TU 5.965-4027 GOST 9466	30.6 / 23.4	N/D
		Deposited metal	26.65	max 1.72; depth up to 1 mm
5	Sv-03Kh15N35G7M6B Flux OF-10	Deposited metal PNAE G-7-10-89	40.7 / 29.5	N/D

methods. Deposited metal should feature a high resistance to micro- and macrocrack formation, should have rather high strength, respective ductility and impact toughness, should form compressive stresses during surfacing and have a high resistance to initiation and propagation of fatigue cracks [5], rather high corrosion and fatigue-corrosion resistance.

In view of above, it became necessary to conduct research aimed at selection of the optimum available welding consumables for surfacing of critical zones of equipment operating in sea water.

Several interrelated problems had to be solved when choosing consumables for surfacing of pump components:

- to protect the pump rotor working surfaces and stagnant zones of pump bodies from corrosion failure at contact with sea water by surfacing of corrosion-resistant materials without any essential deterioration of the initial properties of base metal (BM) of the items both during the period of operation and shut-down;

- to provide hardness $HRC_e \geq 30$ and PC protection of the working surfaces of pump rotor part components, subjected to corrosion-mechanical wear under the conditions of sea water, by surfacing method;

- to provide the specified technical operating life of bearings of not less than 30 years in the contact coal-plastic pair FUT (to TU 5.966-11704) and anti-corrosion deposit with hardness $HRC_e \geq 30$ on 38KhM and 40Kh carbon steels (GOST 4543-71) for pump intermediate shafts.

Experimental trials of KhN65MV alloy suitability for solving the first defined task were done along with other welding consumables (see the Table).

PC resistance of the deposited metal was determined by the chemical method to GOST 9.912-89 envisaging accelerated testing in 10 % solution of $FeCl_3 + 6H_2O$.

Samples of 20 × 30 × 4 mm size, 5 pieces per one test, were cut out of the upper layers of seven-layer deposits produced with the following welding consumables:

- KhN65MV (EP-567) wire ---- argon arc surfacing;
- E-03Kh23N27M3D3G2B (OZL-17U) electrodes ---- electric arc surfacing;
- E-07Kh19N11M3G2F (EA 400 / 10U) electrodes ---- electric arc surfacing;
- PP-Np-07Kh12M3N3G2 (PP-AN-163) wire ---- automatic submerged-arc surfacing with AN-26C flux.

The tests were conducted in three cycles for 5 (1), 24 (2) and 48 (3) h. Total testing duration is 77 h. Conditional pitting rate was used as the evaluation result. The depth and the number of pits per a unit area were determined as additional indices with the results given in the Table. Specimens cut out of the metal deposited by PP-Np-07Kh12M3N3G2 (PP-AN-163) wire had considerable losses (Figure 1, a). Depth of individual pits was down to reach 2 mm. Specimens cut out of the metal deposited by electrodes E-03Kh23N27M3D3G2B (OZL-17U) had minor losses of mass and one spot failure per 1 cm² (Figure 1, c). Pits were not found on the surface of the specimens cut out of the deposited metal KhN65MV (EP-567), (Figure 1, d). Mass losses were absent. The experiments proved that the test results are in good agreement with calculated PRE values.

Specimens from the metal deposited by KhN65MV (EP-567) wire having the highest PC resistance were subjected to the test at a higher temperature (+40 °C) to GOST 9.912-89. Losses in mass were absent. Metal deposited using alloy Kh65MV is also stable against intercrystalline corrosion. The tests were carried out by RD 24200.15-90 procedure.

Thus, metal deposited with KhN65MV alloy wire showed the highest PC resistance.

As is known [11, 12], stainless steels and alloys having the required corrosion resistance are prone to tearing in the friction pairs in a number of cases. This requires taking measures on improvement of their hardness. The latter is achieved by mechanical hardening by roller treatment, high frequency mechanical peening and explosion treatment.

KhN65MV alloy, having a high corrosion resistance, provides up to HB 220 (HRC 18) hardness in

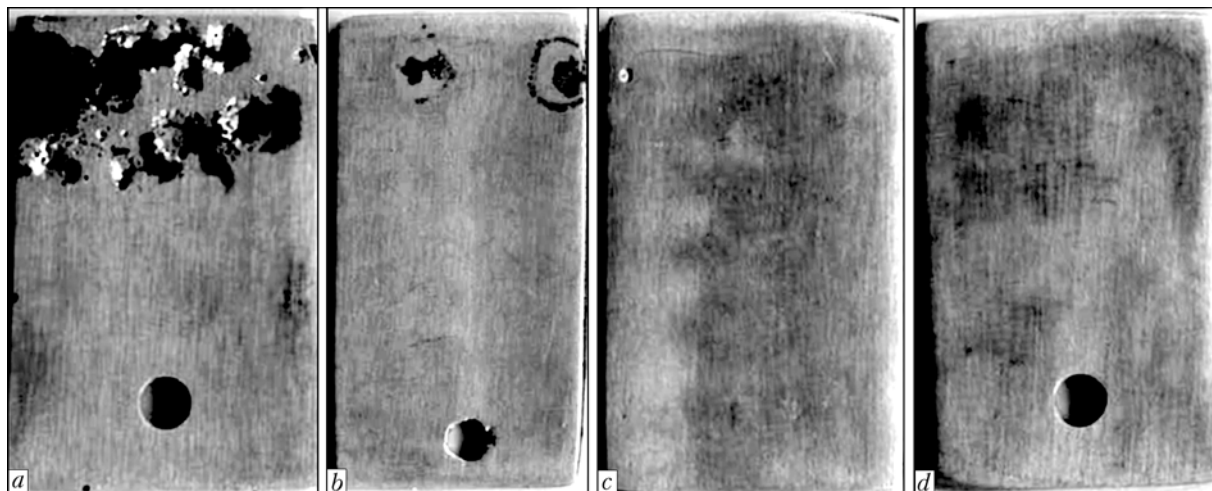


Figure 1. Appearance of specimens of metal surfaced by different consumables after PC testing: *a* — PP-AN-163 flux-cored wire, PRE = 19, PC depth of up to 2 mm, mass losses of up to 10.5 g/(m²·h); *b* — EA 400/10U electrodes, PRE = 27, PC depth of up to 0.5 mm, mass losses of up to 1.72 g/(m²·h); *c* — OZL-17U electrodes, PRE = 34, PC — 1 point per 1 cm², mass losses of up to 0.6 g/(m²·h); *d* — EP-567 (KhN65MV) alloy, PRE = 66, PC was not found, no mass losses

the deposited metal that is lower than required (HRC 35–40) for the zones subjected to corrosion-mechanical wear.

When solving the task connected with hardness increase and inducing compressive stresses in the deposited layer of KhN65MV alloy, roller treatment of the corrosion-resistant layer was used taking into account the known recommendations [11, 12].

Maximum hardness reached HV 412 on the surface of the deposited metal after deformational hardening. Hardness of the hardened layer over the deposit cross-section also depends on roller treatment modes. Hardness distribution along the deposit cross-section depending on the number of passes is given in Figure 2. The depth of hardened layer with HV 320 hardness reached 2.0–2.5 mm after three passes. Such treatment raises the deposit resistance to tears and mechanical wear in friction pairs. However, there is practically no data on the corrosion-mechanical wear of hardened deposited metal and hardening influence on its corrosion resistance when operating in sea water, which necessitated performance of investigations in this direction.

Comparison testing was conducted by the method of short-time loading [13] that allows getting enough

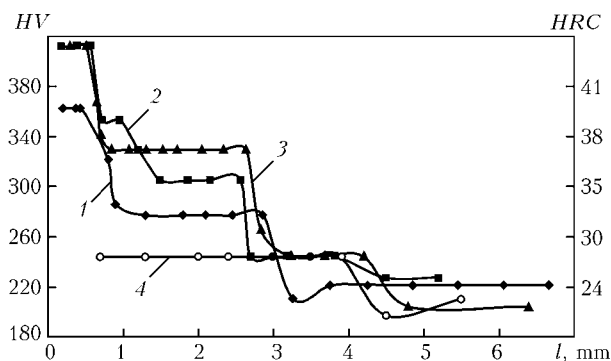


Figure 2. Hardness distribution along the cross-section of corrosion-resistant metal deposited by KhN65MV alloy with different number of roller treatment runs: 1–3 — after one, two and three runs, respectively; 4 — as-welded

experiment data for statistical processing rather quickly in a number of cases. Another advantage of short-time testing also is the possibility of reliable assurance of constant assigned conditions of loading and wear of the contact surfaces of tested material and mating body during the entire time of the friction unit operation.

Linear wear (h — groove depth on the surface of tested material) was chosen as the main index characterizing the properties of tested materials at constant loading and fixed traveled path length. The procedure cannot be used for calculation of friction pair residual operating life, but can allow comparative evaluation of friction pair wear resistance.

The diagram of friction unit with water tank is given in Figure 3. Wetting with sea water was performed by partial dipping of the rotating roll into the tank. Linear wear was determined at constant loading $F_N = 100$ N, slip velocity of 1.1 m/s and fixed traveled path length ($L = 200, 300, 400, 500, 600$ and 700 m).

Wear of metal deposited with application of such filler materials as Stellite 6, bronze, KhN65MV alloy (hardened deposit) was tested in comparison with BM (12Kh18N10T steel). Plate from V3K alloy was used as the mating body. The test results are given in Figure 4. Materials are arranged by decrease of maximum wear (grove depth h' , mm) as follows: 12Kh18N10T (HB 200) — 0.128 mm; bronze UTP34N

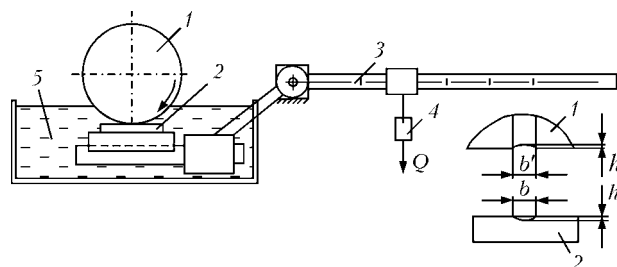


Figure 3. Diagram of friction component for comparative tribotechnical testing: 1 — cylindrical specimen with tested deposit; 2 — mating body specimen; 3 — lever; 4 — movable load; 5 — tank with synthetic sea water

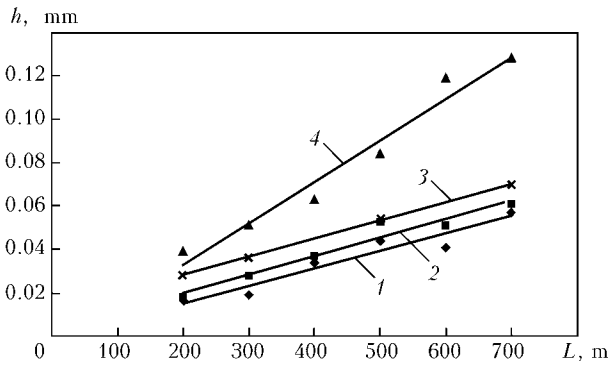


Figure 4. Linear wear of deposited metal (1 — Stellite 6; 2 — KhN65MV alloy; 3 — bronze UTP34N) and BM (12Kh18N10T steel) at constant load $F_N = 100$ N and fixed length of mating body traveled path

material (HRC 22) — 0.074 mm; KhN65MV alloy (HRC 39) — 0.061 mm; Stellite 6 (HRC 50) — 0.058 mm.

Thus, KhN65MV deposit hardened by roller treatment up to HV 412 (HRC_e 35–40) hardness, has higher resistance to corrosion-mechanical wear in comparison with stainless steel and bronze, and can be recommended for pump rotor part component subjected to such a type of wear.

Studies on bearing workability in the contact pair of coal-plastic FUT + KhN65MV deposit as applied to countershafts from high carbon steel were conducted in two stages. First the technology of countershaft surfacing with KhN65MV alloy, which would not impair BM properties, was optimized. Optimization of the technology and studies of the welding process influence on the deposited metal and BM were carried out* on samples from 40Kh steel of 210 mm diameter that had been heat-treated and provided mechanical properties not lower than CR 440.

Deposited layer of Kh65NMV type was produced in manual TIG welding with filler wire KhN65MV over an underlayer of 07Kh25N13 type taking into account the requirements of standard technical docu-

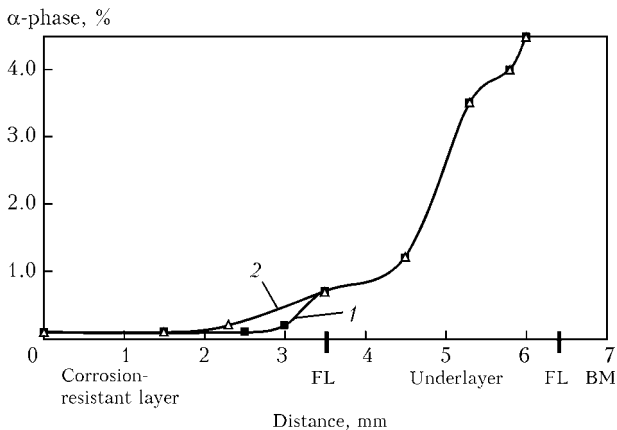


Figure 5. Distribution of α -phase along the deposited metal cross-section: 1 — hardened specimen; 2 — specimen before hardening; FL — fusion line

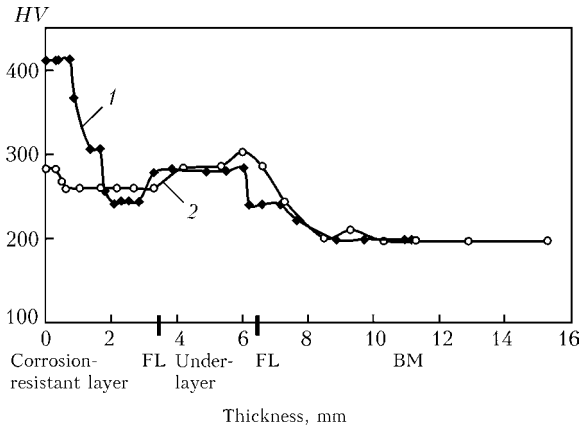


Figure 6. HV hardness distribution along the thickness of deposited layer and BM: 1 — hardened specimen; 2 — specimen before hardening

mentation [14, 15]. Distribution of α -phase over the deposited metal cross-section (Figure 5), hardness (Figure 6) and microstructure of BM deposited and adjoining sections were determined.

Quantity of α -phase decreases from 50 % in the interlayer along the line of underlayer fusion with

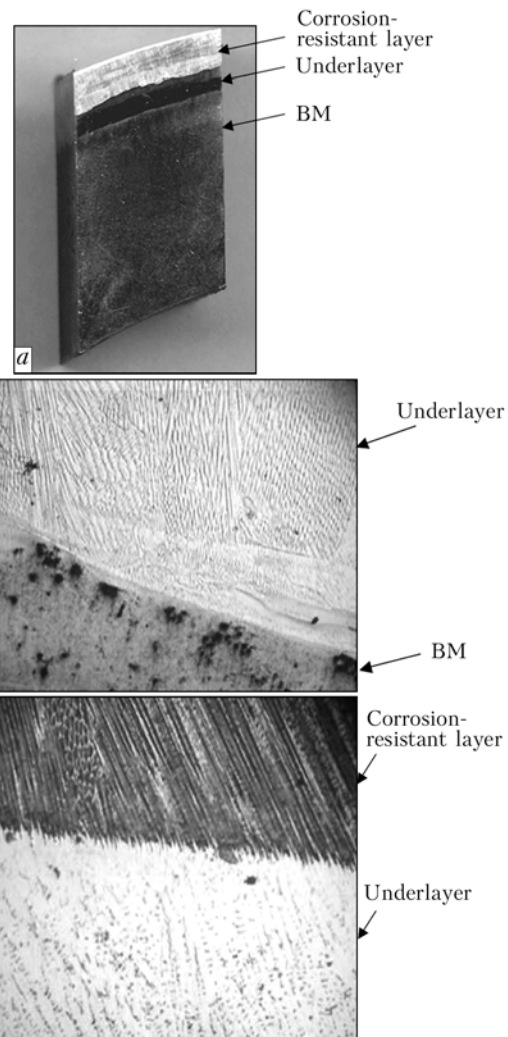


Figure 7. Two-layer surfacing of BM from 40Kh steel with 07Kh25N13 steel underlayer: a — appearance; b — fusion line of underlayer with BM ($\times 50$); c — fusion line of KhN65MV corrosion-resistant layer with 07Kh25N13 underlayer (b, c — $\times 250$)

* T.A. Chugaj, A.A. Lomako and B.T. Kobzar («M.V. Frunze Sumy NPO») participated in performance of the work.



BM to 0.8–1.0 % in underlayer at the distance of 2.0–2.5 mm from the fusion line with BM (Figure 5). In the corrosion-resistant layer (KhN65MV) the quantity of α -phase changes from 0.1 % on the surface of corrosion-resistant deposited metal to 0.7 % on the underlayer–corrosion-resistant layer fusion line. The interlayer of the deposited metal near the fusion line of underlayer with BM has the maximum hardness HV 280–300 (Figure 6). BM hardness decreases from HV 280 along the fusion line with the underlayer to HV 240–223 at the distance of 0.6–1.8 mm from fusion line, BM hardness beyond the HAZ being HV 187–200. No microcracks were found along the fusion line, or in the deposited metal (Figure 7).

Thus, KhN65MV deposited metal and the method of its deposition on 40Kh steel through an interlayer provides BM corrosion protection (40Kh steel) without impairing its properties.

Friction pairs of FUT coal-plastic + corrosion-resistant materials determine the wear of contact surface during comparative tribotechnical testing. Antifriction properties of FUT type coal-plastics were studied in sufficient detail [13, 16]. Taking into account that FUT + hardened steel, FUT + bronze pairs and other [16] are often used in pump bearings, testing of the influence of material nature, including deposited metal of KhN65MV type, on friction pair wear resistance was carried out. Comparison tests were conducted by the previous procedure at constant loading of 250 N, slip velocity of 1.0–1.1 m/s and surface roughness $R_a = 0.6$ –1.0. The following friction pairs were tested: KhN65MV + FUT; 12Kh18N10T + FUT; BrA9Zn4N4Mts1 + FUT; BrO10F1 + FUT; BrO10Ts2 + FUT.

Dependence of FUT contact surface linear wear (h_{max}) on the length of traveled path is given in Figure 8. KhN65MV + FUT friction pairs have the highest value of $h_{max} = 0.2$ mm on the fixed length of the traveled path $L = 600$ m. The lowest value is found for BrO10Ts2 + FUT friction pairs ($h_{max} = 0.016$ mm). Wear of FUT contact surface in the pair with KhN65MV deposited material is about 10–12 times higher than the wear of FUT contact surface in the pair with BrO10Ts2.

Results of the conducted investigations of friction pairs are in good agreement with the results of the data in work [16] in that the nature of metal essentially influences the wear resistance of FUT coal-plastic in the friction pair. Thus, corrosion-resistant deposited metal KhN65MV should be used in the friction pair with FUT, considering the real operating conditions of this pair.

CONCLUSIONS

1. Deposited metal of KhN65MV type including that hardened by roller treatment provides a high common corrosion resistance and pitting corrosion resistance of VA type pump component surface at operation in sea water. Moreover, it can be recommended for com-

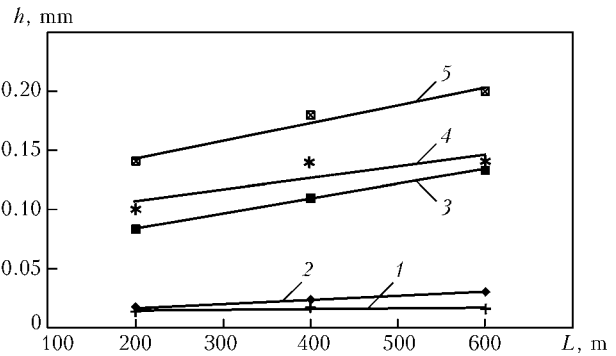


Figure 8. Dependence of FUT contact surface linear wear on traveled path length at constant loading $F_N = 250$ N: 1 — BrO10Ts2; 2 — BrO10F1; 3 — BrA9Zn4N4Mts1; 4 — 12Kh18N10T steel; 5 — KhN65MV (hardened)

mon corrosion and PC protection of parts and components, operating under the conditions of corrosion-mechanical wear.

2. Hardened deposited metal of KhN65MV type in the pair with FUT is inferior to bronze + FUT pair by tribotechnical parameters and can be recommended only taking into account the real operating conditions of the item.

1. Ulianin, E.A. (1991) *Corrosion-resistant steels and alloys*. Refer. Book. Moscow: Metallurgiya.
2. Voronenko, B.I. (1995) Corrosion resistance of current austenitic-ferritic (duplex) stainless steels. Special types of corrosion (Review). *Zashchita Metallov*, 31(2).
3. (1987) *Corrosion*: Refer. Book. Ed. by L.L. Shrajner. Moscow: Metallurgiya.
4. Chendler, K.A. (1988) *Corrosion of vessels and marine structures*. Leningrad: Sudostroenie.
5. Kravtsov, T.G., Kravtsov, V.T. (2004) New surfacing material for recovery and corrosion protection of shafts under cyclic loading service conditions. In: *Proc. of 3rd Int. Conf. on Welding Consumables*. Dnepropetrovsk.
6. (1983) *Sea corrosion*. Ed. by N.N. Shumakher. Moscow: Metallurgiya.
7. Chukalovskaya, T.V., Shcherbakov, A.I., Chigirinskaya, L.A. et al. (1995) Corrosion-electrochemical behavior of electrode pairs of coal-plastic-metal in corrosive media. *Zashchita Metallov*, 31(2).
8. (1974) *USSR register: Rules of classification of sea vessel construction*. Vol. 2. Leningrad: Transport.
9. (1975) *Materials for short-term seminar of September, 29–30, 1975*. Ed. by Yu.M. Belov, A.E. Vajnerman. Leningrad.
10. Babaev, A.N. (1975) About conditions of conducting fatigue and corrosion-fatigue tests of specimens and transferring their results to real propeller shafts with a deposit. In: *Materials for short-term seminar of September, 29–30, 1975*. Leningrad.
11. Khaet, G.L., Stenko, D.A., Brusilovsky, B.A. (1959) *Experience of Novokramatorsk Machine-Building Works on roller treatment of large parts*: Transact. of TsNIITMASH. Moscow: Mashgiz.
12. Polevoj, S.N., Evdokimov, V.D. (1986) *Hardening of metals*: Refer. Book. Moscow: Mashinostroenie.
13. Tochilnikov, D.G., Ginzburg, B.M. (2002) Procedure of fast tests of antifriction polymers. *Voprosy Materialovedeniya*, 31(3).
14. *OST 5.9573–84*: Surfacing shipbuilding carbon and alloyed steels with aluminium bronzes, copper-nickel alloy and corrosion-resistant steels. Standard technological process, acceptance rules and testing methods.
15. *OST 26-01-858–94*: Welded vessels and apparatuses of nickel and corrosion-resistant alloys on nickel base. General specifications.
16. Anisimov, A.V., Bakhereva, V.E. et al. (2002) Study of the influence of mating body material on indices of coal-plastics at friction with water wetting. *Voprosy Materialovedeniya*, 31(3).



BLOCK OF BIAS AND CATHODE POWER OF ELECTRON BEAM GUN USING INVERTER-TYPE CONVERTERS

N.K. CHAJKA

OJSC «Selmi», Sumy, Ukraine

The paper deals with the approach to application of inverter-type converters for powering the cathode and forming the control voltage of electron beam guns to reduce the overall dimensions of the block of bias and power of the cathode. This enables neutralizing the negative impact of leakage inductance of high-potential transformer, which increases with introduction of insulation between the windings to ensure the potential decoupling.

Keywords: electron beam welding, electron beam gun, cathode power, bias voltage, inverter, potential decoupling

As in electron beam welding machines the gun cathode is under a potential equal to accelerating voltage, relative to the machine case, special decoupling should be envisaged in the circuits providing the cathode power and bias voltage. In ELA-15, ELA-30, ELA-60 power units the potential decoupling is performed by special high-potential decoupling transformer, which operates at 50 Hz frequency [1]. At transition to the inverter-type source of accelerating voltage the overall dimensions of the bias and cathode power block are comparable with the dimensions of the accelerating voltage source proper. In this connection it became necessary to reduce the block dimensions. For this purpose transition to a higher frequency was used in power transmission circuits. In this case, however, the high-voltage insulation between the windings of the high-frequency high-potential transformer has a rather large volume compared to the greatly reduced volumes of the core and windings. Increase of the relative volume taken up by high-voltage insulation between the windings of high-potential decoupling transformer leads to an increase of leakage inductance L_{S1} , L_{S2} of

the primary and secondary windings, respectively. The higher the potential for which the high-voltage decoupling transformer is designed, the larger the leakage volume taken up by insulation and the greater the leakage inductance, which is a parasitic parameter for the transformer. Leakage inductance creates an inductive resistance, connected in series with the load (T-shaped equivalent circuit of the transformer [2]):

$$X_L = 2\pi FL_S \text{ [Ohm]},$$

where F is the frequency, Hz; $L_S = L_{S1} + L_{S2}$ is the total leakage inductance, H; L_{S1} is the inductance of the primary winding; L_{S2} is the inductance of secondary winding; L_{S2} being reduced to L_{S1} .

From the above expression it follows that the higher the frequency at which the transformer operates, the higher the inductive resistance connected in series with the load, and the lower the effectiveness of such a system of energy transmission. To overcome such a situation, it was decided to use a converter of direct voltage into alternating voltage with series resonance circuit at the output, in which the circuit inductance will be the leakage inductance. At coincidence of the conversion frequency with that of the circuit, the current in the latter, according to the vector diagram of currents and voltages given in Figure 1, will be equal to $I_R = U/R_n$ [3], where R_n is the load resistance reduced to the primary winding, i.e. generator voltage is completely applied to the load.

This solution is protected by a Ukrainian patent [4]. Figure 2 shows the circuit of a device for implementation of this solution, which is a half-bridge circuit with resonance load. Pulse-width modulation of controlling pulses was used to control the output voltage. KR1114EU4 microcircuit or its analog can be used as the pulse-width modulator, and field transistors IRFP 460 --- as keys.

The transformer can have two or more secondary windings and two screens, which are located on the low-voltage and high-voltage sides, and designed for protection of the elements at breakdowns in the electron beam gun. The screen located on the high-voltage side, is connected to the common part of the accelerating voltage source, which, in its turn, is connected

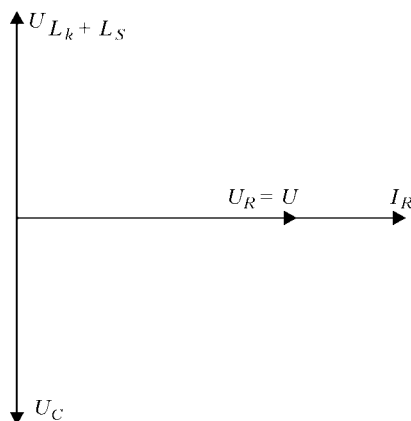


Figure 1. Vector diagram of voltages and currents of the circuit at the frequency equal to the resonance frequency: U — power circuit generator voltage; U_C — voltage in circuit capacitance; U_R — voltage on the load reduced to the primary winding; L_k — external circuit inductance; $U_{Lk} + L_s$ — voltage on the total circuit inductance

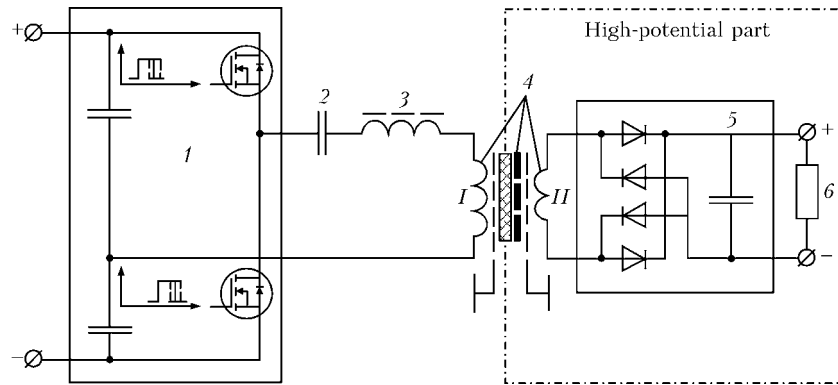


Figure 2. Schematic of a device for power transfer with high-potential decoupling: 1 — key inverter; 2 — capacitor; 3 — inductance; 4 — transformer with a high-potential insulation between the windings; 5 — rectifier with filter; 6 — load

to the gun cathode. The key inverter has pulse-width modulation [5] for output voltage control. The frequency of conversion of the key inverter is equal to the resonance frequency of the series circuit formed by capacitor 2, inductance 3 and more seldom by leakage inductance of transformer 4. At a sufficiently high conversion frequency external inductance 3 can be eliminated, using the transformer leakage inductance as the circuit inductance.

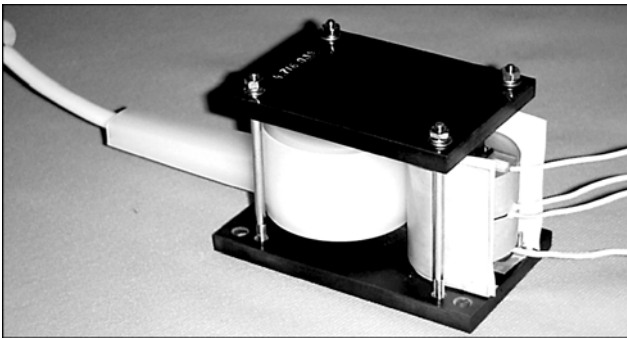


Figure 3. Appearance of high-potential decoupling transformer

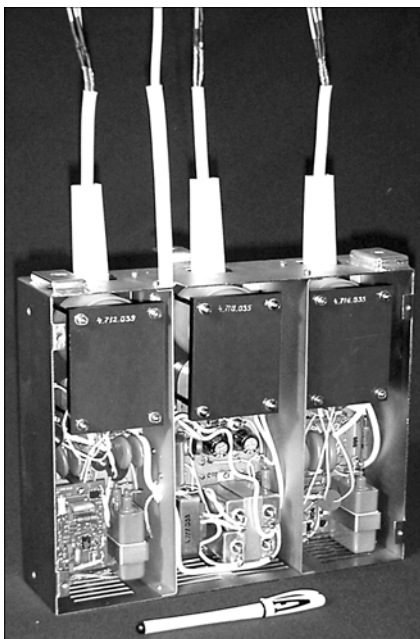
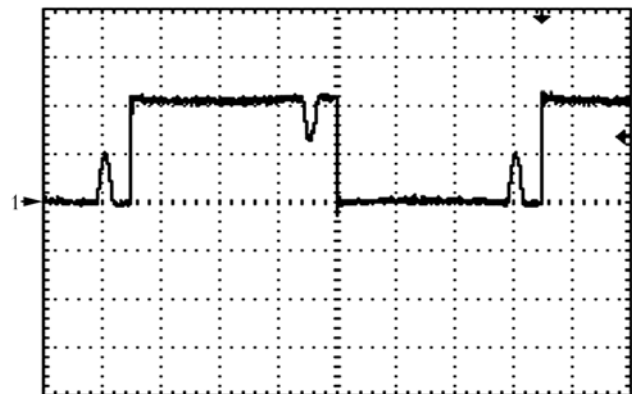


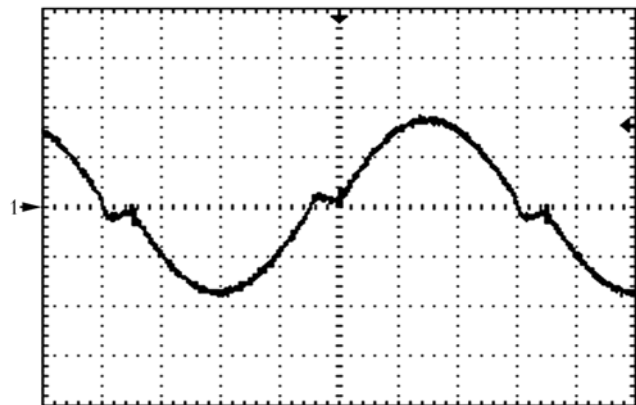
Figure 4. Appearance of block of bias and cathode power with the removed front cover

The presented approach of power transfer with a high-potential decoupling was used as a basis to develop a block of bias and cathode power designed for power unit of welding machines with an inverter source of accelerating voltage. The block includes three channels — filament power, cathode bombardment voltage and bias voltage. The main element in each channel is the high-potential decoupling transformer of a unified design having a different number of turns in the channel secondary windings.

Transformer primary windings are at a low potential, while the magnet cores are at a high potential. High-potential decoupling is ensured by primary



CH1 100 V *a* M 10.0 μs



CH1 1.00 V *b* M 10.0 μs

Figure 5. Oscillograms of the source-drain voltage of upper key (a) and voltage on the measuring resistor $R_m = 1$ Ohm of circuit current at maximum duration of the control pulse (b)



winding insulation using a polyethylene capsule having the shape of a cylinder with an axial channel for the magnet core. Polyethylene thickness is selected proceeding from the values of the working and testing voltages. The capsule consists of the upper and lower halves, which are connected by a step flange to increase the distance of overlapping over the surface. A spout extends from the side surface of the capsule lower half on the level of its base, through the inner channel of which the taps from the primary winding and shield run. The spout length is selected to be such that the transformer could stand the test voltage (90 kV in this case). M2000 NMS-IP-110A core is used as the magnet core.

Figure 3 gives the appearance of a high-potential decoupling transformer, and Figure 4 — the appearance of the bias block. Overall dimensions of the block without the extending spouts of the transformer are $288 \times 245 \times 86$ mm. A similar block in ELA-6 power unit produced by OJSC «Selmi» (Sumy), with the traditional circuit with high-potential decoupling transformers operating at 50 Hz frequency, has the overall dimensions of $450 \times 250 \times 440$ mm.

Figure 5 gives the oscillograms of the source–drain voltage of the upper key and circuit current, the half-waves of which are the key currents at maximum pulse duration of the bombardment channel converter as the most power-intensive.

The converter operates at 16–20 kHz frequency, and at direct current and voltage of 200 V it provides 80 mA current at 1000 V voltage on the load with 12 kOhm resistance, which corresponds to the power of 80 W.

The block was tested on a mock-up of ELA-6VCh power unit and has the following output parameters:

Filament current at 0.5 Ohm load, A	10
Bias voltage, kV	5
Bombardment current at 1 kV voltage, mA	80
Working potential of the block relative to the power unit case, kV	60

The given achieved results are not the limit. At development of a bombardment source for tungsten cathode heating more than 150 W power at the efficiency of 90 % was obtained in the same transformer.

It should be noted that the devices made with the proposed circuit are not susceptible to short-circuiting in the load, as in this case the key current decreases.

1. Varashin, E.M., Tyshchuk, M.E. *Separation transformer*. USSR author's cert. 1494052. Int. Cl. H 01 F 27/28. Publ. 15.07.80.
2. Rychina, G.A. (1976) *Electroradioelements*. Moscow: Sov. Radio.
3. Dobronevsky, O.V. (1971) *Reference book on radio electronics*. Kiev: Vyscha Shkola.
4. Chajka, M.K. *Device for conversion of input direct current energy into output direct current energy with high-potential decoupling*. Pat. 74594 UA. Int. Cl. H 02 M 3/28, H 01 J 37/06, B 23 K 15/00. Publ. 16.01.2006.
5. Kostikov, V.G., Nikitin, I.E. (1986) *High-voltage electric power sources REA*. Moscow: Radio i Svyaz.

TECHNOLOGY OF MULTILAYER ARGON-ARC WELDING OF HARDENING HIGH-STRENGTH STEELS USING NON-AUSTENITIC WIRES WITHOUT PREHEATING AND HEAT TREATMENT



Contacts: Prof. Savitsky M.M.
E-mail: savitsky@paton.kiev.ua

The principle of the offered technology consists in control of thermal cycle of argon-arc non-consumable electrode welding without preheating and heat treatment of hardening high-strength steels, that gives an opportunity to use the non-austenitic welding wires of not high alloying, including those with an increased carbon content. Welding is performed using a standard welding equipment.

Technology provides such advantages as minimizing the consumption of welding consumables, power consumption, welding stresses and strains, labor content, cost of welded products. In addition, equivalent strength, high reliability and long life of the welded joint are attained under the different service conditions. Technology has been implemented at the enterprises of Ukraine.

Application. For manufacture of drilling machinery (exploring and industrial), load-carrying shafts, mining and metallurgical equipment, products of aircraft industry and general machine building.

Proposals for co-operation. Development and implementation of technologies of welding and manufacture of experimental-industrial batches of welded products on the contract base.



THESES FOR SCIENTIFIC DEGREE

The E.O. Paton Electric Welding Institute of the NAS of Ukraine



On May 17, 2007 **M.D. Rabkina** (PWI) defended the Doctor's Thesis on the subject «Influence of Structural-Mechanical Anisotropy of the Steel Rolled Stock on Welded Structure Resistance to Lamellar Fracture».

The dissertation is devoted to studying the regularities of initiation and propagation of lamellar fractures of welded joints and development of theoretical principles and technological measures of their prevention at all the stages of development and operation of welded structures, allowing for the texture of the base metal and operating conditions, including temperature, load and impact of hydrogen-containing media.

It is experimentally established that lamellar cracks appear in two forms: low- and high-temperature. The first is characterized by lowering of fracture toughness on the «lower shelf» of its temperature dependence and increase of the brittle-tough transition temperature T_{br} . The second is characterized by lowering of fracture toughness on the «upper shelf» of its temperature dependence without any noticeable change of T_{br} . The main cause for development of the low-temperature lamellar cracking is the predominant presence of a family of crystallographic cleavage planes $\{001\} \langle 011 \rangle$ in the steel rolled stock, which develops at the temperature of the end of rolling corresponding to the ferrite region. High-temperature lamellar cracking is due to the texture of non-metallic inclusions resulting from hot rolling. Both the kinds of cracking can have a lamellar-brittle and lamellar-tough component, as well as their combinations. Regularities of dislocation distribution during deformation of the low-alloyed steels depending on the direction of the applied load, have been studied. Chaotically

distributed dislocations are localized in the region of non-metallic inclusions causing their cracking or delamination from the matrix. Dislocations located in the form of walls, are indicative of structure fragmentation. New concepts of the causes of welded structure failure due to the base metal texture, allowed defining the requirements to Z-steels for nodal tubular connections. Results of investigations of test steel batches based on 09G2S grade with different values of temperature of the end of rolling are the basis for formulating technical conditions for critical welded structures. A dependence is established between the lamellar fracture resistance and HAZ structural elements in low-alloy steel welded joints. Based on the results of theoretical and experimental studies, an approximate formula has been developed, which allows determination of the width of the overheating section, depending on the cooling rate $w_{6/5}$ in the range of 1–10 °C/s; theoretical methods of evaluation of crack resistance characteristics K_{Ic} and δ_{Ic} were developed by the results of standard mechanical testing allowing for the dimensions of structural elements. Regularities of initiation and development of lamellar cracking of structural shells of a petroleum processing complex because of hydrogen diffusion into the zone of elastoplastic distortion of the crystalline lattice have been studied. It arises in decarbonised zones as a result of pressure of hydrogen and/or methane both at the initial stages of initiation and in the prefracture zone ahead of the avalanche crack front, and consists in interaction of individual microcracks and pores. Decarbonisation of structural steels is accompanied by inheriting of the material structure and proceeds, unlike the existing concepts, at low values of temperature and pressure of hydrocarbon vapours (less than 0.2 MPa). This results in development of lamellar cracks, which, depending on relative dimensions of the crack h_j/r_i , fracture toughness K_{Ic} and thickness of sound metal interlayer can either develop, or acquire the shape of bubbles. At low values of metal fracture toughness ($K_{Ic} < 30 \text{ MPa}\sqrt{\text{m}}$) growth of lamellar-hydrogen cracks is found, which is promoted by crystallographic orientation $\{001\} \langle 011 \rangle$. Proceeding from physico-mechanical investigations of the metal of fragments of the dismantled structures it was established that the residual life of structures after long-term service in hydrogen-containing media is determined by the degree of damage of the case shell by lamellar-hydrogen cracks.



On May 30, 2007, **A.E. Korotynsky** (PWI) defended the Doctor's Thesis on the subject «Highly Efficient Sources for Arc Welding Based on Induction-Capacitance Converters».

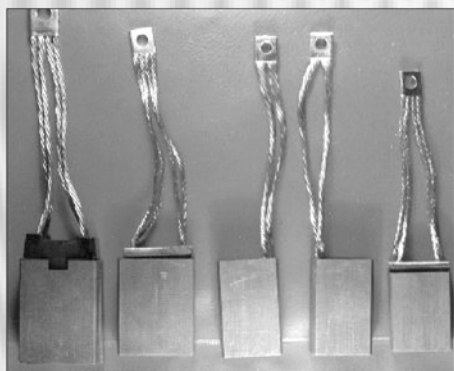
Dissertation is devoted to investigation, development and introduction into production of new energy-efficient processes, as well as mobile welding-technological complexes with improved characteristics of energy efficiency, electromagnetic compatibility and weight-dimensional parameters. It is shown that application of inductance-capacitance converter provides a high energy-efficiency due to increased efficiency and power factor, improves the indices of resourcesaving (consumption of copper is reduced 1.5–1.8 times, of transformer steel — 1.8–2.2 times), yields the highest indices of electromagnetic compatibility, which is due to selective properties of the welding contour.

Detailed theoretical and experimental investigations of resonance processes in welding inductance-capacitance converters (WICC) at different degrees of contour mistuning have been conducted. It is established that depending on the welding process (MMA, TIG, MIG/MAG), the necessary degree of mistuning is selected, which is optimum for providing the arcing stability, as well as other welding-technological properties (forming, spattering, defect formation, etc.). It is shown that the most acceptable method for increasing WICC power is transition to a modular principle of their construction. In this connection, methods of coherent analysis of interaction of welding currents of the switched on modules were developed, and new methods were proposed for power adjustment in arc welding.

New two-contour circuits of resonance sources have been proposed and studied, characterized by an increased arcing stability, which allow successfully conducting AC welding process using electrodes with a basic coating. It is shown that in WICC the most promising method for welding current adjustment is the discrete-time one, which does not disturb the setting of the resonance circuit. To develop high-frequency WICC, it proposed in the work to use devices with distributed parameters, which were selected to be an artificial long line closed at the end and a quasi-inducon.

By the results of this work, 15 types of new sources were introduced into production, as well as five welding-technological complexes based on inductance-capacitance converters.

DIFFUSION BONDING AND BRAZING OF DISSIMILAR MATERIALS



Technological processes of diffusion bonding in vacuum of ceramics, graphite and also these materials with metals have been developed. Technologies of bonding ceramics on the base of aluminium oxide, silicon nitride, silicon carbide, piezoceramics and others are offered. Technologies of bonding of ceramics and graphite with titanium, copper, steel, refractory and heat-resistant alloys have been developed for multi-component systems with and without use of interlayers. Technological processes and designed equipment guarantee the high quality of the joints.

Purpose and application. Technological processes are designed for welding and brazing of products made from ceramics, graphite, including different combinations with metals. They are used in instrument industry, radio electronics, electrophysical equipment, power engineering and others.

Status and level of development. Technology and equipment for welding cermet sectioned tubes of electron accelerators are implemented at NIIIEFA (St.-Petersburg, therefore).

Proposals for co-operation. Signing of contract is possible.

Main developers and performers: Prof. Yushchenko K.A., Dr. Nesmikh V.S., Lead. Eng. Kushnaryova T.N.

Contacts: Prof. Yushchenko K.A.
Tel./fax: (38044) 289 2202



NEWS

NKMZ SHIPPED OUT THE EQUIPMENT FOR A STEEL-MELTING FURNACE TO UZBEKISTAN

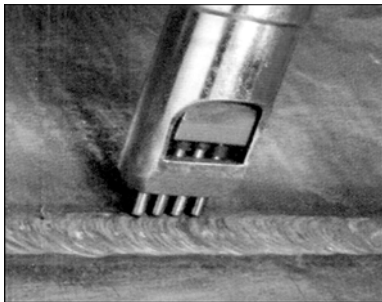
Novo-Kramatorsk Machine-Building Works (NKMZ) (Kramatorsk, Donetsk reg.) finished supplying equipment for a fundamental renovation of 100-ton arc steel melting furnace in Uzmetkobminat Works (Uzbekistan, Bekabad). With implementation of this contract, NKMZ for the first time entered the market of electric steel melting equipment. The NKMZ specialists have proven not only the viability of the new engineering solutions, but also their superiority over the existing

ones. Improvement of performance of steel-melting arc furnace of 100 t capacity envisaged by NKMZ specialists, will allow Uzbek metallurgists reducing almost 2 times the unscheduled downtime and increasing production of quality metal.

On the other hand, with the furnace commissioning NKMZ will complete the steel-melting cycle and will have the reference-lists on all the units of the modern steel melting complex.

STRENGTHENING TREATMENT OF WELDED JOINTS

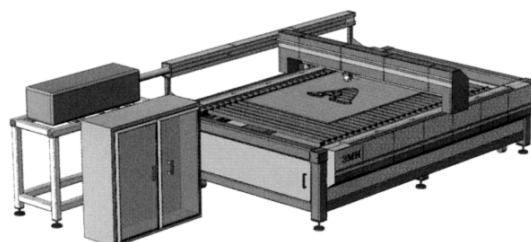
OJSC «MAGNIT plus» (St.-Petersburg) offers «Shmel» technological system designed for strengthening treatment of welded joints of metal structures operating at alternating and constant loads by the method of impact deformation at ultrasonic frequency. The complex provides a lowering of mechanical stresses in the welded joints and base metal, creates a strengthening layer with increased resistance to cracking.



Technical characteristics of the system are as follows: working frequency of 26–28 kHz, output power of 500 W, power voltage of 220 V, weight of 21 kg, overall dimensions of 36 × 390 × 420 mm.

SLP-02 SYSTEM

Now and in the near future laser and plasma cutting technologies will become the most widely used processes of cutting and treatment of sheet material due to their simplicity, reliability, safety and cost-effectiveness compared to any other processes. Machine tools of this type are capable of cutting any materials, namely plastic, steel, including stainless and high-alloyed steels, cast iron, copper, brass, bronze, alu-





minium, titanium and other materials, and are also successfully used for engraving and marking.

CJSC «Zavod Mekhatronnykh Izdelij» (Moscow distr.) mastered the manufacture of tables of this series, in particular SLR-02, for highly efficient and sound cutting of sheet material.

SLR-02 consists of a three-coordinate table of gantry type, CO₂-laser with 200 W output mean power, system of beam delivery to the object, as well as controlling controller. The table proper is constructed from linear modules manufactured by STS (Italy). The modules are made from precise aluminium profile with integrated roller slideway bearings. Assemblies of module fastening to the bed plate allow compensating the non-straight-

linearity of the module proper. Reinforced polyurethane belts are used in the transmission. The drive is provided by synchronous servomotors with precision planetary reduction gears. Mounting corrugated protection is possible as an option.

Laser system can be fitted with CO₂-lasers with average output power of 300 and 500 W. More powerful slot RLS-1000 and RLS-250 lasers can be mounted at customer demand.

Engineers of this plant developed equipment, in which precision components in the table design and locally made laser make an ideal combination. Thus, it was possible to achieve a high accuracy of cutting and low price of the item.

NEUTRIX INSTRUMENT FOR TUNGSTEN ELECTRODE SHARPENING

«Unitekh» (Dubno, Rovno distr.) offers Neutrix --- a unique instrument of its kind for sharpening tungsten electrodes. A portable grinding machine is incorporated into the developed instrument, which guarantees reproducible high-quality grinding of tungsten electrodes for arc plasma welding, TIG welding and «orbital» welding of pipes, while meeting the most stringent requirements of environmental protection.



Owing to its mobility Neutrix instrument is ideal for mounting operations and other tasks which require a portable grinding machine. For stationary operation

it can be supplied with the fastened support bed plate and large filter for dust collection. Neutrix instrument has the following significant advantages:

- necessary tip angle is smoothly set using the sharpening angle scale. Sharpening angles from 7.5 to 90° correspond to 15 to 180° angles for the electrode;
- experimental disk allows three-times use of the diamond disc on three grinding planes;
- special clamping device allows sharpening short tungsten electrodes of 1.0-1.4 mm diameter and up to 15 mm length (for complex operations, including automatic welding of pipes);
- accurate determination of the wear length is achieved using an adjustable gauge, which enables minimum electrode consumption and minimum diamond disc wear. Adjustable gauge also allows removing flash from tungsten electrodes (more than 1.6 mm diameter) for welding aluminium;
- ability of observation of the sharpening process through the viewing glass and checking the grinding pressure to avoid electrode annealing at sharpening;
- built-in suction and portable filter for dust collection are an important feature of Neutrix instrument.

In such a modification Neutrix is the only available shaping instrument for tungsten in the world market.



INTERNATIONAL CONFERENCE «Ti-2007 IN CIS»

Traditional annual International Conference «Titanium in CIS» arranged by the International Association «Titanium» was held on 15–18 April 2007 in Yalta (Crimea, Ukraine). The Conference was attended by more than 250 specialists from Ukraine, Russia, Tajikistan, USA, Germany, Italy, Japan, China, Luxemburg, South Korea and other countries. Presentations at the Conference were made by titanium scientists and experts from the leading research institutions and industrial enterprises of Ukraine, Russia and other countries: State Research and Design Institute of Titanium, E.O. Paton Electric Welding Institute (NAS of Ukraine), G.V. Kurdyumov Institute of Metal Physics (NAS of Ukraine), I.N. Frantsevich Institute for Materials Science Problems (NAS of Ukraine), H.V. Karpenko Physico-Mechanical Institute (NAS of Ukraine), Institute of Geological Sciences (NAS of Ukraine), Donetsk National Technical University, Zaporozhie State Engineering Academy, Company «Zaporozhie Titanium-Magnesium Works», O.K. Antonov Aircraft Science and Technology Complex, OJSC «All-Russian Institute of Light Alloys», Federal State Unitary Enterprise All-Russian Institute of Aircraft Materials (FSUE) R&D Institute for Structural Materials «Prometej», Moscow Aviation Institute MATI — K.E. Tsiolkovsky Russian State Technical University, Urals State Technical University UPI, A.A. Bajkov Institute of Metallurgy and Materials Science (Russian Academy of Sciences), OJSC RITM, FSUE Giredmet, University of Technology MISiS, FSUE A.A. Bochvar Russian Research Institute for New Materials, OJSC «Corporation VSMPO-AVISMA», OJSC «Sukhoi Design Bureau», Russian Space Corporation «Energiya», OJSC «Chepetsky Mechanical Factory», etc. Over 90 papers were presented totally.

Representatives of the Zaporozhie Titanium-Magnesium Works covered in detail the main areas of efforts on upgrading the technology for production of titanium sponge in Ukraine and further development of its facilities. It should be noted that in 2007 the Works has started construction of a metallurgical workshop to produce ingots and slabs by the electron beam cold hearth melting method, and is exploring currently the possibility of construction of a rolling workshop to produce titanium sheets and plates.

Much attention was given at the Conference to issues related to upgrading of the technology for production and improvement of the quality of titanium sponge and titanium ingots. In addition to the Zaporozhie Titanium-Magnesium Works, this issue was also the subject of presentations made by specialists from the Corporation VSMPO-AVISMA, State Research and Design Institute of Titanium, E.O. Paton Electric Welding Institute, Company VILS, etc.



It is the opinion of the Conference participants that the process of magnesium-thermic reduction of titanium chloride will still be the key process for production of titanium during the next decades, and that the electron beam technology will play an increasing role in production of titanium ingots, along with the vacuum-arc remelting technology. It should also be noted that the intensive research efforts on utilisation of the electroslag and plasma-arc remelting technologies in metallurgy are still underway.

The E.O. Paton Electric Welding Institute presented papers dedicated to investigation of the quality of metal produced by the electron beam and arc slag remelting technologies, compacting of titanium chips, dynamic load resistance of new domestic titanium alloy T110, and to improvement of the technologies for welding titanium and titanium-base alloys through applying activating fluxes and superposition of a transverse magnetic field on the arc. The papers presented by specialists of the E.O. Paton Electric Welding Institute generated high interest among the Conference participants.

Much consideration was given at the Conference to the issues associated with application of titanium in aircraft engineering, ship building, power engineering, manufacture of medical-application parts (endoprostheses, implants, instruments, etc.), and manufacture of titanium semi-finished products (plates, forgings, rods, tubes).

The problem of manufacture of semi-finished products from titanium alloys with improved physical-mechanical properties is addressed currently both through development of new titanium alloys, such as Ti-Si based alloy, and through development of efficient methods and parameters for thermo-mechanical deformation of existing alloys.

There were many presentations dedicated to improvement of performance of parts made from titanium

alloys by using different types of surface treatment (coating, nitriding, oxidation, etc.).

The market of titanium has been characterised lately by a considerable growth of output of titanium sponge and products made from it. So, whereas in 2005 the world production of titanium sponge was 112,900 t and in 2006 --- 136,400 t, it is expected that the output in 2007 will be 155,000 t. The most dramatic increase in volumes of production of titanium sponge was fixed in China: 5000 t in 2004, 9500 t in 2005, 18,000 in 2006, and 28,000 in 2007. The share of China in the world production of titanium sponge increased from 6.0 % in 2004 to 13.2 % in 2006. And it is expected to grow to 18 % in 2007. According to the domestic production plans, Chinese enterprises schedule to produce 85,000 t of titanium sponge in 2010, and 105,000 t --- in 2012. The volumes of consumption of titanium in the Chinese industry also grow, but not as rapidly as production of titanium sponge and ingots of titanium alloys. For example,

consumption of rolled products in China increased from 10,000 to 15,000 t in 2005–2007. Therefore, the Chinese industry has almost completely met its own demand for titanium, and starting from the second half of 2006 it has been actively entering the world market by offering to supply big batches of titanium. Because of a substantial increase of offers, the prices for titanium have stopped growing and even started decreasing. According to forecasts made by some Conference participants, they may fall to their economically grounded level --- US\$ 6--7 per kilo, which opens up good prospects for increasing the scopes of application of titanium in different civil industry sectors.

In conclusion, we would like to note a high level of arrangement of the Conference and express gratitude to its organisers represented by CJSC Inter-State Association «Titanium» and its Chairman A.V. Aleksandrov.

Prof. C. V. Akhonin, PWI

RAILWAY TRANSPORT. WELDING 2007 (Workshop in Kakhovka)

Traditional 5th Workshop «Railway Transport. Welding 2007» was held on the 16th of May 2007 at the Open Joint Stock Company «Kakhovka Plant for Electric Welding Equipment» (KZESO). The Workshop was attended by about 30 leading specialists in the field, representing railway car building, car repair, switch, electric car and railmotor car repair, and machine building factories of Ukraine (Dnepropetrovsk, Zaporozhie, Kerch, Kremenchug, Krivoj Rog, Stakhanov, Nikolaev), Russia (Novoaltajsk, Bryansk, Istie, Novosibirsk, Perm, Roslavl, Tver, Torzhok), Pridnestrovskaya Moldavian Republic (Tiraspol), and Georgia (Tbilisi). Representatives of the Welding Society of Ukraine, International Association «Welding», Journals «Avtomaticheskaya Svarka» and «Svarshchik», as well as heads and chief specialists

of the main departments of KZESO also took part in the Workshop.

This year Workshop was characterised by an expanded geography of the attendees, participation of a large number of young specialists, and opportunities to communicate with colleagues on prospects of upgrading of the production processes, as well as application of the latest scientific achievements in manufacturing.

The Workshop was opened by Ya.I. Mikitin, Chairman of the Board of Directors and Director General of KZESO. He dwelt briefly on the history of the Plant, and noted the role of B.E. Paton, who as early as at the end of the 1950s had determined the profile of activity of the Plant in manufacture of electric welding equipment. Then Ya.I. Mikitin high-





lighted the leading positions of the Plant in production of a number of unique pieces of the equipment that are 15–20 years ahead of the world achievements. At present the staff of the Plant is about 2400 people, and it has remained almost unchanged since many years ago. The volumes of production grew 2.5 times compared with the Soviet period. And in the near future (1–2 years) they may grow another 2 times, because the Plant has mastered the manufacture of new products — a series of on-route machines.

Ya.I. Mikitin highly appreciated the role of the close and efficient collaboration of the Plant with science. It is the collaboration of KZESO with the E.O. Paton Electric Welding Institute that prevented disintegration of the Plant in the 1990s, and, on the contrary, allowed finding the economic ways of strengthening this collaboration.

KZESO sees the pledge of its successful development in collaboration of the advanced research, modern production and reliable financing. KZESO strongly intends to remain ahead of its competitors in the welding equipment market. The on-route machines, which are being mastered currently at the second production site, have no analogues in Ukraine, and the snow-removing machines — no analogues in the world. The same applies also to the flash butt welding machines for making railway frogs.

Production of KZESO has been certified according to ISO 9000 since 2006. Every year the Plant passes the audit. Professional workers are concentrated at the main departments of the Plant. For example, 74 people are working at the Chief Designer's Department, and over 80 people — at the Chief Technologist's Department.

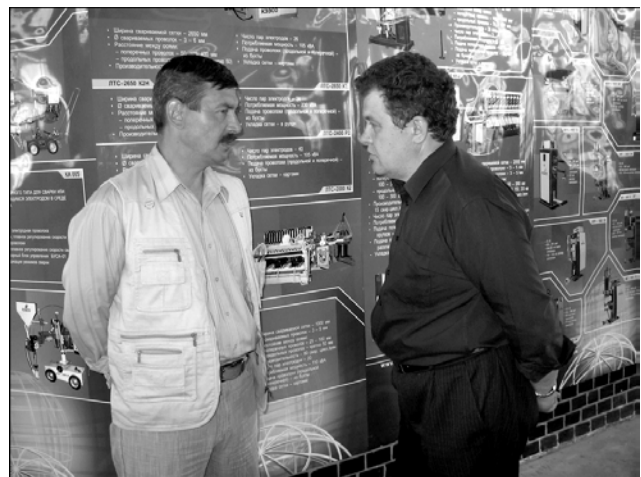
KZESO is manufacturing now more than 100 types of welding equipment, including transformers, rectifiers, special power sources, semi-automatic welding devices, machines for resistance seam welding, automatic devices for electroslag welding, and machines for flash butt and spot welding. KZESO is working on the so-called «branch» principle of design and manufacture of equipment, e.g. for motor-car industry, or for operation under special conditions. Production of lines and machines for the manufacture of grids, which are in high demand in the building industry, is being mastered now. KZESO is the world market leader in manufacture of mobile rail welding



systems (99.9 % of the systems in operation were manufactured by KZESO), the volume of the applied stationary rail welding machines manufactured by KZESO constituting 60 % of the total world fleet of such machines.

Topical problem for the nearest future is replacement of obsolete main pipelines and construction of the new ones. Here the focus is on utilisation of pipes with a wall thickness of 32 mm, which should provide their long service life. New welding equipment to meet increased requirements for welded joints is needed to handle this problem. Russian Joint Stock Company «Gazprom» has already made an agreement with KZESO on supply of new machines. Among the samples of new equipment mastered by KZESO are also mobile machines for welding of railway frogs (they will also outstrip the corresponding foreign developments by 15–20 years).

Ya.I. Mikitin covered also the social aspect of life of the Company. KZESO has a sanatorium-preventorium (70 man/month), 2 recreation centres, and a boarding house. The workers have the subsidised factory canteen. During the last 15 years KZESO has paid for education of more than 400 workers at the



higher education institutions, who are now successfully working at the factory.

Then the presentations at the Workshop were made by the industry representatives. Yu.V. Butenko, Chief Welder of Production Company «Mashzorya-Proekt», highly estimated semi-automatic devices KZESO KIU-401 (unit VS-300B), 25–30 pieces of which are now in operation at the Company. He noted the need to arrange production of machines for argon-arc welding to meet requirements of ship building enterprises.

V.M. Ilyushenko, Head of Department at the E.O. Paton Electric Welding Institute, told about a positive experience of PWI in «running-in» of new models of the semi-automatic devices produced by KZESO, which makes it possible to optimise and bring them to a consumer level within the short terms. At the same time, he noted the necessity to master production of the inverter-type power units, equipment for automation of the submerged-arc welding processes, twin-electrode gas-shielded welding process (Time Twin), and hybrid processes. The E.O. Paton Electric Welding Institute has developments for the technology of semi-automatic welding in different spatial positions to conduct repair operations, which can be taken into account in designs of semi-automatic devices produced by KZESO. PWI has also developed a promising composition of electrode material for resistance spot welding machines.

Representative of Limited Liability Company «Transmash», as well as representatives of other factories gave their high estimation to the KZESO equipment for arc welding, and expressed their interest in

buying different types of semi-automatic devices and power units.

Participants of the Workshop were invited to visit the exhibition section at a shop, where V.I. Okul, Chief Engineer of KZESO, told them in detail about advantages of the exhibited equipment for arc and flash butt welding, demonstrated promotion models of resistance multi-spot welding and on-route machines, and answered numerous questions asked by the Workshop participants.

In conclusion of the Workshop, S.V. Dukh, Chief Designer, spoke in detail about principles of the work underlying designing of the equipment, as well as technologies, peculiarities of production and selection of components, including control systems.

It should be emphasised that the information presented by the Director and leading specialists of KZESO is very impressive. KZESO is expanding, it widens production and ranges of equipment and machines being manufactured by focusing on training and upbringing of staff, certification of production according to the European standards, and strengthening of social security for its employees.

The Workshop participants expressed their gratitude to the representatives of KZESO for their excellent organisational efforts, continuous upgrading of the equipment, expanding its ranges, and their striving for meeting the market demands.

*Prof. V.N. Lipodaev, PWI
Dr. A.T. Zelnichenko, PWI*

M.L. ZHADKEVICH IS 70

Prof. L.M. Zhadkevich, Doctor of Technical Sciences, corresponding member of the NAS of Ukraine, noted specialist in the field of materials science, metals technology and special electrometallurgy, and Deputy Director of the E.O. Paton Electric Welding Institute, was 70 on the 12th of July, 2007.



He started to be involved into problems of the technology of metals in 1955 at the Kujbyshev Metallurgical Works, whereto he was appointed after graduating from a technical school. There he passed the path from a pressman to a chief of the country-largest pressing workshop. Then he completed education at the All-Union Correspondence Polytechnic Institute, and became one of the leading specialists in the field of materials science and pressure treatment of metals. Production of blanks and assemblies of high-strength aluminium and other alloys for machine- and ship-building, aircraft engineering and rocket construction was arranged under the leadership of M.L. Zhadkevich.

In 1977, M.L. Zhadkevich was appointed to the Kiev Zonal Research Institute for standard and experimental design of residential and public buildings, where he headed a division for experimental aluminium constructions and developed technologies for production of aluminium parts. He was leading the activity on mastering the technologies for pressing and fabrication of standard and unique building alu-



minium structures in Brovary, Voronezh, Khabarovsk and Kishinyov.

M.L. Zhadkevich has been working at the E.O. Paton Electric Welding Institute since 1984. He was a director of the Pilot Plant for Special Electrometallurgy from 1985. Under difficult conditions of restructuring of the economy of the country, by handling organisational and research problems he managed to provide successful functioning of the Plant in building of a new generation of equipment and technologies for electroslag casting of billets for heavy and power engineering, electron beam welding of large-size units of rockets from super strong aluminium alloys, hardening and repair spraying of blades for gas turbine and other power generation parts and units, ship building and defence industry.

Since 1993 L.M. Zhadkevich has been the Deputy Director in research activities at the E.O. Paton Electric Welding Institute, and Head of Department «New Physical-Technical Methods for Welding and Special Electrometallurgy». He was the first to develop new multi-component nickel- and cobalt-base alloys for hardening and repair technologies. He elaborated scientific principles of simulation of complex electrometallurgy processes, as well as production of nanocrystalline and other materials with high service properties.

Theoretical and experimental studies performed by L.M. Zhadkevich at a high scientific level are of interest to specialists involved in development of welding and related technologies. Being a supervisor of a research area, he trained 4 doctors and 3 candidates of technical sciences. M.L. Zhadkevich is the author of over 420 scientific papers, including 8 monographs. Equipment, materials and technologies developed under the leadership of M.L. Zhadkevich have been widely applied in fabrication of critical aerospace structures, power generation equipment, parts used

in defence industry, instrument making, etc. They are covered by dozens of patents and author's certificates, and noted with many medals and diplomas.

M.L. Zhadkevich combines to advantage the research and scientific-organizational activities. He is a member of the Inter-Departmental Commission on State Program «Titanium of Ukraine», member of the Inter-Departmental Commission on non-ferrous metallurgy, member of the Scientific Board of the E.O. Paton Electric Welding Institute, Thesis Defence Board of the E.O. Paton Electric Welding Institute, Board of Directors of the Joint Ukrainian-American Experimental Centre «Pratt & Whitney--Paton», and member of the editorial boards of a number of publications.

For his contribution to the progress of materials science, and development of high-efficiency technologies for production and processing of new materials in particular, as well as for his fruitful scientific-organizational activity, M.L. Zhadkevich was awarded the Order of the Red Banner of Labour, medals, honorary title «Honoured Scientist and Technician», and State Prize of Ukraine in the field of science and technology. He is a corresponding member of the National Academy of Sciences of Ukraine, and a full member of the Academy of Technological Sciences.

We cordially congratulate the hero of the jubilee and wish him from the bottom of our hearts good health, personal happiness and great success in accomplishment of his creative plans.

*E.O. Paton Electric Welding Institute
of the NAS of Ukraine
Editorial boards of
«Avtomaticheskaya Svarka» and
«The Paton Welding Journal»*